

Decision-making framework for enhanced thermal resilience of façade-retrofits

Building Technology Master Thesis

Student: Alina Verena Wagner

Student number: 5635616

Main mentor: Dr. Alessandra Luna Navarro

Second mentor: Dr. Eleonora Brembilla

Acknowledgements

This master thesis and the past months have been a journey of unfolding knowledge, exploration, and personal development. As the final period of my academic education, my thesis concludes on two extremely enriching years in the Building Technology Master programme of the University of Technology in Delft. The programme itself, but especially my thesis project, redefined my horizon. I had the chance to learn a lot deeper about what it means to be a design engineer of the built environment, creating the surrounding of our future. With blurring boundaries, I can now say that I am convinced to be “somewhere between architecture, engineering and science” - we all need to listen, gather knowledge, and collaborate to be able to design solutions for a healthier, sustainable, and resilient built environment. I am grateful that I was able to listen to and learn from the interdisciplinary team of the AE+T department and all my fellow Building Technology students, thank you.

For my master thesis, I had the help, guidance, and support of many people. First of all, I would like to express the biggest “thank you” to Dr Alessandra Luna Navarro. As my main mentor, she was guiding me with her endless curiosity and enthusiasm. Her energy, knowledge, and scientific accuracy helped me to find the right path throughout the whole process. Sometimes lost in the boundless depth of research, her constant availability reminded me that I do not have to solve difficulties and doubts alone. A special thanks also to my second supervisor, Dr Eleonora Brembilla. Her expert knowledge helped me to solve several specific questions and improving my research significantly. Both have been supporting me professionally but also mentally, while inspiring me with their passion for research.

Additionally, I would also like to thank Dr Simona Bianchi and Pedro de la Barra Luegmayer. Their expertise was of great help in parts of the research, which allowed me to progress more efficiently. Furthermore, I would like to extend my sincere thanks to Prof. Dr Atze Boerstra. The weekly meetings of my student assistant job were a welcome change out of the thesis routine. I highly appreciated his input and understanding towards my thesis process.

This journey however would not have been the same without the support of my family. My parents, Christine and Robert, gave me their invaluable trust in me as a person and in my competence. They provided me with the necessary strength to “climb this mountain”. Now that I am enjoying the view, I am aware of the “wings” they equipped me with. I also thank with deepest gratitude my sister for her advice and presence before and during the whole master’s programme. As the first person to reach out, Anna was reconstructing and healing my self-confidence repeatedly. Thank you.

And finally: thank you to all my friends. Through distance, but still connected, sharing thoughts with my friends in Germany made me gain different perspectives. However, the closest were all my friends in Delft. I am extremely grateful for their daily support and cheer-up. They believed in me and my project at times when it was hard for me to do so. Lotte and Eva as my decision-makers and personal support group. And Pranay who joined my journey through the unknown – it would have never been the same without the daily company as study-buddies Thank you for being there with me and for me when going through those ups and downs of our thesis.

Solely by choosing this specific topic, this thesis has introduced me to the depth of scientific research on building/façade performance. While first not realizing the possible detail, I am incredibly thankful for my professional and personal growth, with everybody accompanying me.

Abstract

Climate extremes are becoming increasingly frequent and intense worldwide, with greater pressure on ecosystems, the built environment, and humankind. Heat waves, in particular, are overheating indoor spaces and thermal comfort as one of the major comfort requirements of buildings is disrupted or, in the most extreme situations, lost. In extreme cases, this can lead to life-threatening circumstances and explains the high morbidity and mortality during past heat wave events. It is crucial to urgently develop a more climate-resilient built environment, that can effectively respond to the future climate hazard of heat waves. Hereby, the building envelope has a key role to mitigate the impact of the exterior environment on the occupants' indoor comfort. Accordingly, exploring possibilities of façade design for "future-proof" buildings is important to reduce health risks and improve the daily quality of life. However, the lack of comprehensive research on assessment methods for evaluating the influence of façade design on building thermal resilience proves the current challenges of implementing the concept of "resilience" in a practical manner.

This research aims to improve the design process of retrofit options, increasing thermal indoor comfort during heat waves, and enhancing long-term building thermal resilience. It includes the development of resilience indices, based on the assessment of the facade's performance at the different stages of a resilient building reponse during extreme heat periods. By conducting a systematic literature review focusing on thermal resilience terminology and corresponding assessment methods, the study identifies limitations and gaps in current research. A novel method is proposed, which incorporates future climate scenarios and multiple resilience indicators. While most existing research solely relies on the measurement of a single indicator to measure thermal resilience, this thesis demonstrates the importance of combining multiple resilience indicators to comprehensively assess the influence of façades on building thermal resilience. The proposed framework aims to be universally applicable and adjustable, while assessing the short- and long-term impacts of retrofit interventions on the performance of the façade. The resulting index visualizes how various façade retrofit variables can influence thermal resilience at the building level, which provides a deeper understanding of dependencies and thus enhances improved decision-making during the development of façade retrofits.

Content

Acknowledgements	1
Abstract	3
Content	4
List of figures	6
List of tables	9
Introduction	10
1.1 Problem statement	13
1.2 Research gap	13
1.3 Research objective	13
1.4 Research question and sub questions	14
1.5 Methodology	14
1.6 Research outline	16
Literature review	17
2.1 Characteristics of extreme heat events	18
2.1.1 Indices to identify heat waves	19
2.1.2 Influences of heat waves on occupants	20
2.2 The role of the facade on the improvement of thermal comfort	22
2.3 Definition of resilience	23
2.4 Systematic literature review	24
2.4.1 Definition of resilient façade and building design	25
2.4.2 Quantification methods of resilience in façade design	27
2.4.3 Retrofit strategies for heat wave resilience of facades	33
2.5 Conclusion of literature review	35
Definition of resilience indicators	37
3.1 Development of a Future Resilience Index	38
3.1.1 Definition of resilience indicators	38
3.1.2 Calculation of resilience indicators	40

3.2	The final index	44
Building performance simulation methodology		46
4.1	Introduction of methodology	47
4.1.1	Outline and workflow of index calculation	48
4.2	Hazard analysis - heat wave weather data	50
4.3	Definition of case study	51
4.3.1	Base case simulation set-up	52
4.3.2	Inputs and range of variation	53
4.4	Sensitivity analysis	55
4.4.1	The Sobol method	57
4.5	Morphing of future weather data	60
Results		61
5.1	Sensitivities of variables	62
5.2	Output performance distribution	64
5.3	Identification of best performing scenarios	65
5.4	Variable values comparison	66
5.5	Index evaluation and final rating of design cases	70
5.6	Discussion of research results	74
5.7	Conclusion	77
Materialisation and design		79
6.1	Materialisation of parameter values	80
6.2	Materialisation of parameter values	83
Conclusion and outlook		85
7.1	Conclusion	86
7.2	Limitations of research	90
7.3	Future challenges	91
References		93
Appendix A		105
Appendix B		106

List of figures

- Figure 1:** Schematic representation of climate-change-related changes in temperature distribution. (a) Illustrates the shift of the average climate, with the temperature distribution of the present climate moving towards a generally warmer climate. (b) Depicts the increase in temperature variability, resulting in a distribution with a greater number of extreme temperature values. adapted from: IPCC, 2012, p. 7..... **12**
- Figure 2:** Research outline source: own..... **16**
- Figure 3:** a) Global surface temperature changes in °C relative to the 1850-1900 period, with solid, coloured lines representing predicted increases for IPCC scenarios (SSP1-5). b) Visualization of risk assessment in the Reasons for Concern (RFC) framework, depicting five broad categories of future concerns. Colours represent different risk levels: "Very high" (purple), "High" (red), "Moderate" (orange), and "Undetectable" (white). adapted from: H.-O. Pörtner et al., 2022, p. 17..... **18**
- Figure 4:** a) The research focus scale of the eleven in-depth reviewed papers b) Number of papers published per year source: own..... **24**
- Figure 5:** The relation of a heat wave's duration and intensity to a resistant, robust, and resilient building's response. The plot surface area is divided into categories of "short/long" and "intensive/extensive" heat waves, with power outages occurring in "short-intensive" and "long-extensive" heat wave scenarios. Orange dots are positioned to represent the assumed intensity and frequency that the corresponding building design can withstand. adapted from: Attia et al., 2021, p. 6..... **25**
- Figure 6:** Number of quantitative/qualitative research of the state-of-the-art considered in literature review source: own..... **27**
- Figure 7:** Illustration of the resilience performance graph (a) based on based on the concept of the resilience triangle (b). The heat wave period is divided in the disruption and recovery period, marked by the start and the end of the extreme temperature event (in a) a cold snap). Twelve segments result from the specification of the two disruption periods, three thermal comfort thresholds and the application of penalty values. a) adapted from: Homaei and Hamdy, 2021, p.5 b) source: own..... **29**
- Figure 8:** Illustration of the resilience performance graph (a) based on the concept of the resilience trapezoid (b). The trapezoid graph is characterized by the addition of the extremis period, representing the delay during the response to heat wave conditions. Twelve segments result from the specification of the two disruption periods, three thermal comfort thresholds and the application of penalty values. The dashed lines (in a)) represent possible trends of real cases. a) from: Ji et al., 2022, p.3 b) source: own..... **29**
- Figure 9:** Preferred simulation software of state-of-the-art source: own..... **31**
- Figure 10:** Weather data used in the reviewed state-of-the-art source: own..... **31**
- Figure 11:** World map with locations of reviewed case studies. source: own..... **32**
- Figure 12:** Location of case studies based on Koppen climate classification (in Tropical monsoon climate (Am), Cold semi-arid climate (BSk), Hot desert climate (BWh), Temperate oceanic climate (Cfb), Hot-summer Mediterranean climate (Csa), Warm-summer Mediterranean climate (Csb), Hot-summer humid continental climate (Dfa), Warm-summer humid continental climate (Dfb), Subarctic climate (Dfc), Monsoon-influenced hot-summer humid continental climate (Dwa) source: own, based on Koppen climate classification..... **32**
- Figure 13:** Stages of the resilience process during the design and operational period of a building source: Attia et al., 2021..... **38**
- Figure 14:** Resilience performance graph with identified stages of resilience. Performance influenced by aging and impact of disruption (heat wave event). After disruptive event performance might reach level above or below designed

performance (depending on the response during the disruptive event) source: own; adapted from Attia et al., 2021	39
Figure 15: Cyclic process of resilience: resilience stages (black) and stage characteristics (white) source: own.....	39
Figure 16: Relation within resilience terminology: The four stages of a resilient response are linked to resilience criteria, which define specific resilience indicators. These indicators can be quantified using resilience indices. This approach enables the quantitative measurement of "resilience," providing a means to assess and evaluate resilience in a numerical manner. source: own.....	40
Figure 17: Resilience indices categorized with example calculation methods source: own	41
Figure 18: Measurement of resistance performance index: The proposal quantifies the temperature difference between the thermal comfort threshold level and the initial measurement of the thermal comfort indicator at the onset of a heat wave. The resulting resistance performance index shares the same unit as the chosen thermal comfort indicator. A smaller resistance index indicates better performance, as it signifies a reduced difference from the comfort threshold. source: own	42
Figure 19: Measurement of robustness performance index: The proposal measures the integral of the thermal comfort indicator's measured values over time, when it exceeds the thermal comfort threshold during the simulation period. A smaller robustness index signifies more comfortable conditions, indicating less severe overheating in terms of both magnitude and duration. source: own	42
Figure 20: Measurement of recoverability performance index: The proposal measures the time required for the reduction of the thermal comfort indicator measurement to reach comfortable conditions (below the thermal comfort threshold). The resulting recoverability index shares the same unit as the time measurement (e.g., hours). A smaller recoverability index indicates a shorter time span needed to achieve comfortable conditions. source: own.....	43
Figure 21: Proposal for evaluating the resilience performance of the façade, based on three indices: resistance, robustness, and recoverability. The overall performance is represented as a cumulative index, calculated by summing the individual indices for each weather data input. The solid lines in the figure represent the results of a single analysis, corresponding to one façade proposal with a specific weather data input. source: own.....	44
Figure 22: The adaptive capacity as the average of the facade's performance throughout the analysed climate scenarios. source: own	44
Figure 23: Calculation of the "Future resilience index" (FRI): The cumulative index is determined by summing the overall performance under current heat wave conditions (using 2015 weather data) and the adaptive capacity index (averaging the facade's performance across analysed climate scenarios). source: own	45
Figure 24: Methodology of decision-making workflow: The proposal considers the façade's vulnerability in terms of its current state and the local hazard and exposure to heat waves. Based on the performance comparison of ideal retrofit options and of the base case, the final façade retrofit is designed. source: own	47
Figure 25: Simulation workflow methodology: the workflow methodology includes the two loops of the sensitivity analysis (orange line) and the evaluation loop, rating the performance of the developed design cases (dark grey line). source: own.....	49
Figure 26: Heat wave identification using daily mean temperature as an indicator. Heat waves are defined by temperatures surpassing the Spic threshold (99.5th percentile), with the duration determined by the start and end moments based on the Sdeb threshold (97.5th percentile). Interruptions within the heat wave occur when temperatures fall between the Sdeb and Sint thresholds (95th percentile). adapted from: Ouzeau et al. (2016)	50
Figure 27: Bird's-eye view of the "Maxvorstadt" district in Munich, showcasing the distinct urban plan characterized by a repetitive pattern of residential buildings. source: (Hallo München, 2021).....	52

Figure 28: Illustration of the simplified modelling process where numerical models are used to simulate complex natural systems. These models aim to reproduce the processes and behaviour observed in the natural system, creating a parallel representation of each other. adapted from: Rosen (1991)	56
Figure 29: Illustration of the schematic methodology for sensitivity analysis. Variable combinations are sampled to create an input array, where each row represents a unique combination. Numerical output is calculated for each combination, and the sensitivities of variables are derived based on the variance of the output when changing the input. adapted from: Saltelli et al. (2008).....	56
Figure 30: Procedure of Sobol sensitivity analysis source: own	59
Figure 31: Predicted future CO2 emissions considering annual predicted anthropogenic (human-caused) emissions over the period from 2015 until 2100. Shown by the five narratives SSP1-1.9/2.6	60
Figure 32: Result of the Sobol sensitivity analysis. Input variables on the x-axis with corresponding Sobol's total indices, ST (greyscale) and first order indices, S1, in front (in highlight colour). a) results for the resistance index, b) for the robustness and c) for the recoverability. source: own	62
Figure 33: Frequency distribution of the resistance (a), robustness (b), and recoverability (c) output indices on the x-axis; frequency count on the y-axis; mean per index as black dashed line. source: own	64
Figure 34: Kernel-density estimate for the z-factor for each indicator, the x-axis: distance to the mean in number of standard deviations solid line: mean of each output distribution; dashed line: 5th percentile. source: own.....	65
Figure 35: Comparison of performance outcome with the recoverability on the x-axis, the resistance on the y-axis and the robustness on the z-axis: most resistant scenarios in dark green, most robust in green, and scenarios with the shortest time of recovery blue; scenarios with the assumes best overall performance in orange. source: own	66
Figure 36: Heat map of variable values (horizontal) and best- (a) and worst- (b) performing variable combinations (one scenario design in one vertical column) of the best five performing ones of resistance (left), robustness (centre) and recoverability (right) input variables: specific heat of interior finish, g-value of window, infiltration, U-value of glazing and thermal conductivity of insulation. source: own	67
Figure 37: 3D plot of the most contradicting variables: the specific heat of the interior finishing (x-axis), the thermal conductivity of the insulation (y-axis) and the infiltration (z-axis) with the top five performing scenarios per indicator (each scatter illustrates one scenario) with the best performing ones of the resistance (dark green), robustness (green) and recoverability (light blue); overall best performance in dark orange, second best overall performance in light orange source: own.....	69
Figure 38: Boxplot of the SET hourly data with ventilation requirements (exterior temperature min. 15 degrees) during the simulation period per design scenario (dark green: "res" case; green: "rob" case; blue: "rec" case; orange; "perf" case; grey: base case) and year (left: 2015; centre: 2050; right: 2080) source: own	71
Figure 39: Boxplot of the SET hourly data with ventilation requirements (exterior temperature min. 15 degrees) during the simulation period per design scenario (dark green: "res" case; green: "rob" case; blue: "rec" case; orange; "perf" case; grey: base case) and year a) 2015; b) 2050; c) 2080. source: own	72
Figure 40: Boxplot of the SET hourly data during the simulation period with ventilation requirement (exterior temperature min. 25 degrees) per design scenario (dark green: "res" case; green: "rob" case; blue: "rec" case; orange; "perf" case; grey: base case) and year a): 2015; b) 2050; c) 2080. source: own	72
Figure 41: Empirical-based classification scheme "A/B/C" proposed for the overall thermal resilience performance of facades, considering their resistance, robustness, and recoverability. source: own.....	77
Figure 42: Section in 1:20 of case study façade in its current state. source: own	81
Figure 43: Section in 1:20 of case study façade retrofit proposal with retrofitted elements in red, source: own	82

Figure 44: Thermal resilience indices performance of retrofit proposal (solid line) compared to base case (dotted line) in 2015 (dark red), 2050 (red) and 2080 (light red). source: own **83**

Figure 45: Performance of facade's current state (base case in dotted line) and retrofit (solid) in regard of a) the adaptive capacity and b) the FRI source: own..... **84**

List of tables

Table 1: Resilience indices in the state-of-the-art of thermal resilience assessment. The discussed indices include measurements of common thermal comfort indices with additional measurements of the duration and severity of the extreme temperature event. source: own **27**

Table 2: State-of-the-art thermal comfort metrics and their measurements, divided in environmental and personal factors. source: own **30**

Table 3: Tested facade retrofit options of the state-of-the-art: measures are divided into measures related to façade elements, ventilation strategies, and remaining other measures. Per reference the most effective measures are highlighted. source: own **34**

Table 4: Simulation parameters of the case study building in its current state (definition of base case scenario). source: own **52**

Table 5: Material properties of exterior wall of case study construction. Properties in alignment with EnergyPLUS material property input. source: own **53**

Table 6: Material properties of added insulation. Properties in alignment with EnergyPLUS material property input. source: own **54**

Table 7: Range and distribution of facade variables for retrofit options source: own **55**

Table 8: Material properties of design cases as per research results source: own **69**

Table 9: Index calculation for design cases with unrestricted ventilation including calculation with predictive weather data. Indices are normalized and cumulated, before the FRI is derived. source: own **70**

Table 10: Index calculation for design cases with restricted ventilation (exterior temperature min. 25 degrees) including calculation with predictive weather data. Indices are normalized and cumulated, before the FRI is derived. source: own **73**

Table 11: Derivation of design values for reduced thickness insulation while meeting thermal resistance requirements. source: own **80**



Introduction

- 1.1 Problem statement
- 1.2 Research gap
- 1.3 Research objective
- 1.4 Research question and sub-questions
- 1.5 Methodology
- 1.6 Research outline

Climate change is significantly affecting geographical and biological systems, leading to increased temperatures and more extreme local weather events. The latest report of the Intergovernmental Panel on Climate Change (IPCC) predicts a significant increase in temperature and precipitation extremes, pluvial floods, droughts, and storms. There is “very robust evidence” of the fact that the world will “very likely” be faced with a larger amount of hot and cold days. But heat waves are not only becoming more frequent, but also more intense and appear over a longer period (Seneviratne et al., 2021). Consequently, indoor temperatures are exceeding the comfortable range, increasing the threat especially for the most vulnerable part of the population. The larger number of severe heat waves and limited possibilities to adjust therefore has an immense effect on the number of heat-related diseases and mortality.

The building envelope strongly influences the health objectives of the occupants and is therefore getting increased attention as an integral influence on the indoor environment. However, even though the façade is planned more and more consciously regarding energy consumption and resource efficiency, extreme weather conditions are often overlooked. As a result, during heat waves, the functionality of the façade as a protector from outdoor impact is decreased significantly. While air-conditioning is an effective method to restore comfortable indoor conditions, it is energy-intensive and contributes to the urban heat island effect.

There is an urgent need for façade solutions that can adjust to future needs. While climate change mitigation strategies are well-studied, there is limited knowledge on how to adapt to the inevitable impacts of climate change. The IPCC proves that even if human-induced greenhouse gas forcing as the main driver of extreme events is eliminated, heat waves would be unavoidable (Seneviratne et al., 2021). Hence, it is crucial to incorporate predictions and future scenarios into the design process to be prepared for the circumstances to come. This requires to go beyond past knowledge with approved values and design resilient façade systems that guarantee efficient performance at any point, responding to new circumstances (Patterson, 2022).

While the preparedness for such extreme temperature events is one part of the concern, another one is the awareness of the scarcity of building materials. There is an urgency for a more circular construction industry, which uses the given resources more carefully. Façade solutions that improve the performance during seasonal events compromise optimal functioning during other periods, resulting in inefficient material usage. Passive house strategies for example are optimized for colder periods, but they are more likely to overheat in warmer conditions. It is crucial to achieve careful material selection when designing holistic façade designs that perform well at all times, including during extreme temperature peaks (Ozarisoy, 2022).

Future-proof façade design requires high flexibility and the possibility to respond without compromising on a healthy indoor thermal environment. This shift of thinking is changing key design parameters and demanding the debate of new considerations and constraints. Not only the past and the most common are important to consider, but also the future with new circumstances, new requirements, and new conceptions must be taken into account.

With the general warming of the globe of 2 degrees, the intensity of hot extreme periods will be expected to double, compared to the situation with global warming stabilized at 1.5 degrees – with 3 degrees global warming quadrupled (Seneviratne et al., 2021). Figure 1, derived from the IPCC Special Report on Extremes (SREX, IPCC, 2012), provides a schematic representation of how the current climate is predicted to be influenced by a general shift in average temperatures and alterations in variability.

The current average temperature shifting to a warmer temperature range (Fig. 1 a)) and the probability of temperature extremes increasing (Fig. 1 b)) can be related to climate change. Thus, the increase of globally averaged heat wave intensity, probability and duration can be predicted to additionally intensify in future (Perkins et al., 2012).

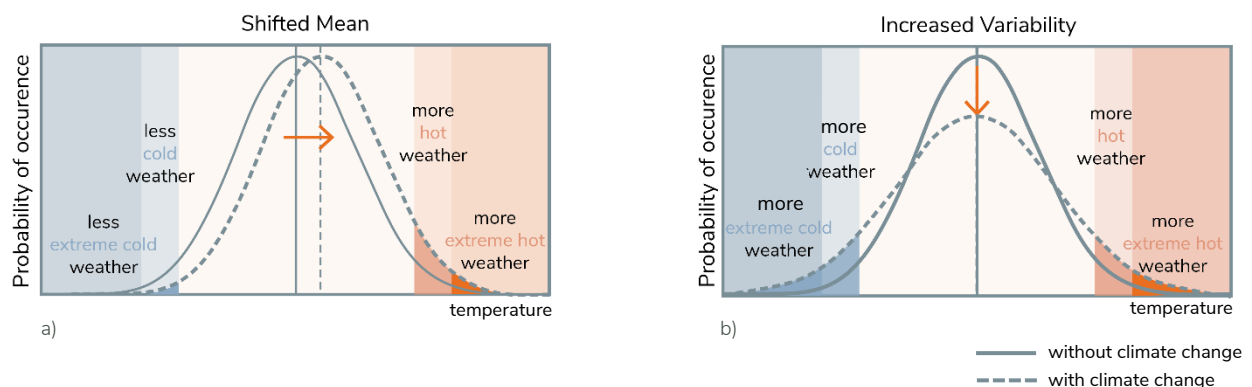


Figure 1: Schematic representation of climate-change-related changes in temperature distribution. (a) Illustrates the shift of the average climate, with the temperature distribution of the present climate moving towards a generally warmer climate. (b) Depicts the increase in temperature variability, resulting in a distribution with a greater number of extreme temperature values. adapted from: IPCC, 2012, p. 7

Heat waves count globally as one of the deadliest of occurring weather events, even with their current intensity and frequency (Holmes et al., 2016). With an immense impact on human health, thousands of deaths can be related to past heat waves. Especially within the vulnerable groups of the population like the elderly and children, a high morbidity is recorded during heat wave periods. An estimate of 70000 deaths can be connected to the heat wave of 2003 in Europe; with 54000 heat-related deaths in Russia in 2010 (Coumou & Rahmstorf, 2012; McMichael & Lindgren, 2011).

In addition to the high mortality rates, extreme heat is also affects productivity and the general well-being of human beings (Zuo et al., 2014). Although buildings are intended to protect their occupants, they often suffer from overheated indoor spaces during heat wave periods. To avoid excessive temperatures, fuel-intensive mechanical air conditioning is often used. Currently, cooling needs account for 16% of total building electricity consumption, but this is predicted to rise to 61% of global net energy consumption (IEA, 2018; Santamouris, 2016). Moreover, peak electricity demand during heat waves can lead to power shortages, further increasing the risk of occupants who rely on mechanical cooling. Thus, mechanical cooling alone is not sufficient to protect from heat stress during heat waves. Solving the problem of overheating in the built environment while minimizing energy-intensive cooling strategies is one of the most challenging tasks of the industry in the coming decades (Attia et al., 2021; Bilardo et al., 2019).

To adjust to the upcoming challenges, there is an urgent need for buildings that are designed in such a way to be able to reduce the risk of heat waves for occupants. The United Nations (UN Department of Economic and Social Affairs, n.d.) within their sustainability goals is calling for “inclusive, safe, resilient and sustainable cities and human settlements”. Consequently, rethinking building design to be prepared for the future heat, quickly draws attention to the term “resilience”. While a common understanding is shared between the different discussions about resilience, there are various definitions, which need to be discussed depending on the focus of the research. Hence, to be able to translate the theoretical character of the term “resilience” itself to practical applications, a generally approved definition and assessment method need to be developed (Attia et al., 2021). As an intermediary between outdoor environmental conditions and indoor comfort, the building envelope is having a key role in guaranteeing thermal comfort conditions during heat wave periods. Accordingly, exploring possibilities of façade design for thermal

resilient buildings is crucial to cope with the future climate while reducing health risks, improving the daily quality of life, and achieving the UN sustainability goals.

1.1 Problem statement

"Resilience" has gained increased attention as a crucial concept in building design strategies to withstand future climate change-related hazards, such as heat waves. In this context, the building envelope plays a crucial role between the outside and inside environment, making it a focal point for thermal resilience in building design. The design of the building envelope should aim to protect occupants from heat stress, always ensuring thermal comfort.

However, currently, there are no existing guidelines or methods specifically dedicated to façade design that enhances building thermal resilience. As a result, "resilience" in the built environment remains abstract and difficult to measure. To address climate-change-related extreme heat events, there is a need for methodologies that can assess thermal resilience in the built environment effectively.

1.2 Research gap

The state-of-the-art research in chapter 2 introduces different assessment methodologies of thermal resilience to extreme temperatures in the built environment. However, current methods lack suitable approaches to quantify the influence of façades on a building's thermal resilience and provide guidance to designers and occupants in making conscious choices regarding appropriate façade design that performs well during heat waves. Proposed quantification methods overlook the existence of multiple stages of resilience, thus failing to capture the different abilities required for enhancing resilience in different stages. Furthermore, the assessment methods primarily focus on the building level, neglecting the significant influence of the façade on occupants' thermal perception during extreme temperature periods. Moreover, none of the assessment metrics consider future weather predictions, which is a crucial aspect in assessing thermal resilience in façade design.

In summary, the current body of research lacks a comprehensive assessment framework that considers the influence of façades on building thermal resilience, incorporates the different stages of a building's response to heat waves through corresponding resilience indicators and includes future heat wave scenarios. A comprehensive framework should aim to be universally applicable, adjustable, and provide insights into the short- and long-term performance of interventions.

1.3 Research objective

There is an urgent need to enhance the thermal resilience of existing facades to withstand future heat waves. However, there is no universally accepted building standard, nor thermal comfort metric on thermal resilience, to which professionals can relate while designing retrofits or new constructions. Therefore, the objective of this thesis is to develop a decision-making framework, which can be used when designing retrofits for improved thermal indoor comfort during present and future heat waves. The framework will include the definition of a resilience index, which consists of multiple resilience indices, which assess the

façade's abilities in different stages of disruption. The developed framework aims to be adjustable, based on interest and location, which makes it proposedly commonly applicable.

To meet the research objective, the following research sub-objectives can be determined:

- development of a structured overview of the current understanding and assessment of occupant thermal comfort during extreme heat events;
- In-depth analysis of sufficient indicators quantifying the thermal resilience performance of façades during heat waves;
- Improvement of existing methodologies assessing facades' thermal resilience during extreme heat events by introducing advancements in terms of comprehensiveness of resilience indication and inclusion of future weather data;
- Determining limitations of the proposed method by applying the developed procedure to an example case.

1.4 Research question and sub questions

The above-mentioned problem statement and research objectives lead to the following research question:

“How can we evaluate the influence of façades on building thermal resilience during heat waves?”

The thesis as well as the literature review is divided into three focus topics: “thermal comfort in extreme heat”, “resilience” and “façade design”. To be able to give a scientific response to the research question, the following sub-questions are raised:

1. **“How do future climate-related heat waves change building requirements for façade construction?”**
2. **“How is the influence of façade on building thermal resilience to extreme heat assessed? What are commonly used metrics?”**
3. **“How could current assessment methodologies of building thermal resilience be improved?”**
4. **“What are relevant façade parameters to be considered for retrofitting improving occupants' thermal comfort during extreme heat events?”**
5. **“What are the most important façade parameters influencing resilience indicators?”**

1.5 Methodology

In order to meet the research objectives and to answer the research questions and sub-questions, this thesis is split into five related parts:

Literature review

A first explorative literature review puts the topic of the thesis into a broader context to understand its relevance in the building industry, global society, and climate change consequences. Special attention is put on the definition of temperature extremes, heat waves and their impact on the built environment and its occupants. This also includes thermal comfort under extreme heat conditions. Altogether, the explorative literature review answers the first sub-question.

The second part of the literature review is focused more specifically on the topic of resilience in façade design. Systematically, eleven relevant papers on quantification methods of thermal resilience during extreme weather disruptions are analysed regarding their definition of resilience, their proposed resilience evaluation method and the therewith tested retrofit options. The main objective hereby is the investigation for available methodologies of measuring the resilience of facades to extreme heat, which answers the second sub-question. The consideration of the tested retrofit options, touched upon the fourth research question. The output of the literature review defines the research gap and is generally important input for the further progression of the research.

Definition of resilience indicators

With an additional literature study, resilience indicators are defined: Resilience criteria are translated to resilience indicators with their corresponding resilience indices, with their common calculation methods found in scientific literature. An analysis of the different calculation methods finally concludes on the third sub-question.

Development of building performance methodology

The application of the proposed quantification method requires the definition of a simulation methodology. The proposed framework combines dynamic building performance simulation (EnergyPLUS engine), with the postprocessing of the results in Python, using multiple additional libraries such as Pythermalcomfort (Tartarini & Schiavon, 2020), SALib (Herman & Usher, 2017), Eppy (Santosh, 2022) and NumPy (Harris et al., 2020). It eventually results in the final rating of the outcome, which indicates the most suitable retrofit design for the chosen location, improving the façade's thermal resilience to heat waves.

Evaluation of method

For the evaluation of the method, a case study is introduced. For the location of Munich, the specific meaning of a "heat wave" is defined. Based on that, an EPW weather file is adjusted in such a way that it includes, over the simulation period of 43 days, real weather data from two past heat waves in Munich from 2015. Within Munich, the district "Maxvorstadt" is chosen as one to display common German residential, urban blocks. The base case scenario is set up based on the analysis of the given case study data.

Following the proposed workflow, a sensitivity analysis is conducted. The aim is to identify the most influential façade parameters with the highest impact on the façade's performance in each of the resilience stages. Thus, four design cases describe the best-performing input variations: the best-performing ones per indicator and the one with the assumed best overall performance. To evaluate the hypothesis of the proposed assessment framework, the final rating of the design cases is analysed. Hereupon, the "best" design is materialized.

Finally, with a profound knowledge of the topic, limitations of the research and future research possibilities are pointed out. This concludes the proposed methodology as a valuable decision-making method during the design of retrofits that improve the façade's thermal resilience. Limitations in terms of the proposed performance evaluation method are acknowledged.

1.6 Research outline

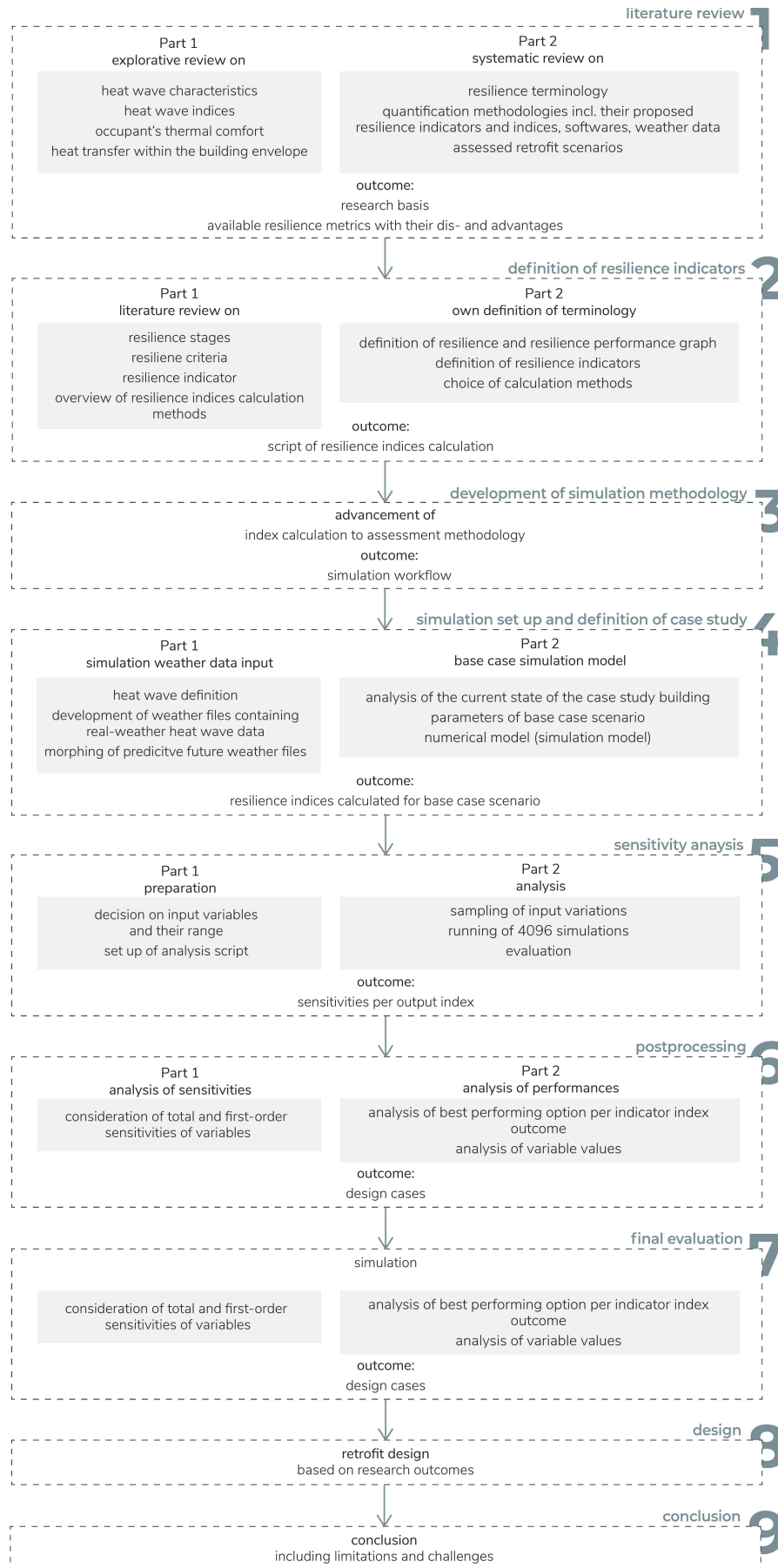


Figure 2: Research outline
source: own



Literature review

- 2.1 Characteristics of extreme heat events
 - 2.1.1 Indices to identify heat waves
 - 2.1.2 Influences of heat waves on occupants
- 2.2 The role of the facade on the improvement of thermal comfort
- 2.3 Definition of resilience
- 2.4 Systematic literature review
 - 2.4.1 Definition of resilient façade and building design
 - 2.4.2 Quantification methods of resilience in façade design
 - 2.4.3 Retrofit strategies for heat wave resilience of facades
- 2.5 Conclusion of literature review

2.1 Characteristics of extreme heat events

With the global temperatures rising, the probability of temperature extremes is increasing (IPCC, 2012). The IPCC claims: “New evidence strengthens the conclusion from the IPCC Special Report on Global Warming of 1.5°C (SR1.5) that even relatively small incremental increases in global warming (+0.5°C) cause statistically significant changes in extremes on the global scale and for large regions (high confidence)” (Seneviratne et al., 2021, p. 1518). Through climate projection models scientists are modelling “scenarios”, assuming different greenhouse gas concentrations, population levels etc. Numerical models describe, analyse and simulate the complex interactions between the Earth’s atmosphere, oceans, and land surface (Paul J. Schramm et al., n.d.). The IPCC climate scenarios are based on the comparison of the output of several climate projection models. The proposed narratives (SSP narratives) sort them in several categories based on realistic storylines addressing driving forces of future greenhouse gas emissions. Four storylines represent disparate future development in terms of the global demographic change, and the economic and technological development. Figure 3a shows the predicted variation in global surface temperature for the SSP1-5 narratives. Obvious is that for all five narratives, the risk and impact of extreme weather events remains within a range of “high” or “very high”, stated with confidence (Fig. 3b).

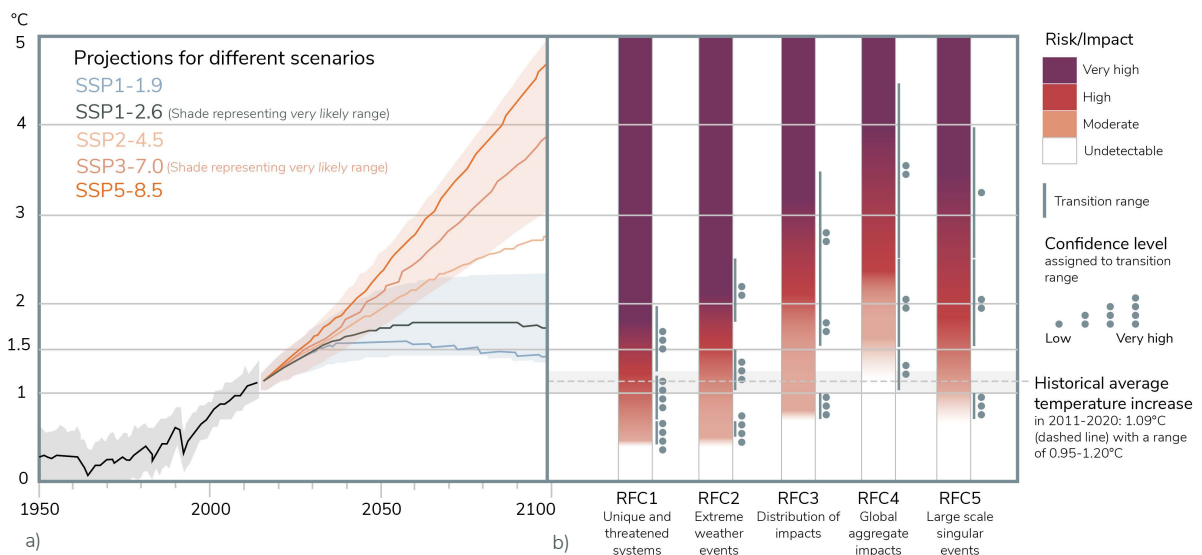


Figure 3: a) Global surface temperature changes in °C relative to the 1850-1900 period, with solid, coloured lines representing predicted increases for IPCC scenarios (SSP1-5). b) Visualization of risk assessment in the Reasons for Concern (RFC) framework, depicting five broad categories of future concerns. Colours represent different risk levels: "Very high" (purple), "High" (red), "Moderate" (orange), and "Undetectable" (white).

adapted from: H.-O. Pörtner et al., 2022, p. 17

Thus, it can be said that extreme weather events are closely related to human-induced greenhouse gas emissions since the pre-industrial time, which counts especially for temperature extremes (Seneviratne et al., 2021). The IPCC demonstrates that “some recent hot extremes would have been extremely unlikely to occur without human influence on the climate system” (Seneviratne et al., 2021, p. 1517).

Temperature extremes are “the occurrence of a value of a weather or climate variable above (or below) a threshold value near the upper (or lower) ends of the range of observed values of the variable” (The Intergovernmental Panel on Climate Change, 2020). Extreme climate is considered as “a pattern of extreme weather that persists for some time, such as a season” (Seneviratne et al., 2021, p. 1522). Extreme weather events, on the other hand, occur rarely, which makes them well-defined in location and time. An extreme weather event might be unique in its strength, which also means that it is often considered a “surprise” (H.-O. Pörtner et al., 2022).

To identify extreme events, it is common to either compare relatives (percentiles) or absolute values. If the assessed value is above or below the described threshold, the event is considered extreme. However, depending on the chosen thresholds, different events can be called 'extreme'. Variables are the comparison values - an event that would have been extreme in the 20th century compared to the average might not be 'extreme' anymore compared to the new 'normal' of the rapidly changing climate.

In case of extreme heat events, the threshold is exceeded either on the bottom average (extreme cold) or the top average (extreme warmth). So-called "heat waves" are generally defined as a period of consecutive days with excessively hotter conditions than normal (Pattenden, 2003; Trigo, 2005). Even though heat waves are commonly associated with summer conditions, heat waves can also occur in other seasons (Perkins & Alexander, 2013).

To summarise, it is important to note that the severity and frequency of heat waves are increased due to human-made climate change. However, special attention needs to be given to the analysis of heat waves: Extreme temperatures are exceeding the local average maximal temperatures significantly, which leads to heat stress on humankind as well as the built environment. The following section explores how to identify heat wave periods.

2.1.1 Indices to identify heat waves

To be able to identify heat waves and measure their impact, heat waves and their extreme heat indices need to be defined. However, those depend strongly on the geographical location due to the variance in response to extreme heat (Meehl & Tebaldi, 2004). Additionally, indices also vary based on the field of study: Heat waves are having a significant impact on various natural and human-made systems, and the range of the focus of the study, e.g., agriculture, human health, electricity, general infrastructure, etc. puts attention on certain kinds of impacts. Therefore, different variations of metrics are used, which makes them depend on location and purpose. It is noted that different studies considering heat waves and their impacts might have different outcomes, depending on the metrics chosen. There is not one established for all purposes. Several indices are proposed, that can be adjusted.

The following sections will first introduce various possible heat wave indicators. While the author is aware that "extreme temperatures" can describe temperature highs as well as temperature lows, this thesis will from now solely focus on the heat extremes.

In general, heat waves differ in terms of **frequency**, **duration** and **magnitude** (Perkins & Alexander, 2013). Each heat wave definition, therefore, consists of an assessment method to quantify **one** or **multiple** of those aspects, depending again on the focus of the study.

To assess the **frequency** and **magnitude** of occurring heat waves, the most commonly used indices are based on either **fixed** or **relative** thresholds. Fixed (absolute) thresholds are based on the exceedances of a set value. However, the exact threshold value is strongly dependent on local climate conditions, which makes it not relevant for research including various locations or comparisons. Therefore, fixed thresholds do have the advantage of being easier received also from the non-scientific audience, but are not applicable for studies ranging over larger areas e.g., with locations in different climate zones (Koffi & Koffi, 2008). Relative (percentile) thresholds have been introduced to define heat waves with respect to predominant local climate conditions. Larger data sets of the prevailing climatic conditions of one location are being analysed, which finally regulates the threshold. Hence, within a study of a larger region, the same definition of a heat wave can be used. Due to the fact that the definition of the threshold is based on the analysis of

prevailing climate conditions, it can be argued that percentile thresholds also include the cultural background of a regional population (Robinson, 2001). As to the IPCC (2001), it is advised to use the 90th percentile threshold as a comparison. The result will sort abnormally high temperatures and gives therefore promising data as a heat wave frequency indication.

The definition of the **duration** of a heat wave varies per research. The most commonly used is a period of **three** (Nairn & Fawcett, 2013) or **six** consecutive days (Fischer & Schär, 2010; Junk et al., 2019; Perkins & Alexander, 2013).

Heat wave indices are then combining the definitions by identifying the heat wave as per the number of days (duration) above a selected threshold (magnitude) or counting the number of heat waves in a selected period (frequency). In summary, it is important to understand what relevant characteristics of a heat wave have an increased impact on the thermal performance of facades.

In addition to the duration, magnitude, and frequency, also the maximum night-time temperatures should be considered as a heat wave indication. Due to the loss of night-time relief, high night-time temperatures during heat waves are having an immense impact on human health (U.S. Environmental Protection Agency, n.d.). Therefore, indices like TN90p, which measures the occurrence of warm nights above the 90th percentile, or the daily minimum temperature should be considered.

As humidity is also an important factor when it comes to how a human body copes with heat, the apparent temperature (T_a) defined as the “heat index” can potentially also be used for a more detailed indication of a heat wave. As a combination of air temperature and relative humidity, it more realistically covers the impact of a heat wave. However, Perkins (2015) argues that those kinds of indices cannot be retrieved directly from climate data and are therefore not being used commonly.

To summarize, there are no general metrics on the identification of heat waves. However, it can be concluded that the **frequency**, **magnitude**, and **intensity** of heat waves as well as **night-time air temperatures** and **humidity** are key factors to be considered.

2.1.2 Influences of heat waves on occupants

Heat waves have a significant impact on humans and human-made systems, as they reach the point, where systems are no longer able to adapt to heat. It is necessary to understand the definition of human thermal comfort and the consequences of thermal discomfort.

Thermal comfort is defined as “that condition of mind that expresses satisfaction with the thermal environment and is assessed by subjective evaluation” (ASHRAE, 2017a, p. 3). The definition highlights that evaluating comfort is a cognitive activity that incorporates numerous factors influenced by physical, physiological, psychological, and other processes (ASHRAE, 2017b). The conscious mind appears to form judgments regarding thermal comfort and discomfort based on direct sensory experiences of temperature and moisture on the skin, internal body temperatures, and the effort required to maintain a stable body temperature (Berglund, 1995; Gagge, 1937; Hardy et al., 1971). Achieving comfort involves consciously or unconsciously initiating behaviours guided by perceptions of temperature and moisture, such as adjusting clothing, changing activities, altering posture or location, adjusting thermostat settings, opening windows, expressing dissatisfaction, or leaving the environment (ASHRAE, 2017b).

Fanger (1970) is one of the first ones to define “thermal comfort” as the conditions where humans have a neutral thermal sensation (neither feeling cold or warm). To keep a body in heat balance, the body

temperature is necessary to be kept within a narrow limit of $\pm 1^{\circ}\text{C}$ at 37°C (while resting). To keep an adequate core temperature, there is often a heat flow between the body and the environment, which depends on the metabolic heat produced by the human body and the heat gained or lost from / to the environment (Epstein & Moran, 2006). Thereby, several physiological responses of the human body maintain the adequate core temperature: in a warm surrounding those are sweating, respiration and vasodilation. When the body is sweating, it loses heat through the sweat's evaporation from the skin surface. Respiration describes the heat exchange with the environment through breathing. With a warmer surrounding, the body allows more blood to flow near the skin (vasodilation), enhancing heat loss through radiation and convection (Gagge et al., 1967; Havenith & Fiala, 2015). Conversely, in a colder surrounding, a body reduces the blood flow near the skin's surface (vasoconstriction). Shivering additionally helps to increase the body's core temperature by increasing metabolic activity (Gagge et al., 1967; Havenith & Fiala, 2015).

In general, to assess the thermal comfort of individuals, the heat balance of the body's heat losses and heat production is evaluated (Havenith & Fiala, 2015). For the in-depth analysis of all factors influencing the heat losses/production of the human body, several drivers of the heat transfers would need to be included (Havenith & Fiala, 2015). Thus, different methods present a simplified methodology, including a selection of relevant factors. One of the most commonly used thermal comfort metrics is the so-called Predicted Mean Vote (PMV) (Fanger, 1970). For the calculation of the PMV six key parameters are taken into consideration: air temperature, mean radiant temperature (MRT), air velocity, humidity, clothing level and metabolic heat production (Fanger, 1970). The thermal sensation ranges from "-3" as "cold", to "0", as "neutral" and "+3" as "hot". On the bases of the PMV, the Predicted Percentage of Dissatisfied (PPD) people can be derived, which gives information about the assumed percentage of people that are in thermal dis-/satisfaction within a space.

It has been realized that as soon as occupants would find themselves in a "discomfort" situation, they would start actively seeking improvement of the thermal situation (Parsons, 2002). The Adaptive thermal comfort model (ACM), described by ASHRAE (2017a) includes typical human responses to warm/cold sensations like adapting the clothing level, the opening/closing of windows, etc. and is specifically recommended when designing for naturally ventilated, free-running conditions.

There is however a significant difference between thermal discomfort and heat stress. While the physiological response of the human body can maintain the heat balance during thermal discomfort, in heat stress, the body is not able to keep the balance (Holmes et al., 2016). The body temperature is continuously increasing. When the 'core' temperature is higher than 38°C - 39°C , the human body might collapse – at 41°C a heat stroke is very likely (Parsons, 2002).

In heat wave periods, the adaptive thermal comfort model might be more accurate than traditional thermal comfort models, which are purely considering the physiological response. However, the heat stress on occupants can be extreme and out of discomfort/overheating conditions of common thermal comfort regulations. Thus, it can be said that current standards do not include recommendations on building design considering heat waves and the risk for occupants. For example, the guide of the Chartered Institution of Building Services Engineers (CIBSE) for overheating in European buildings (2013) defines the overheating risk of buildings based on the hours of exceedance of a threshold derived from a simulation using weather data from a design summer year (DSY) (Nicol, 2013). As DSY only represents warm, but not extreme summer conditions, it is not appropriate when investigating thermal comfort in extreme periods.

As Homaei and Hamdy (2021b) point out, when investigating thermal comfort during heat waves, it is also important to consider the temporal aspect of the disruptive event. At the start of the heat wave, indoor

temperatures are constantly increasing, which, due to the pessimistic state of mind of the occupants, worsens the thermal comfort compared to the objective assumption. When the conditions are improving again, occupants think more positively about the situation. This also boosts the enhancement of their thermal comfort condition.

2.2 The role of the facade on the improvement of thermal comfort

Three main types of heat transfer can be identified between the indoor environment and the façade: long-wave radiation from warm or cold façade surfaces, the transmission of short-term solar radiation through glazed areas and convection due to incoming air flows and air temperature differences (Huizenga et al., 2006). More specifically, opaque enclosure parts influence thermal comfort through mainly conduction but also by convection within wall and roof cavities. Whereas transparent and translucent façade elements influence thermal comfort by incoming short-term solar radiation, and, especially after sunset by convective and conductive heat flows. The in- and outflow of air through leakages, ventilation and openings influence thermal comfort through convection (Ted Kesik & Liam O'Brien, 2019).

Conduction

Thermal conduction describes the thermal energy transfer at atomic level. On façade level, conduction occurs within a wall and its components, but also between the wall and the surrounding air (indoors and outdoors). The flow of heat through materials from higher to lower kinetic energy depends on the material of the façade component, including its thermal conductivity, its thickness, the area, and the temperature difference between out- and indoors. Therefore, the conduction heat flow of a building envelope is strongly connected to its **thermal conductance**, which is described by the so-called **U-value** and its reciprocal, the **R-value** (Linden et al., 2013). While **thermal conductivity** describes how well a material can transfer heat, the property of the “**specific heat**” captures the amount of energy needed to create a temperature change of 1 degree Celsius within the material. This makes the specific heat of a material a critical characteristic of the façade regarding its influence of conductive heat flow on occupant thermal comfort (Luna Navarro et al., 2021).

Convection

Convection describes the heat transfer between a solid and a fluid (liquid or gas) or also between fluids (Ted Kesik & Liam O'Brien, 2019). The energy is transferred as the fluid (e.g., air) is in brief contact with the heat source. Within the building envelope, this plays an important role at the outside and inside surface or within a cavity: because of the increased speed of the outside wind, the convection heat flow is larger outside, however, also indoors, the convective heat transfer depends on the air speed and the surface temperature, and therefore also on the indoor ventilation system (Linden et al., 2013). Convective heat transfer therefore largely depends on the **air tightness** in regard to incoming cool or warm air (Luna Navarro et al., 2021; Ted Kesik & Liam O'Brien, 2019). Hereby, also the temperature difference between the exterior and the interior environment is important, as higher differences lead to higher pressure and thus to an increased convective heat flow through gaps etc.

Radiation

Radiative heat flow describes the continuous heat transfer between colder and warmer objects. All objects are emitting electromagnetic radiation and absorb energy from other objects (Linden et al., 2013). This emission, however, can differ in wavelengths, which makes the sun the largest emitter of short-wave radiation, and most of the colder objects long-wave emitters (Ted Kesik & Liam O'Brien, 2019). In relation

to façade characteristics, radiative heat flows are especially important for glazed surfaces for the incoming directly long-wave solar radiation gain (Luna Navarro et al., 2021). Indirectly emitted gain is first absorbed by the opaque construction parts and then reemitted into the indoor space in short-wave radiation (Designing Buildings Ltd., 2022). Also, notably warm, or cold surfaces should be considered, as those influence thermal comfort when being in ultimate proximity. Therefore, it can be said that in terms of radiative heat transfer, the **solar heat gain coefficient (g-value)** and the **type of glazing** are the most crucial façade characteristics (Ted Kesik & Liam O'Brien, 2019). The g-value measures the ability of glazing or window elements to transmit solar radiation into the indoor space. Thus, a lower g-value means that a lesser percentage of heat is transmitted. Whereas the type of glazing describes the glazing's properties including its materials and potential coatings. Those influence the amount of solar radiation absorbed, reflected, or transmitted.

2.3 Definition of resilience

The term resilience as defined by Britannica is “the ability to become strong, healthy, or successful again after something bad happens”, but also “the ability of something to return to its original shape after it has been pulled, stretched, pressed, bent, etc.” (Encyclopædia Britannica, n.d.). While one definition is related to human psychology, the other one shows a connection to material characteristics. Indeed, “resilience” is a term used in various professions and situations. Thus, it is important to understand its exact meaning and its origin.

In the mid-19th century, Charles Darwin has been the first one to describe “resilience” in his work “On the Origin of Species”, which published his research on the evolutionary science of species (Simon Levin, 2013). In the 1970s and onwards, “resilience” has then been becoming an important term in the ecological sciences, primarily connected to ecosystem and species population-related studies (Patterson et al., 2017). Holling (1996) then made the distinction between engineering and ecological resilience, while discussing them in terms of their aspects on equilibria. These definitions are still valid and are now drawing the line between different definitions of resilience.

The “**engineering resilience**” is a concept focused on one equilibrium, the resistance to a disturbing factor and in case of disturbance, the speed in return to the equilibrium state (Holling, 1996). Resilience concepts within various disciplines are based on the “engineering resilience” e.g., physics, economics, psychology, and sociology.

The “**ecological resilience**” is seeing a system without one specific equilibrium, but with various “stability states” (Holling, 1973). Instabilities and disruptions can trigger the change to another state. Therefore, the focus hereby is on the magnitude of disruption and absorption capacity until the system is forced to change.

Other terms, like “**evolutionary resilience**”, have been defined, which put emphasis on the fact that a system can “evolve” over time and therefore rearrange its configuration (Boschma, 2015; Simmie & Martin, 2010). However, as the “evolutionary resilience” can be seen as a sub-definition of ecological resilience, within this thesis, they are seen as strongly connected, if not the same.

It is important to note that those definitions are vague, thus depending on the statement or research, the definition might get reinterpreted, which might lead to confusion. For example, the term “bounce back”, which is often used while explaining the resilience concept, can be considered as part of the ecological resilience approach (Attia et al., 2021), or on the contrary, it can also be an indicator of the engineering resilience definition (Patterson et al., 2017).

In any case, the term resilience describes the ability of a system to respond to **shocks**. Being vulnerable, the system is **exposed** to “possible, future occurrence(s) of natural or human-induced physical events that may have adverse effects on vulnerable and exposed elements” (Paul J. Schramm et al., n.d., p. 69), called **hazards**. Thus, high **vulnerability** to those hazards (system related), plus high exposure, as the external circumstances of higher hazard risk, lead to a more severe shock. A resilient system however can recover from the shock and return to its original state (the equilibrium).

2.4 Systematic literature review

To improve the thermal resilience conditions of the current state of the art within façade design, an extensive summary of the ongoing research on the topic is necessary. Therefore, a systematic literature review of the topic has been conducted: The search term “TITLE-ABS-KEY ((façade OR “building skin” OR envelope OR building) AND (resilience OR resilient) AND (thermal OR indoor AND comfort))” gave a large output of 199 results. When selecting relevant papers, the focus was given to the professional fields of the built environment, while excluding papers from different fields. From the remaining research papers, those analysing the impact of heat waves on the urban scale have also been excluded, as well as papers not specifically focused on resilience.

It has been first discussed to remove “building” from the search term. However, within the final selection of the reviewed papers, only one paper focuses entirely on the façade level (Patterson, 2022). , the final selection includes the **eleven** most relevant papers. Six of the eleven papers focus their research on resilience in the whole building context (Attia et al., 2021; Lassandro & Di Turi, 2019; Rajput et al., 2022; Schünemann et al., 2022; Sun et al., 2021, 2021) four on the building as well as on the façade level (Homaei & Hamdy, 2021a; Ji et al., 2022; C. Zhang et al., 2021; Zuo et al., 2014), and only one is exclusively focused on resilience on façade level (Patterson, 2022).

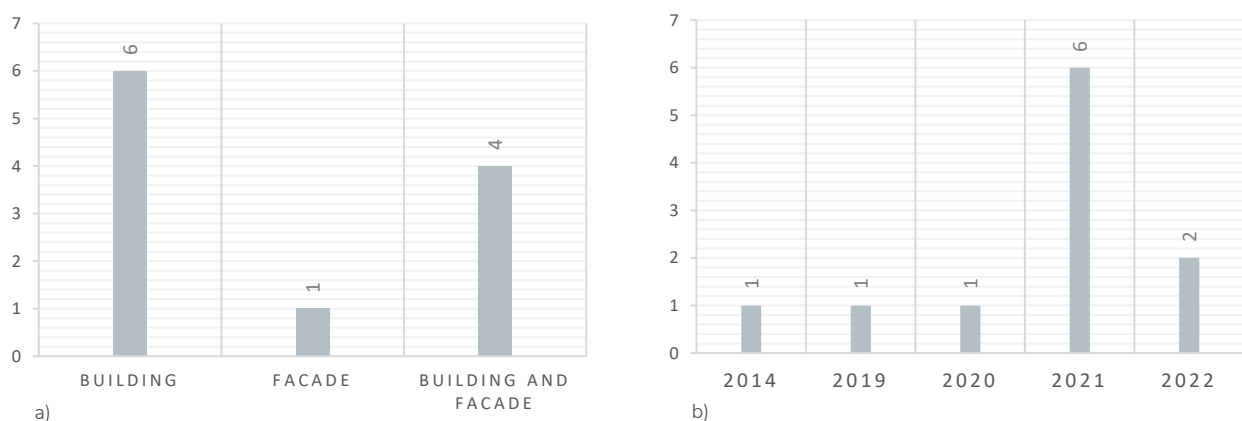


Figure 4: a) The research focus scale of the eleven in-depth reviewed papers
 b) Number of papers published per year
 source: own

The years of publication (Fig. 4b) give a clear indication of the growth of attention on resilience in façade and building/façade design. Since the Paris Agreement in December 2015 (United Nations, n.d.) seven reports of UN sustainability goals have been published, where the UN (UN Department of Economic and Social Affairs, n.d., tit. Goal 11) is specifically calling to “(...) make cities and human settlements inclusive, safe, resilient and sustainable”. A sustainable built environment is therefore directly connected to resilient

cities and buildings. Of the eleven chosen papers, one has been published in 2014, before the Paris Agreement, and ten from afterwards. Even though it is solely a small number of papers, it can be used as an indicator of increased interest in research/industry for resilient solutions in the built environment.

The following describes the results of the literature review: resilience definitions, quantification methods as well as research results of tested retrofit options.

2.4.1 Definition of resilient façade and building design

Each of the reviewed papers is arguing with its own distinct definition of “resilience”. However, when linking them to the corresponding **resilience criteria**, which express the **system's abilities** to meet resilient conditions, the general definition of “resilience” becomes tangible. Based on those, one can define **resilience indicators** (Siu et al., 2023). Thus, the resilience indicators make the building's performance measurable (Attia et al., 2021). This puts special attention on a defined terminology related to resilience performance.

In general, in the conceptual context of discussing resilience definitions, the scale becomes almost negligible, and the scale is referred to as the “system” level.

Given that three of the papers do not emphasize the definition of thermal resilience (Rajput et al., 2022; Sun et al., 2020, 2021), or directly equate resilience with overheating intensity (Schünemann et al., 2022), the focus is on the remaining.

Attia et al. (2021) refer to the official definition of the UN report (2016) of disaster risk reduction and describe resilience as “(...) the ability of a system, community or society exposed to hazards to resist, absorb, accommodate, adapt to, transform and recover from the effects of a hazard in a timely and efficient manner, including through the preservation and restoration of its essential basic structures and functions through risk management”. The paper further distinguishes between four periods of a resilient response: **vulnerability, resistance, robustness, and recoverability**. In general, a system is vulnerable to failure. Thus, vulnerability describes the pre-condition of the system to be sensitive to disruption. Within the disturbance, the pre-failure phase, where the system is still capable of keeping the performance within a certain threshold, is the “resistant period”. Whereas “robustness” describes the reaction of the system post-failure (Fig. 5) (Attia et al., 2021).



Figure 5: The relation of a heat wave's duration and intensity to a resistant, robust, and resilient building's response. The plot surface area is divided into categories of "short/long" and "intensive/extensive" heat waves, with power outages occurring in "short-intensive" and "long-extensive" heat wave scenarios. Orange dots are positioned to represent the assumed intensity and frequency that the corresponding building design can withstand. adapted from: Attia et al., 2021, p. 6

Homaei and Hamdy (2021a) define a resilient system to be “able to prepare for, absorb, adapt to and recover from the disruptive event”. **Preparation, absorption, adaptation, and recovery** are important abilities. Similar defines Ji et al. (2022) resilience: “(...) the capacity of a subject to anticipate, absorb, adapt to and/or rapidly recover from a disruptive event” (Cabinet Office, 2011).

Zhang et al. (2021) in their qualitative review of resilient cooling strategies define the built environment as resilient when “(...) buildings and their systems to continue functioning as intended in the face of natural hazards imposed by climate change” (Alfraidi & Boussabaine, 2015, p. 1). Further, it is distinguished between the **absorptive, adaptive, and restorative capacity** as well as the **recovery speed**. While the absorptive capacity indicates how well the system can withstand failure in the first place, the adaptive capacity describes the system’s ability to change to eventually improve its performance during the current and future disruptive periods. The restorative capacity depicts the ability to reach the performance as before the failure. The recovery speed measures the speed of the restorative process.

For Patterson (2022) resilience is the “(...)capacity to adapt to changing conditions and to maintain or regain functionality and vitality in the face of stress or disturbance. It is the capacity to bounce back after a disturbance or interruption of some sort” (Resilient Design Institute, n.d.). Thus, the focus is on the strong connection between **durability** and **adaptability**; both required abilities to reach resilience. He argues for adaptable, simple systems with increased repair possibilities, reducing the effect of current disruptive events and the ability to respond to future extremes.

Lassandro and Di Turi (2019) define a resilient system as one that “(...) adapts or transforms itself to fit to shocks or changes and to attain new and better-adapted configuration”(Friedland & Gall, 2012; Matthews et al., 2014). They argue: to enhance resilience, the system’s criteria include **reliability, adaptability, and mitigation ability**. The aspect of the reliability also incorporates the aspect of durability, as a system can only be reliable during its whole life cycle under given conditions when it is durable.

The range of proposed resilience criteria is wide; however, similarities can be drawn. Four of the reviewed papers (Attia et al., 2021; Homaei & Hamdy, 2021a; Ji et al., 2022; C. Zhang et al., 2021) define certain resilience criteria per part of the disruptive period; Attia et al. (2021) refer to them as **stages of resilience**. The pre-condition (**vulnerability** (Attia et al., 2021) or **preparation** (Homaei & Hamdy, 2021a)), is followed by the pre-failure stage, where the system’s resilience is defined by its **resistance** (Attia et al., 2021), its **absorption** (Homaei & Hamdy, 2021a) or its **absorptive capacity** (C. Zhang et al., 2021) – all three referring to the ability of the system to withstand the failure. During the failure period, the **robustness** (Attia et al., 2021), the **adaptation** (Homaei & Hamdy, 2021a) and the **adaptive capacity** (C. Zhang et al., 2021) capture the system’s response to the shock of failure – is it able to adapt to the shock conditions? How robust is the system’s performance in shock conditions? Further, the **recoverability** (Attia et al., 2021), the **recovery** (Homaei & Hamdy, 2021a), the **restorative capacity** as well as the **recovery speed** (C. Zhang et al., 2021) describe the system’s ability to get back to pre-shock conditions: in terms of characteristics enhancing the recovery or/and in terms of its speed.

The remaining two papers do not define resilience stages, but emphasize both the importance of **durability** (Patterson, 2022) or related: **reliability** (Lassandro & Di Turi, 2019). Both combine it with the criteria of the system’s **adaptability** (Lassandro & Di Turi, 2019; Patterson, 2022). However, one highlights the self-learning aspect of a system, which should be able to “shift from a normal state to another one, through a dynamic transformation in response to disturbance and mutable conditions” (Lassandro & Di Turi, 2019, p. 2), whereas Patterson (2022) implies the user an active role.

2.4.2 Quantification methods of resilience in façade design

Resilience, even when clearly defined, is due to its abstract character hard to measure. With correlation in terms of resilience indicators found in the reviewed papers, there are large disparities in translating the specified resilience indicators to numerical, comparable indices.

The distinction can be made between qualitative and quantitative proposals: the qualitative methods assess resilience without numeric description, whereas quantitative methods propose a numeric translation from resilience indicators to indices (Fig. 6). While the qualitative proposals (Attia et al., 2021; Patterson et al., 2017; Patterson, 2022; C. Zhang et al., 2021) are interesting in terms of their comprehensive analysis of the terminology, the following discusses in-depth the different proposals on how to quantify numerically resilience of façades during extreme climate events (Homaei & Hamdy, 2021a; Ji et al., 2022; Lassandro & Di Turi, 2019; Rajput et al., 2022; Schünemann et al., 2022; Sun et al., 2020, 2021).

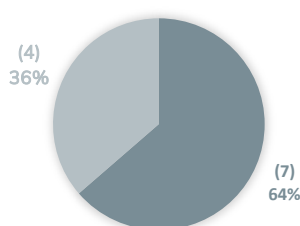


Figure 6: Number of quantitative/qualitative research of the state-of-the-art considered in literature review
source: own

The proposed methods, base their proposal assessing resilience performance on **resilience indices** and/or on **thermal comfort indicators**. While thermal comfort indicators mean common, established thermal comfort metrics, resilience indices can add depth to the same. Thus, each method describes its measurement with chosen thermal comfort metrics but does not necessarily propose a (novel) resilience index.

Table 1: Resilience indices in the state-of-the-art of thermal resilience assessment. The discussed indices include measurements of common thermal comfort indices with additional measurements of the duration and severity of the extreme temperature event. source: own

	Resilience index	Heat index HI	Standard effective temp. SET	Operative temp.	Predicted mean vote PMV	air temp.	duration	severity
Lassandro & Di Turi, 2019	heat response index (HRI)							
Ji et al., 2022	thermal resilience index (TRI) based on weighted unmet thermal performance (WSETH)		x				x	x
Homaei and Hamdy, 2021b	resilience class index (RCI) weighted unmet thermal performance (WUMTP)			x			x	x
Sun et al., 2020	unmet degree hours (UHD)					x	x	x
	heat index hazard hours (HIHH)	x					x	x
	standard effective temperature unmet degree-hours (SETUHD)		x				x	x
	predicted mean vote exceedance hours (PMVEH)				x		x	x

Sun et al., 2021	n.a.	x						
Schünemann et al., 2022	overtemperature degree hours (TDH)					x	x	x
Rajput et al., 2022	n.a.					x		

Six (Homaei & Hamdy, 2021a; Ji et al., 2022; Lassandro & Di Turi, 2019; Rajput et al., 2022; Schünemann et al., 2022; Sun et al., 2020, 2021) of the seven quantitative assessment methods discuss resilience performance based on measurements of the indoor thermal comfort. The seventh measures only outdoor thermal comfort indicators. Thus, the **Response Index to Heat Waves (HRI)** (Lassandro & Di Turi, 2019) will be excluded from further analysis. Based on solely measurements of the exterior operative temperature, surface temperature, etc., the performance of the proposed façade is assessed in terms of its effect on outdoor thermal comfort, which is not of interest within this thesis. However, their method of weighting the parameters regarding the given importance on the individual analysis, improves the importance of the metrics as an improved decision-making process for stakeholders, especially for building policies.

Out of the remaining six papers, three of the reviewed papers (Rajput et al., 2022; Schünemann et al., 2022; Sun et al., 2020) choose for their analysis the measurements of the indoor air temperature. The **overtemperature degree hours (TDH)** (Schünemann et al., 2022) as well as the **unmet degree hours (UHD)** (Sun et al., 2020) both add a temporal layer to it: the indices include the additional measurement of the time and the degree of exceedance above a defined comfort threshold (based on the indoor air temperature).

The **Heat Index (HI)** can also be used as a KPI of thermal resilience (Sun et al., 2020, 2021). As explained in Chapter 2.2.1, the heat index, or “apparent temperature” combines measurements of the air temperature with relative humidity and is used as a simplified description of the perception of a human body in extreme heat (Holmes et al., 2016). Also here, the heat index is either used as the only indicator, or with the addition of the temporal layer, e.g. the **heat index hazard hours (HIHH)** (Sun et al., 2021). After the definition of a threshold, the exceedance hours are counted. Therefore, the index captures more detail in terms of the resulting danger for the occupants.

Homaei and Hamdy’s (2021a) choose for their method the operative temperature. Their proposed index, the **weighted unmet thermal performance (WUMTP)**, additionally includes the time and exceedance referring to four thresholds, dividing the performance into an acceptable, habitable and uninhabitable level. It must be noted that the proposed method is specifically assessing climate cold extremes, which makes only the assessment method of interest in this thesis. The further proceeding is based on the “resilience triangle”, which has its origin in seismic resilience (Bruneau et al. 2003) (Fig. 7b). From the temperature measurements, a resilience performance curve can be drawn. The “phase penalty” then divides the graph into a disruption and in a recovery period. Any measurements in the disruptive period are multiplied by a “heavier” penalty to capture the stronger effect of the extreme temperatures on the occupants due to the assumed pessimistic mental conditions right after the shock. The “hazard penalty” further weights the segments of the measurements in the more uncomfortable levels “heavier”, than those in the acceptable level. When applying the phase penalty, six segments of “easy” and “difficult” sections result. Thus, the total integral is divided into twelve segments, each of them with a different set of penalty values. Applying the penalties to the measurements of the indoor operative temperature over time, the WUMTP in degree hours can be calculated (Homaei & Hamdy, 2021a). The total WUMTP of the whole simulated building can

then be compared to a desired performance level, which further defines the **resilience class index (RCI)** (Homaei & Hamdy, 2021b).

Similarly, using the same penalty values, Ji et al. (Ji et al., 2022) develop their index (Fig. 7a). However, the basis of the resilience performance graph, as well as the thermal comfort metric, is different. The resilience trapezoid (Fig. 8b) adds the extremis between the failure and the recovery period; arguably closer to the actual building performance due to its time to respond. Based on measurements of the indoor **Standard effective temperature (SET)** and the introduced thresholds of $SET_{\text{comfort}} = 24.12^\circ\text{C}$, $SET_{\text{alert}} = 28.12^\circ\text{C}$, $SET_{\text{emergency}} = 32.12^\circ\text{C}$, the **weighted standard effective temperature (WSETH)**, as the sum of the resulting segments incl. penalties, can be calculated. Also here, the final output is the **thermal resilience index (TRI)** for one zone, or equally for the whole building.

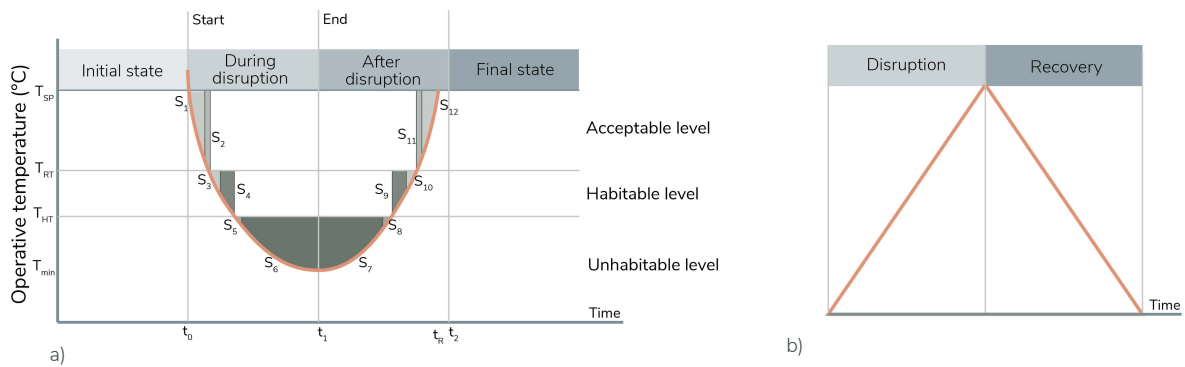


Figure 7: Illustration of the resilience performance graph (a) based on based on the concept of the resilience triangle (b). The heat wave period is divided in the disruption and recovery period, marked by the start and the end of the extreme temperature event (in a) a cold snap). Twelve segments result from the specification of the two disruption periods, three thermal comfort thresholds and the application of penalty values.

a) adapted from: Homaei and Hamdy, 2021, p.5
b) source: own

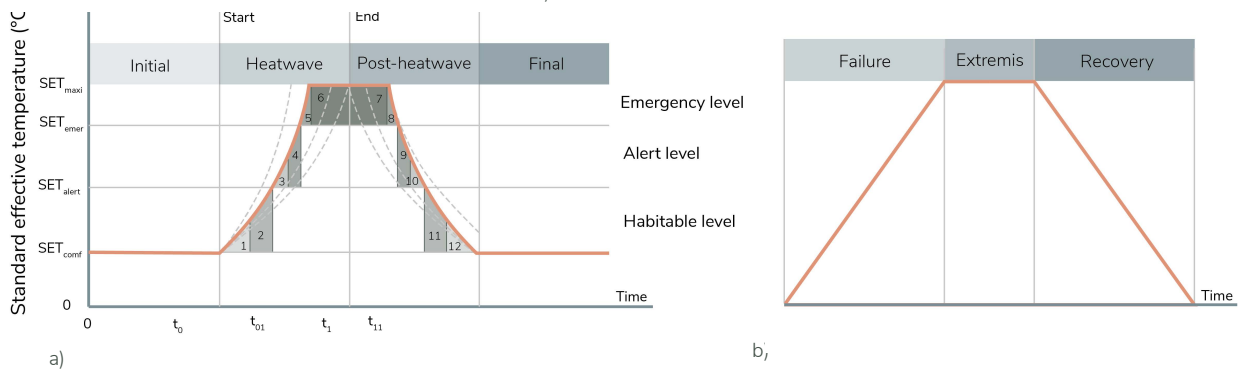


Figure 8: Illustration of the resilience performance graph (a) based on the concept of the resilience trapezoid (b). The trapezoid graph is characterized by the addition of the extremis period, representing the delay during the response to heat wave conditions. Twelve segments result from the specification of the two disruption periods, three thermal comfort thresholds and the application of penalty values. The dashed lines (in a) represent possible trends of real cases.

a) from: Ji et al., 2022, p.3
b) source: own

An overview of the differences between the WUMTP and the WSETH can be found in the Appendix A.

Also, Sun et al. (2021) propose the **SET** as a sufficient thermal comfort indicator during heat waves when including the measurement of the exceedance hours, resulting in the **standard effective temperature unmet degree-hours (SETUHD)**. Accordingly, the **predicted mean vote exceedance hours (PMVEH)** describes the building's performance based on the exceedance of PMV thresholds.

The comparison of the different resilience indices and the thermal comfort indicators (Table 2) shows that the ones measuring only the indoor air temperature include significantly less detail regarding the suitability to depict thermal comfort in extreme heat events than the other ones reviewed. The operative temperature as a simplified measure of occupants' thermal comfort is derived from the mean radiant temperature and air speed. However, as explained by CIBSE (2013), humidity has a lower impact on thermal comfort than expected, however, it is an important factor when both the temperature and the humidity are high. Thus, this makes the air temperature as well as the operative temperature not sufficient as an indicator of thermal comfort during heat waves.

The HI, as an index specifically developed to express heat-related hazard levels for individuals, proves to have the benefit of being a sufficient thermal comfort indicator in different climate zones: the hazard thresholds are based on the response of the human body to temperature and humidity, which changes in different climate conditions.

The PMV and the SET additionally include next to the mean radiant temperature, the air temperature/dry bulb temperature, the relative humidity and the airspeed, also personal factors: the metabolic rate and the clothing insulation, and for the SET also the external work, the body surface area, and the body position. Like this, the SET realistically measures the response of the human body (Y. Zhang et al., 2010) to given temperatures and individual parameters.

Table 2: State-of-the-art thermal comfort metrics and their measurements, divided in environmental and personal factors. source: own

thermal comfort metric				thermal comfort measurements										
				indoor temperature			humidity	velocity	personal factors					
				mean radiant temp.	air temp.	dry bulb temp.	relative humidity	air speed	mean skin temp.	metabolic rate	clothing insulation	external work	body surface area	body position
			PMV	x	x		x	x		x	x			
			operative temp.	x	x			x						
			SET	x		x	x	x		x	x	x	x	x
			HI			x	x							

Seven (WSETH, WUMTP, UHD, HIIH, SETUHD, PMVEH and TDH) out of the eight discussed resilience indicators include another layer of time and severity: The definition of thresholds and the count of time and degree of exceedance adds detail in terms of capturing the building's response to the heat wave as well as the risk for the occupants.

Simulation Software

All seven reviewed papers evaluate their metric by applying it to a chosen case study. As the simulation of the thermal performance requires dynamic thermal modelling, the range of simulation software used is small: Out of the preferred options of IDA ICE or EnergyPLUS, EnergyPLUS has been the more favoured option. Rajput et al. (2022) are additionally using OpenFOAM, ANSYS Fluent or STAR-CCM for Finite Element Modelling as their study requires more detailed modelling of heat transfer, which are divided into nodes (temperatures) and connections (types of heat transfer; airflow).

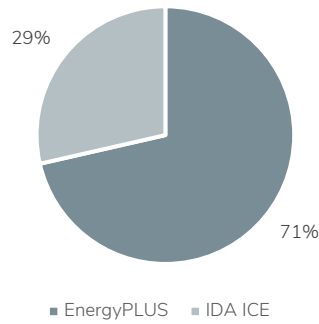


Figure 9: Preferred simulation software of state-of-the-art
source: own

Weather data

For the simulations the type of weather data chosen is important with respect to the analysis of impacts of heat waves: The distinction can be made between the analysis of one specific extreme heat event using specific heat wave data of an **actual meteorological year (AMY)** or using weather data of the predominant weather conditions of the local climate, the so-called **“Typical meteorological year” (TMY)**. Equally, AMY data of one extreme event (Ji et al., 2022; Lassandro & Di Turi, 2019; Sun et al., 2020, 2021) as well as TMY data (Homaei & Hamdy, 2021a; Rajput et al., 2022; Sun et al., 2021) has been found to be used in four of the quantitative studies of the reviewed articles. Focussing on the overheating aspect (Schünemann et al., 2022), and assessing cold extremes (Homaei & Hamdy, 2021b) TMY data has been used. As this makes them less comparable, they have been excluded from the consideration. Therefore, the differentiation becomes clearer, with heatwave-specific data as the more preferred option. Specific data of weather circumstances instead of the predominant year, supposedly tailers the outcome towards the impact of heat waves in general.

Even though it is mentioned as a possible improvement of methodologies (Ji et al., 2022), only Rajput et al. (2022) are using predictive weather data in the form of **“Weather Research and Forecasting” (WRF)** data. The WRF is one of the most commonly used models for climate projection and prediction (Powers et al., 2017). By comparing the results with those done with TMY data of the same location, the research reveals not only insights of the current but also future rating.

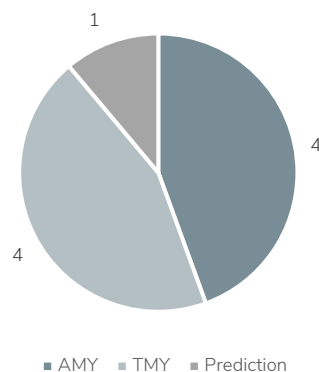


Figure 10: Weather data used in the reviewed state-of-the-art
source: own

Case study location

Since the location with its specific local weather has a large influence on the evaluation of the assessment methodology, it is necessary to also compare the location of the conducted case studies. The different case studies either compare their results in different locations within different climate zones (Homaei & Hamdy, 2021a; Schünemann et al., 2022; Sun et al., 2020, 2021) or evaluate results by locating case studies in different cities within the same climate zone (Lassandro & Di Turi, 2019).



Figure 11: World map with locations of reviewed case studies. source: own

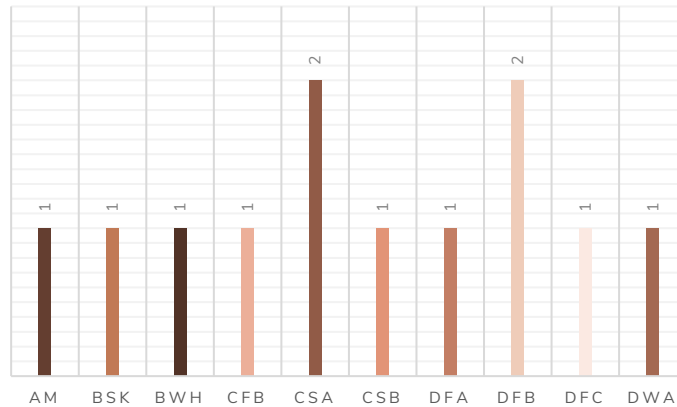


Figure 12: Location of case studies based on Koppen climate classification (in Tropical monsoon climate (Am), Cold semi-arid climate (BSk), Hot desert climate (BWh), Temperate oceanic climate (Cfb), Hot-summer Mediterranean climate (Csa), Warm-summer Mediterranean climate (Csb), Hot-summer humid continental climate (Dfa), Warm-summer humid continental climate (Dfb), Subarctic climate (Dfc), Monsoon-influenced hot-summer humid continental climate (Dwa)) source: own, based on Koppen climate classification

2.4.3 Retrofit strategies for heat wave resilience of facades

As the last part of the review, the selected papers are analysed in terms of their proposed retrofit options. In general, the strategies are almost all focused on the passive building envelope and ventilation measures, however, some papers introduce active measures such as local power generation and thermal storage to cope with power outages during heat waves (Homaei & Hamdy, 2021b; Sun et al., 2020). While the building envelope systems also include investigations of the roof, the envelope measures focusing on the façade have been studied in a separate category.

The improvement potential of separate retrofit strategies in regard to thermal resilience depends on the proposed location as well as on the building conditions and on the combination with other measures (C. Zhang et al., 2021). It is important to note that seven (Attia et al., 2021; Ji et al., 2022; Schünemann et al., 2022; Sun et al., 2020, 2021; Y. Zhang et al., 2010; Zuo et al., 2014) out of eleven reviewed papers conclude their case study with a combination of different measures as the most effective option. The combination of the reduction of solar gain in the form of external shading and natural ventilation (day- and night-time ventilation) has been highlighted as the most promising option (Ji et al., 2022; Schünemann et al., 2022; Sun et al., 2020, 2021).

To further understand the selection specifically of the façade retrofit options, an overview of all mentioned façade measures is made (Table 3): Besides external and internal shading strategies, the proposed glazing retrofits are diverse: to reduce the solar gain, low-E coating (Sun et al., 2021; C. Zhang et al., 2021; Zuo et al., 2014), the reduction of the glazed area (Zuo et al., 2014) and low-cost aluminium shielding (Sun et al., 2020) has been suggested as test measures. While those measures are primarily connected to the g-value, Sun et al. (2021) specifically mention the reduction of the thermal transmittance of the glazing.

Evaluating the impact of external or internal insulation, the results show the beneficial impact of added external wall insulation (Schünemann et al., 2022; Sun et al., 2020; Zuo et al., 2014). Depending on the climate however, added internal insulation might act counteractive for the thermal comfort performance of buildings during heat waves: the Schünemann et al.'s (2022) results of an overheating risk twice as high (in Berlin, Germany) with internal instead of external insulation can be explained through the fact that applying internal insulation to the exterior wall, reduces its heat storage capacity and lets it loose its potential to work as a buffer for incoming solar radiation. To evaluate the retrofit option of added insulation, externally or internally, should however be discussed critically, as the retrofit of the whole exterior wall is one of the more expensive options (Sun et al., 2020).

Other important tested measures include the increase in thermal mass (Rajput et al., 2022; Schünemann et al., 2022; C. Zhang et al., 2021). According to Schünemann et al. (2022), the impact of increased thermal mass is not within the most relevant strategies. With the location on the south façade including shading (Rajput et al., 2022) or by adding Phase Change Materials (PCMs) (C. Zhang et al., 2021), the effect could be improved.

Four papers assess an increase of the albedo value: either of the external façade wall (Sun et al., 2021), through the use of reflective cool materials (Lassandro & Di Turi, 2019; C. Zhang et al., 2021) or through the shielding of windows with aluminium foil (Sun et al., 2020). The increase of the façade and glazing albedo has a positive effect on indoor thermal comfort during heatwaves (Sun et al., 2020, 2021; C. Zhang et al., 2021). However, Lassandro and Di Turi (2019) emphasize a negative effect on the Mean Radiative Temperature and therefore on the thermal comfort of pedestrians.

Green facades as well as ventilated facades could contribute to an improvement of thermal resilience during HWs (Lassandro & Di Turi, 2019; C. Zhang et al., 2021), whereas the reduction of air infiltration, has a negative effect (Sun et al., 2020).

Table 3: Tested facade retrofit options of the state-of-the-art: measures are divided into measures related to façade elements, ventilation strategies, and remaining other measures. Per reference the most effective measures are highlighted. source: own

reference	assessed facade measures	assessed ventilation measures	assessed other measures	most effective measures
Lassandro & Di Turi, 2019	cool materials green facade		green roof	green facade
Zhang et al., 2021	external shading low-e glazing cool materials green facades ventilated facade thermal mass including PCMs	ventilative cooling adiabatic/evaporative cooling compression refrigeration absorption refrigeration including desiccant cooling ground source cooling high-temperature cooling system: radiant cooling	sky radiative cooling personal comfort systems dehumidification	combination
Ji et al., 2022	exterior shading	night ventilation natural ventilation	green roof	external shading + natural ventilation + green roof + night ventilation
Attia et al., 2021	n.a.	n.a.	n.a.	combination of active and passive measures
Homaei and Hamdy, 2021b	n.a.	n.a.	passive desing standard application of batteries implementation of PV system	n.a.
Zuo et al., 2014	insulation reduction window area	n.a.	roof insulation "cool retreats" as areas of the house staying comparatively cool during a heat wave period adjusted occupancy schedule	insulation + reduction of window area + adjusted occupancy schedule
Sun et al., 2020	shading increasing exterior surface reflectance glazing reduced U-value glazing reduced g-value	natural ventilation	roof insulation	window film + natural ventilation
Sun et al., 2021	shielding of windows with aluminum foil reduction of infiltration added insulation low-e glazing shading (overhang)	Natural ventilation	Reduction internal loads cool roof coating shielding of roof with aluminum foil added roof insulation local power generation and thermal storage	natural ventilation+ shielding of windows natural ventilation + reduction of internal heat loads
Schünemann et al., 2022	external insulation internal insulation thermal mass insect screens shading systems sun protection glazing reduction U-value	natural ventilation		ventilation nighttime ventilation plus external shading
Patterson, 2022	n.a.	n.a.	n.a.	n.a.
Rajput et al., 2022	thermal mass	n.a.	n.a.	n.a.

2.5 Conclusion of literature review

Concluding on the first findings of the literature review regarding the characteristics of extreme heat events, it must be said that the most important indication of heat waves are their frequency, magnitude, and duration. Based on absolute or relative thresholds, a period of three or six consecutive days of extreme heat can thus be defined. Most of the time, those indications are based on the air temperature. Depending on the purpose of analysis, the level of detail in terms of the analysis of the hazard, and the study's location, the humidity or the night-time temperature can also be considered.

Further, it is found that for the assessment of thermal comfort during heat waves, the common metrics are not applicable, or would need to be adjusted. Where now only thermal discomfort is assessed, the heat stress during heat waves seems to not be considered.

Certainly, the façade can be identified as one of the main influencers on the occupant's thermal comfort during heat waves: the conductive, convective, and radiative heat flows from the exterior environment are regulated by the wall's properties. Thus, especially, the thermal conductivity and the specific heat and the infiltration of the wall construction, as well as the solar heat gain coefficient and the thermal transmittance of the transparent surfaces can be identified to have a strong impact on the indoor thermal comfort during heat waves.

To reduce the risk for occupants and improve the façade's performance during the disruption periods, the concept of "resilience" can be applied. It includes the reduction of the system's vulnerability and possibly the exposure to heat waves, to improve the system's response during the shock event.

To understand further how the concept of resilience has been applied and evaluated in façade design, eleven recent papers have been reviewed. Their definition used for thermal resilience including the connected resilience criteria, their proposed methods for evaluation including proposed resilience indices, their thermal comfort indicators, the simulation software, weather data, case study location and finally tested façade retrofit solutions have been analysed.

From the literature review, it can be concluded that there is a missing link between the comprehensive definition of resilience criteria and their quantification in the shape of resilience indices. Four papers (Attia et al., 2021; Homaei & Hamdy, 2021a; Ji et al., 2022; C. Zhang et al., 2021) define multiple stages of resilience, out of which only two (Homaei & Hamdy, 2021a; Ji et al., 2022) develop their resilience indices. However, the TRI and RCI do not clearly relate to all of them and are thus not able to capture the defined criteria: E.g., Homaei & Hamdy define their resilience criteria as preparation, absorption, adaptation, and recovery. The WUMTP yet only implies the absorption and arguably also the adaptation. However, the preparation and the recovery are not captured in the index.


Additionally, only the HRI (Lassandro & Di Turi, 2019) enables the weighting of the included parameters. This adds importance to the index as a commonly applicable, adaptable index, but only for exterior thermal comfort in extreme heat.

When discussing the thermal comfort indicators used in the proposed methodologies, it can be concluded that the SET is used to derive two out of the eight discussed indices: the WSETH (Ji et al., 2022) and the SETUHD (Sun et al., 2020). It proves to be a sufficient metric to be used for the assessment of the effect of façades on the thermal comfort of occupants during heat waves. The index reflects a realistic response of the human body to temperatures, with a high level of detail in measurements including personal factors.

When it comes to the appropriate weather data, the importance of future climate on the thermal resilience of facades is inarguable. However, only one of the reviewed papers is including prediction weather data in their simulation (Rajput et al., 2022).

The review of the case study locations of the chosen papers gave an even result. There is further no correlation to be found between the climate data, the KPIs used, and the location chosen. However, it is striking that both Homaei and Hamdy (2021b) and Ji et al. (2022) are locating their case study in the Warm-summer humid continental climate zone (Dfb), which is identified by a cold, continental winter and warm summer, thus by large seasonal differences. The assumption can be made that the proposed retrofit options should give appropriate performance not only during heat waves but also in winter. Since none of the two authors is reasoning their choice of the location of their case study, the assumption is however not confirmed.

It has been found that in most of the studies, the largest improvement of thermal resilience was reached by combining different measures. It includes the variation of external sun shading and natural day- and/or night-time ventilation (Ji et al., 2022; Schünemann et al., 2022; Sun et al., 2020, 2021). While considering only proposed façade related retrofits, internal and external shading options and interventions which focus on the glazing (low-e coating, reduction of glazed area, reduction of U-value and shielding) have been giving positive results in terms of improved thermal resilience throughout the majority of the reviewed papers (Ji et al., 2022; Schünemann et al., 2022; Sun et al., 2020, 2021; C. Zhang et al., 2021; Zuo et al., 2014). The increase of the albedo of the exterior surface of the façade or the glazing can be considered an effective method (Sun et al., 2020, 2021; C. Zhang et al., 2021). The most controversial options are those of increased thermal mass (Rajput et al., 2022; Schünemann et al., 2022; C. Zhang et al., 2021) as well as added external or internal wall insulation (Schünemann et al., 2022; Sun et al., 2020; Zuo et al., 2014).



Definition of resilience indicators

- 3.1 Development of a Future Resilience Index
 - 3.1.1 Definition of resilience indicators
 - 3.1.2 Calculation of resilience indicators
- 3.2 The final index

3.1 Development of a Future Resilience Index

The literature study showed that a commonly used resilience metric for the thermal performance of buildings during heat wave events is non-existent. Proposed resilience criteria and identified indicators, put attention on different aspects of resilience in building and façade design. Establishing an assessment method for resilience in building design is complex, also due to the fact that resilience can be described as a “process that involves several elements” (Attia et al., 2021, p. 3). It draws attention to the fact that (thermal/seismic/etc.) resilience is not only one single property of a building but more an interconnected system of time-dependent characteristics. Even though research defines related, consecutive resilience indicators for the identification of the building’s abilities to enhance thermal resilience (Attia et al., 2021; Homaei & Hamdy, 2021a; Ji et al., 2022; Y. Zhang et al., 2010), they are not translated into suitable quantification methods: the described approaches assess only a fraction of their previously defined criteria (Homaei & Hamdy, 2021a; Ji et al., 2022; Rajput et al., 2022; Schünemann et al., 2022; Sun et al., 2021). Thus, the depth of the analysis of resilience criteria is lost. A “multi-levelled” index would proposedly add adaptability to the index, with the possibility to change it individually depending on the user’s interest and the local climate conditions.

The following describes the development of a novel thermal resilience index for the effect of retrofit options on indoor thermal comfort during heat waves. Based on the building’s resilience stages in regard to the hazard of heat waves, corresponding resilience criteria can be identified. Thereupon, four measurable indicators can be established, which altogether result in the “Future Resilience Index”.

3.1.1 Definition of resilience indicators

Based on the reviewed literature, a resilience performance graph for occupant thermal comfort during heat waves can be drawn. The defined resilience stages are adapted from Attia et al. (2021) (Fig. 13).

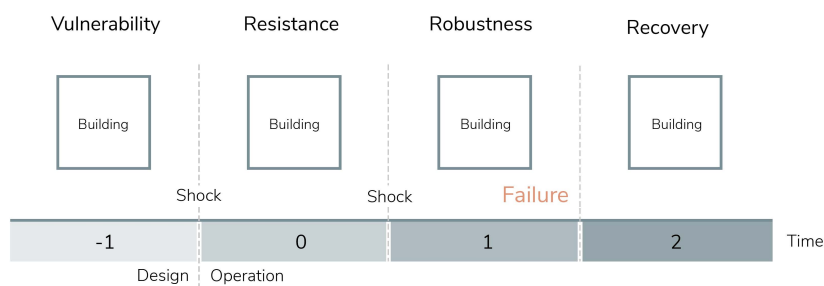


Figure 13: Stages of the resilience process during the design and operational period of a building
source: Attia et al., 2021

“Vulnerability” as the building’s ability to react to different kinds of shocks, describes the pre-shock condition. The performance is not yet influenced. On the one hand, it can be seen as the base condition or even as a necessity to be sensitive to shock and failure (Attia et al., 2021); but on the other hand as the “flip side” of resilience (Folke et al., 2002). In both cases, the vulnerability cannot directly be translated to a measurable index but is based on the analysis of the current building conditions and its exposure to heat waves as the hazard. Thus, that is the reason why the vulnerability is not included.

But another stage has been identified to be important: the “preparation”. It has been found to be essential for a resilient design to be prepared for foreseeable and unforeseeable circumstances (Attia et al., 2021; Homaei & Hamdy, 2021a; Lassandro & Di Turi, 2019; Patterson, 2022). Hence, the preparational stage

describes the period after a disruption and its recovery, where, based on past losses, the system can adapt to or be adapted to short- and long-term prediction scenarios. It captures the important resilience characteristic of enhancing “future-proof” design.

The resulting resilience performance graph can be drawn like this:

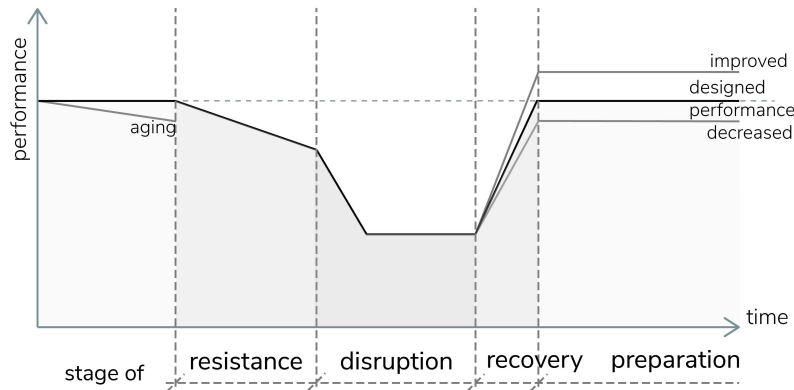


Figure 14: Resilience performance graph with identified stages of resilience. Performance influenced by aging and impact of disruption (heat wave event). After disruptive event performance might reach level above or below designed performance (depending on the response during the disruptive event)
source: own; adapted from Attia et al., 2021

When properly illustrated, the resilience process is cyclic (Attia et al., 2021), representing the iterative effect of heat waves on the building performance: While the preparation is the end stage of one, it is the start of another disruption.

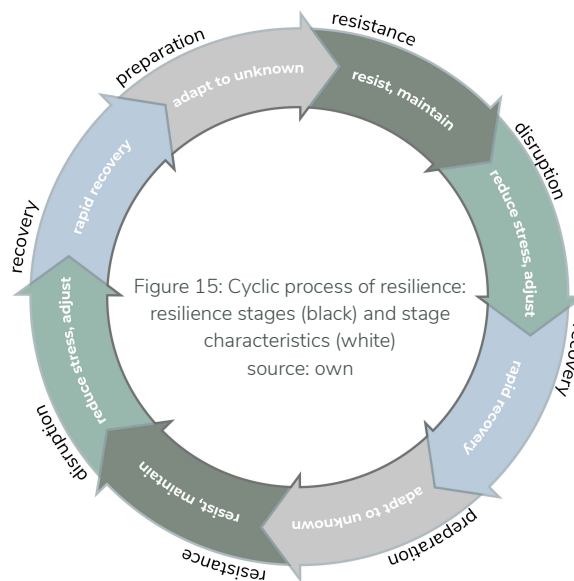


Figure 15: Cyclic process of resilience: resilience stages (black) and stage characteristics (white)
source: own

Further, each stage can be associated with one or multiple **resilience criteria**: abilities, which are necessary to achieve resilience in a certain stage. For the stage of resistance this means to keep the performance within a range of non-disruptive conditions: to **maintain** an acceptable level and to **resist** the shock. Robustness describes the ability to **adjust** performance-influencing parameters, such as the building itself, building services and occupants, during shock conditions to **reduce stress** and the **severity** of the failure (Attia et al., 2021). After the disruptive peak, the system’s ability to **rapidly** reach **pre-shock conditions** and thus the **restoration** of the **equilibrium** is important (Attia et al., 2021; Homaei & Hamdy, 2021a). During the **preparation** period, the focus is on how the building, the façade and the occupants respond to the past disruption: how it adjusts/is being adjusted considering the current performance and future scenarios. It describes the ability to maintain functionality in current climate conditions and in unpredictable future scenarios (Lassandro & Di Turi, 2019).

Finally, based on those criteria, four indicators can be defined (Fig. 16): **resistance**, **robustness**, **recoverability**, and **adaptive capacity**.

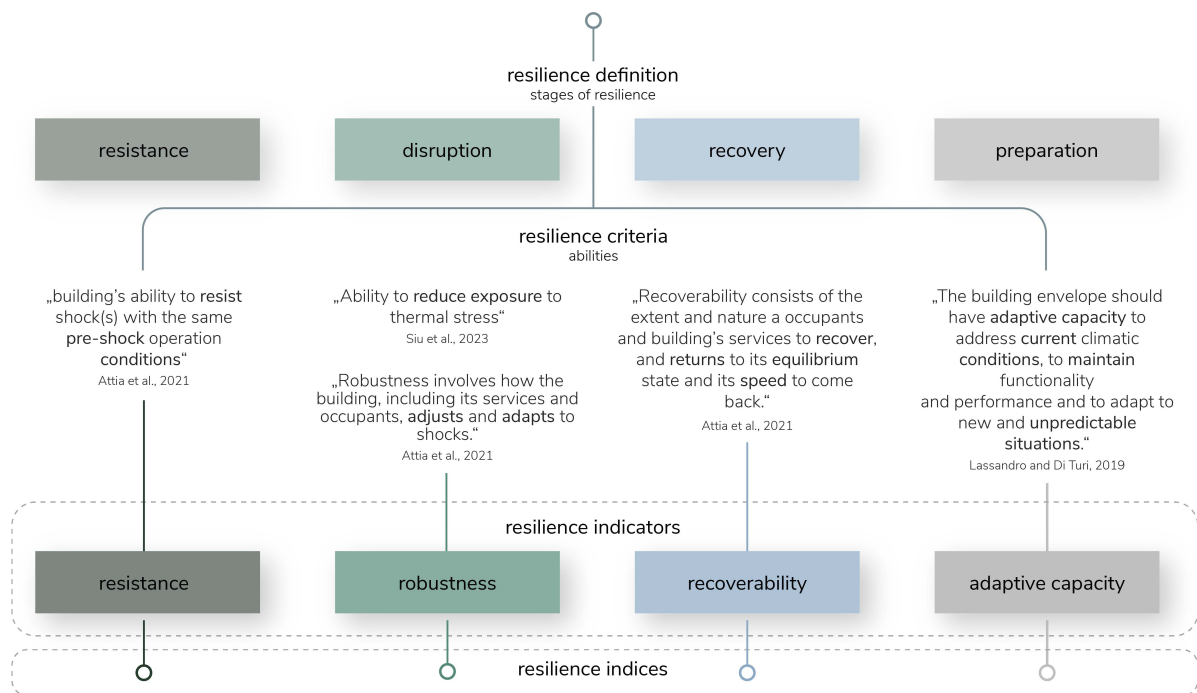


Figure 16: Relation within resilience terminology: The four stages of a resilient response are linked to resilience criteria, which define specific resilience indicators. These indicators can be quantified using resilience indices. This approach enables the quantitative measurement of "resilience," providing a means to assess and evaluate resilience in a numerical manner. source: own

One could argue that the separated abilities are interconnected. E.g., the ability to recover back to comfortable conditions might be possibly improved as soon as the system has an improved resistance, which results in a better starting condition (better performance at the start of the heat wave). However, this remains to be proven. First, it is interesting to see how different façade measures would influence the defined indicators and the overall resilience performance. But how are they calculated?

3.1.2 Calculation of resilience indicators

Resistance, robustness and recoverability are common indicators, used in previous work (Homaei & Hamdy, 2021b; Ji et al., 2022; O'Brien & Bennet, 2016; Sun et al., 2020, 2021; White & Wright, 2020). When sorting their calculation methods per indicator, example indices can be found (Siu et al., 2023) (see Fig. 17). However, note, the categorization is only based on the expressed indicators, and not on the chosen thermal comfort metric. The focus hereby is on the calculation method, whereas the choice of the thermal comfort metric is based on the outcomes of the literature review. The following discusses the findings and concludes on suitable calculation methods per indicator.

Thermal comfort metric and threshold definition

As discussed in Chapter 2.4.2, the standard effective temperature (SET) is the most suitable thermal comfort metric to be used for the analysis of indoor thermal comfort in extreme heat conditions. Thus, the calculation of each of the indicators is based on the hourly data of the SET. The comfort thresholds are defined based on the ASHRAE 7-point scale (ASHRAE, 2017a): PTS = 0 results in a comfortable SET of 24.12°C (habitable level); PTS = 1, sets the alert threshold to a SET of 28.12°C (heat alert level), with the emergency threshold at 32.12°C (emergency level) accordingly (Ji et al., 2022). The habitable level with a comfortable temperature of SET = 24.12°C is used throughout the calculations as a reference threshold.

		robustness			recoverability	
category	time of exceedance	maximal level of thermal stress	time integral of exposure	weighted time integral of exposure	recovery time	
description	Time of exceedance of a critical level of thermal stress	Maximum level of thermal stress reached	Integral of unmet hours: covers magnitude and time of exceedance of thermal stress thresholds	Time integral of exposure including factors to weigh certain stages of exceedance	Time to return to an acceptable/comfortable level after disruptive event	
examples	<p>heat index hazard hours (HIHH): number of hours between first and last moment of exceedance of thermal comfort thresholds: HI 27°C (caution), HI 39°C (danger) for vulnerable people</p> <p>predicted mean vote exceedance hours (PMVEH): number of hours between first and last moment of exceedance of thermal comfort thresholds: PMV 0.7 (grid-on) PMV 3 (grid-off)</p> <p>Sun et al., 2021</p>	<p>Maximum indoor air temperature as a comparison for different simulation results</p> <p>Rajput et al., 2021</p> <p>Maximum Heat Index as a comparison for different simulation results</p> <p>Sun et al., 2020</p>	<p>Unmet degree-hours (UDH): time integral between first and last moment above thermal comfort threshold; threshold based on indoor cooling setpoint in grid-on and grid-off scenarios</p> <p>Standard effective temperature unmet degree-hours (SETUDH): time integral between first and last moment above thermal comfort threshold; SET 28°C (grid-on) SET 30°C (grid-off)</p> <p>Sun et al., 2021</p> <p>Maximum Heat Index as a comparison for different simulation results</p> <p>Sun et al., 2020</p>	<p>Weighted standard effective temperature (WSETH): weighted (based on penalty values) time integral between first and last moment above thermal comfort threshold; SET 24.12°C comfortable</p> <p>SET 28.12°C alert</p> <p>SET 32.12°C emergency</p> <p>Weighted unmet thermal performance (WUMTP): weighted (based on penalty values) time integral between first and last moment above thermal comfort threshold; threshold based on operative temperature (values not applicable as applied to cold snap)</p> <p>Sun et al., 2021</p>	<p>Recovery time (hr) – Time to return to normal state</p> <p>Homaei and Hamdy, 2021</p>	
resistance						
category	adaptive capacity			time until failure	increase of discomfort	
description	Difference of resilience indicators in current and future conditions (ability to adapt and respond)			Passive/active survivability before critical temperature is reached	Temperature at time stamps as indicator how fast discomfort is reached	
				Passive survivability: number of hours before critical temperature is reached	measured temperatures at defined time stamps compared to thermal comfort levels	White and Wright, 2020
						O'Brien and Bennet, 2016

Figure 17: Resilience indices categorized with example calculation methods source: own

Resistance

For the resistance indicator, one could measure the “active/passive survivability”: the time until failure is reached or until the defined critical level is passed with/without considering mechanical cooling/heating (O'Brien & Bennet, 2016). The measurement of the thermal comfort indicator at defined time stamps can also be used as comparable values for a system's resistance (White & Wright, 2020).

To measure the time until failure requires the definition of an additional failure threshold. When at the start of the heat wave, this threshold is reached already, the index would simply be “zero”. Thus, in case the threshold is reached already, the index loses its comparability. It has been chosen to compare the exceedance of the SET above the thermal comfort threshold (SET = 24.12°C) at the start of the heat wave (as per heat wave definition) (see Fig. 18). As the time stamp stays the same for different inputs of the analysis, the outcome is a sufficient indicator of the system's resistance.

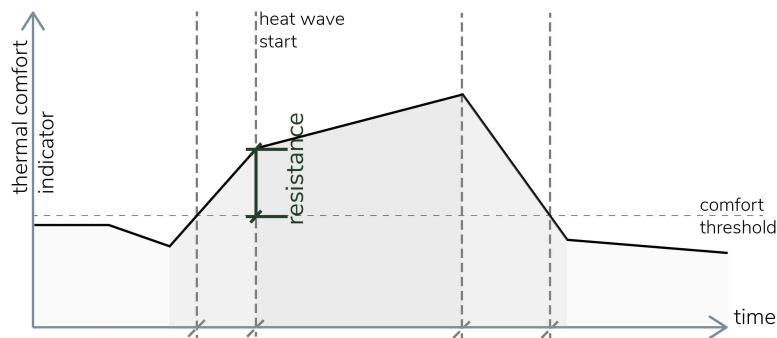


Figure 18: Measurement of resistance performance index: The proposal quantifies the temperature difference between the thermal comfort threshold level and the initial measurement of the thermal comfort indicator at the onset of a heat wave. The resulting resistance performance index shares the same unit as the chosen thermal comfort indicator. A smaller resistance index indicates better performance, as it signifies a reduced difference from the comfort threshold. source: own

Robustness

Most of the literature examples can be categorized as indices for “robustness”. The duration of exceedance above a comfortable or an uninhabitable level is one way of calculating a system's robustness (Sun et al., 2021). Another way is to measure the maximal level of thermal stress; the “peak” of thermal discomfort during the heat wave (Rajput et al., 2022; Sun et al., 2020). To give a more in-depth analysis, both measures can also be combined by using the time integral of exposure as a robustness index. Hence, it can be determined by how much and how long a defined threshold has been surpassed, which adds important details for the assessment of thermal discomfort during heat waves (Sun et al., 2021). To display the occupants' heat stress even further in different stages of the exceedance, weights can be added. Based on the severity of the exceedance segment, the integral segments have more or less influence on the robustness performance (Homaei & Hamdy, 2021a; Ji et al., 2022).

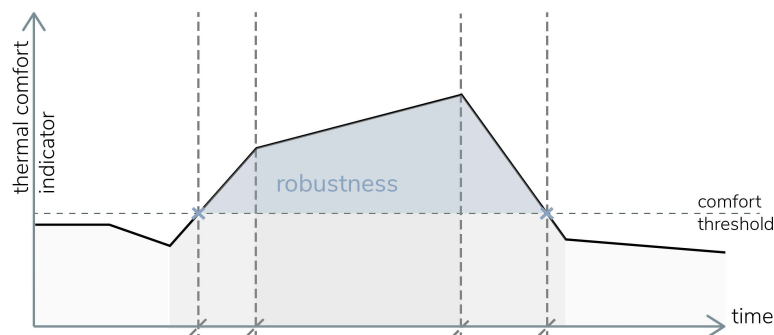


Figure 19: Measurement of robustness performance index: The proposal measures the integral of the thermal comfort indicator's measured values over time, when it exceeds the thermal comfort threshold during the simulation period. A smaller robustness index signifies more comfortable conditions, indicating less severe overheating in terms of both magnitude and duration. source: own

The time integral of exposure has been identified as a sufficient method to calculate the façade's robustness. It can capture not only the maximum reached temperature at an unknown point but also the duration the disruption is taking, as well as by how much the thermal comfort requirements are exceeded.

The weighting of certain segments, of different time periods during the disruptive period, would provide the index with additional information on the actual thermal perception of the occupants. Even though neglected now, it could always be applied.

Recoverability

Based on the available examples in the state-of-the-art research, it is noted that the "recoverability" is not one of the commonly used resilience indices (Figure 20). The given example suggests to measure the time required to get back to a comfortable or "normal" state (Homaei & Hamdy, 2021a). For the analysis of heatwave-related impacts, it is potentially needed to separate the recoverability into day- and nighttime categories, as higher nighttime temperatures significantly increase the health risk for occupants (U.S. Environmental Protection Agency, n.d.).

As there is no reference on how to apply the indicator to actual model outputs, it has been found to be most convenient to define the most extreme value (the value furthest away from the defined comfort zone) within the heat wave period and to count from there until the values are below the comfort threshold again. Since the simulation outcome is showing a high night-time recovery in Munich, it does make sense to measure the recoverability using hourly data. However, the recoverability could also be captured by only counting peak temperatures per day.

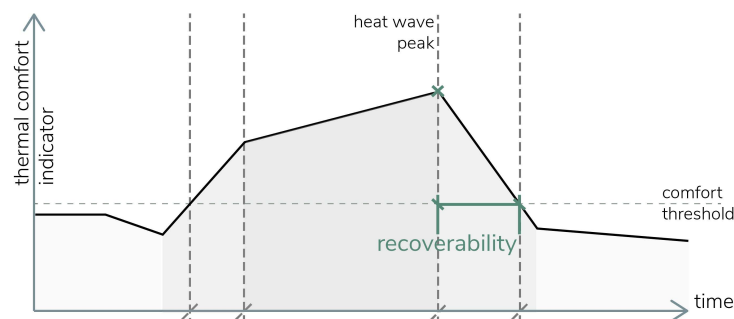


Figure 20: Measurement of recoverability index: The proposal measures the time required for the reduction of the thermal comfort indicator measurement to reach comfortable conditions (below the thermal comfort threshold). The resulting recoverability index shares the same unit as the time measurement (e.g., hours). A smaller recoverability index indicates a shorter time span needed to achieve comfortable conditions. source: own

Adaptive capacity

"Adaptive capacity" is an important term within the resilience discussion, but yet there is no approach how to quantify a system's adaptive capacity. However, based on the outcome of the literature review, a calculation method is defined: The adaptive capacity is defined as the long-term performance, considering the difference in performance in current and future weather conditions. Thus, it takes into account the results of the proposal's performance in each index, in the current and future hazard scenario. In fact, the resulting index puts into perspective how well the chosen option responds and adapts to future weather conditions by calculating the percentual worsening over time.

3.2 The final index

To finally determine the overall performance of the proposal, the “Future Resilience Index” (FRI) is developed. It quantifies the impact of façade interventions on the overall thermal resilience performance of the façade itself. It considers the resulting performance in the façade’s resistance, robustness, recoverability, and adaptive capacity. Thus, it assesses the performance in each stage during the disruption, as well as with future heat wave hazards.

To achieve the same, the following procedure is proposed (see Fig. 21): The overall performance in the current (2015) and future (2050, 2080) is calculated by simply adding the performance output of the indices.

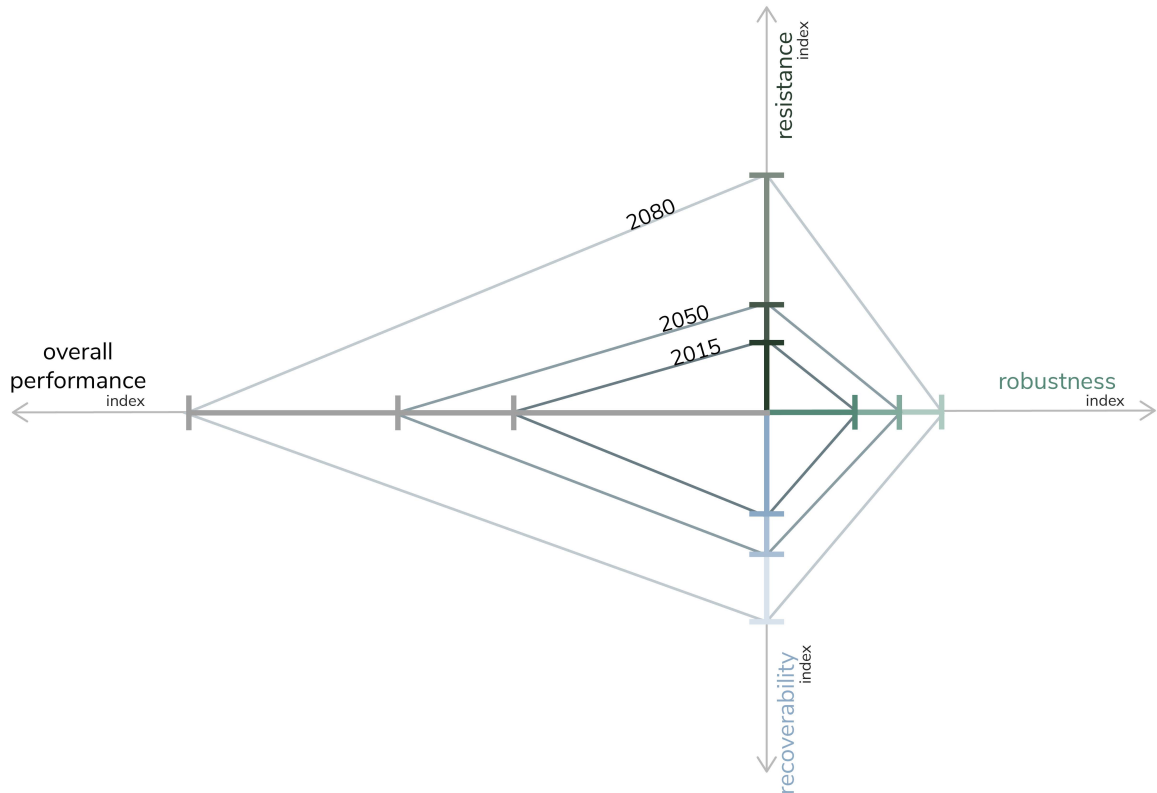


Figure 21: Proposal for evaluating the resilience performance of the façade, based on three indices: resistance, robustness, and recoverability. The overall performance is represented as a cumulative index, calculated by summing the individual indices for each weather data input. The solid lines in the figure represent the results of a single analysis, corresponding to one façade proposal with a specific weather data input.
source: own

Adaptive capacity is defined as the average performance throughout the analysed hazard conditions. With three years analysed, the sum of the overall performance is divided by three, which results in the adaptive capacity index.



Figure 22: The adaptive capacity as the average of the facade's performance throughout the analysed climate scenarios.
source: own

The final index, the FRI, is the sum of the façade's resistance, robustness, and recoverability performance in the current (2015) heat wave scenario, plus the adaptive capacity, considering the future heat wave scenarios (see Fig. 23).

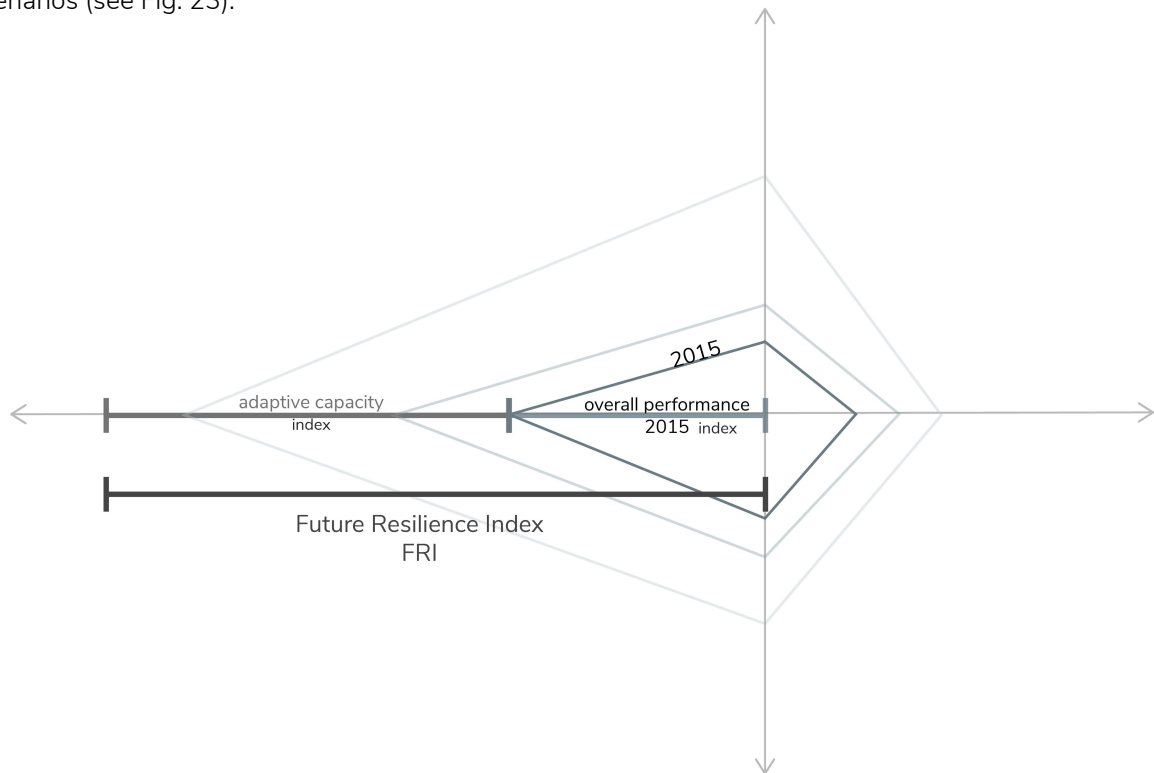


Figure 23: Calculation of the "Future resilience index" (FRI): The cumulative index is determined by summing the overall performance under current heat wave conditions (using 2015 weather data) and the adaptive capacity index (averaging the facade's performance across analysed climate scenarios).

source: own

During the decision-making process, the importance of each resilience indicator can be weighted differently, allowing for varying levels of attention. As the effect of each intervention on each indicator is visible, the assessment process becomes a valuable design tool. The FRI aims to improve the design process, by providing a comprehensive assessment method, enhancing the overall thermal resilience of retrofits.



Building performance simulation methodology

- 4.1 Introduction of methodology
 - 4.1.1 Outline of risk analysis
- 4.2 Hazard analysis – heat wave weather data
- 4.3 Definition of case study
 - 4.3.1 Base case simulation set-up
 - 4.3.2 Inputs and range of variations
- 4.4 Sensitivity analysis
 - 4.4.1 The Sobol method
- 4.5 Morphing of future weather files

4.1 Introduction of methodology

Integrating the FRI into the design process of façade retrofits requires the development of a novel methodology. The proposed workflow aims to offer a framework to identify the best-performing retrofit option(s) that best address the local heat wave hazards.

Firstly, the given risk is determined by analysing the local hazard of heat waves. Based on real weather data, heat extremes and the local definition of heat waves are specified. Secondly, the vulnerability of a building in its current state is evaluated by characterizing its important parameters, which define the base case. The identified parameters are used as numerical input for the simulation model: the base case scenario.

In the design of promising retrofit options, the current construction is analysed to assess possible limitations to be taken into account. To refine retrofit possibilities, local building regulations and standards are considered. Furthermore, the most influential façade parameters with a key role in the retrofit's final performance on the identified resilience indicators are identified. Thus, the design of the retrofit options can specifically focus on selected parameters to increase its efficiency.

The final rating is done based on the assessment of the retrofit performance compared to the performance of the current state of the façade. The numerical output can then be translated into tangible results. The parameter values are materialized. Replaced with actual retrofitting elements, which altogether result in the final design of the retrofit.

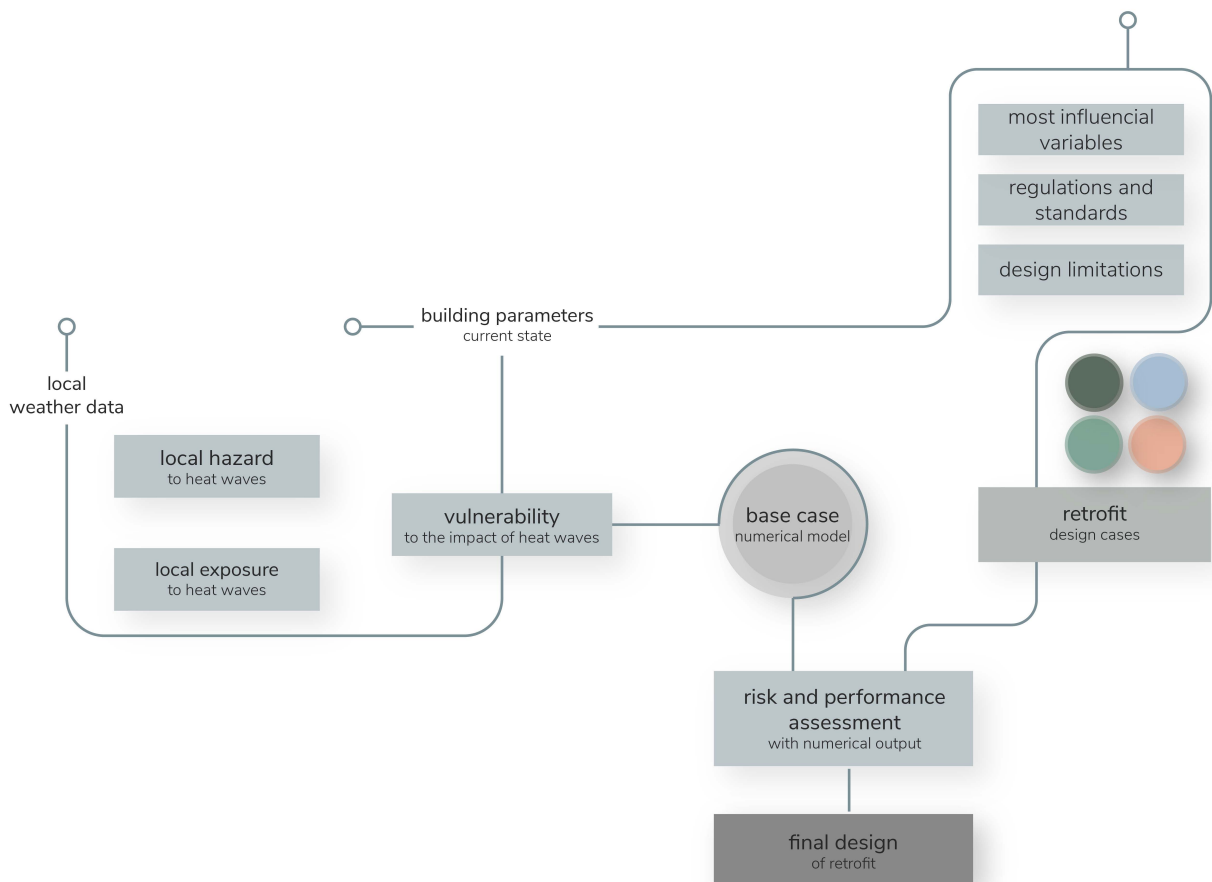


Figure 24: Methodology of decision-making workflow: The proposal considers the façade's vulnerability in terms of its current state and the local hazard and exposure to heat waves. Based on the performance comparison of ideal retrofit options and of the base case, the final façade retrofit is designed. source: own

4.1.1 Outline and workflow of index calculation

The workflow presented can be applied to a variety of situations, including both retrofits and newly constructed buildings. However, it is important to note that the specific parameters and indicators used in the workflow may need to be adjusted based on factors such as the climate, building standards, construction methods, and local circumstances of the surrounding.

The workflow is intended to be adaptable, allowing stakeholders and occupants to tailor the outputs depending on their unique needs and interests. It gives the ability to customize the procedure to unique scenarios and specific requirements by offering a framework for weighing findings. Nevertheless, the basic steps always remain the same (Fig. 24).

The first one is the **definition** of the base case scenario, including all the relevant parameters. Thus, the **simulation model** is **set up**. The EnergyPlus engine works with multiple compatible software. For this thesis, EnergyPLUS has been combined with rhinoceros grasshopper, using the Honeybee, Ladybug and Openstudio tools.

The inputs for the **SET calculation**, which is essential in determining the indicators, are taken from the outputs of the simulation model. Those include **relative humidity**, **indoor air temperature**, and **mean radiant temperature**.

A **sensitivity analysis** is carried out (orange loop in Fig. 24) to determine the factors that have the biggest impact on each of the indicators. The sensitivity analysis is conducted using an EPW file containing AMY data in the simulation period that exhibits two actual heat waves of the year 2015.

Postprocessing the results, four **design cases** can be defined and materialized: The most resistant retrofit scenario, the most robust retrofit scenario and the one scenario that has the quickest recovery. The fourth one performs well in all three indices.

The performance of the four design cases is again simulated (dark grey loop in Fig. 24). This time using not only the AMY weather data of 2015 but also **predicted future weather** data from the same heat wave period. The comparison of the performance (in 2015, 2050 and 2080) for the resistance, robustness and recoverability, results in the **adaptive capacity**. The evaluation of the simulation outputs is used as the design indication for the retrofit design.

To evaluate the resulting thermal resilience of the final design of the façade's retrofit proposal, the resilience indices are again calculated. Finally, the "Future Resilience Index" rates the total thermal resilience of the design case for heat waves in current and future climates.

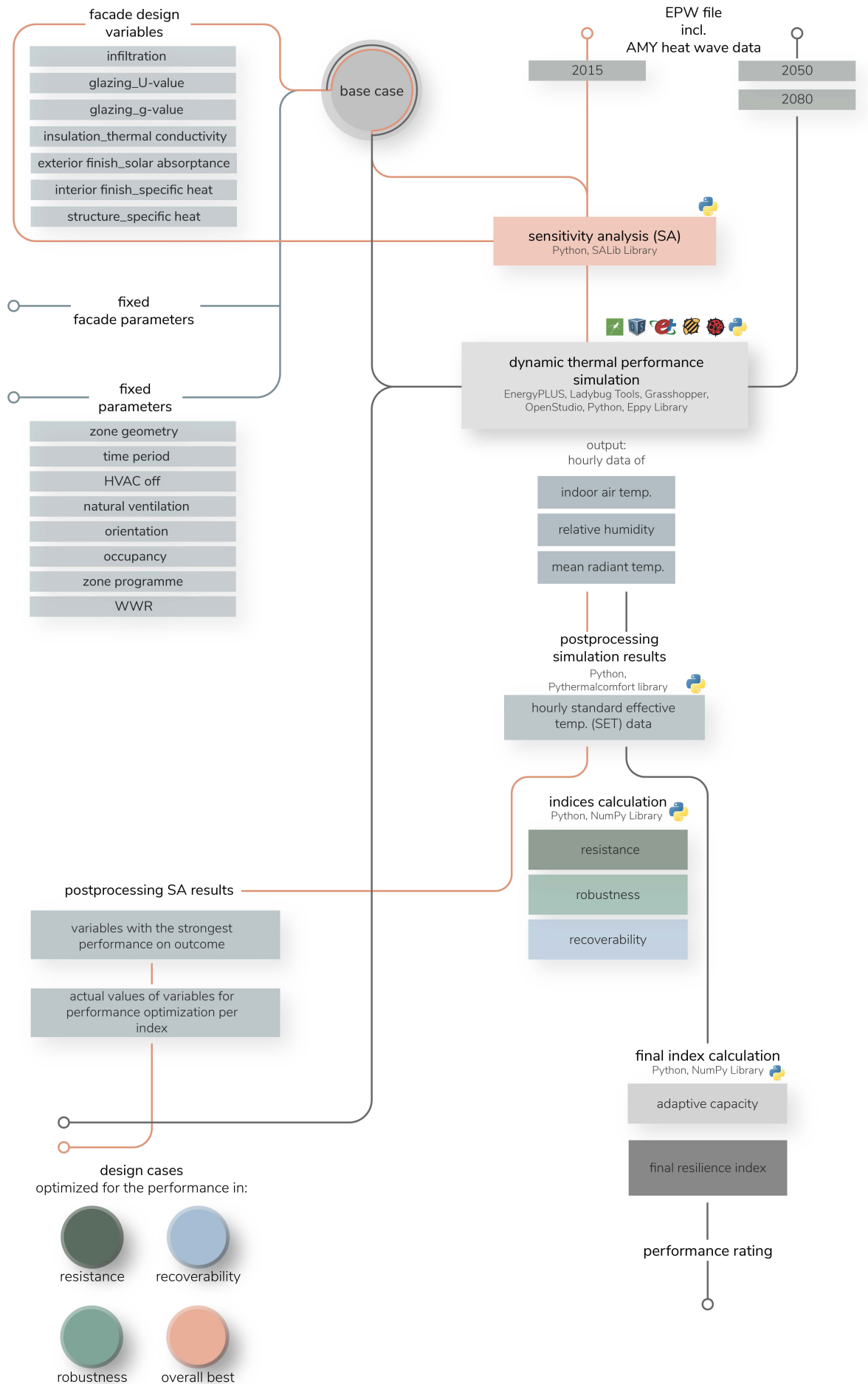


Figure 25: Simulation workflow methodology: the workflow methodology includes the two loops of the sensitivity analysis (orange line) and the evaluation loop, rating the performance of the developed design cases (dark grey line). source: own

4.2 Hazard analysis - heat wave weather data

The previous findings about the variance between heat wave definitions can be confirmed also for Germany: no general definition for heat waves within the country can be found. The German national meteorological service, the “Deutsche Wetterdienst”, is relating their heat warnings to the maximum of the perceived temperature: it is distinguished between “increased thermal stress”, at a perceived temperature of 32 degrees with low differences to night temperatures, and “extreme thermal stress” with temperatures above 38 degrees (Deutscher Wetterdienst, n.d.-a). While this can be used as an indicator of heat stress in Germany, it does not give a clear definition of what differentiates heat waves from high temperatures.

For the analysis of the local hazard to heat waves in Munich, a percentile heat wave definition has been used to identify periods of excessively hotter conditions than normal. While percentile definitions are common, the method, developed by Ouzeau et al. (2016), is not only defining one threshold but multiple thresholds for one location, which define the beginning and the end of a heat wave. As those statistical thresholds are calculated with data from the daily mean temperature of a 30-year period in a specific location, the method is independent of climate zones and can be used throughout different climate zones (Ouzeau et al., 2016). The method is straightforward in its application: the calculation of the thresholds is based on the analysis of the percentile of the historical weather data. Using those thresholds, past, present and future heat waves can be defined.

Ouzeau et al. (2016) proceed as follows: The first threshold (at the 99.5th percentile), the maximum exceeded temperature (T_{pic}) is used to identify the heat wave existence. The second one (T_{deb} , at 97.5th percentile) defines the start and end of a heat wave period: once the mean daily temperature is exceeding the threshold temperature, the start of the heat wave is determined. Same with the end of the heat wave: the moment, where the mean daily temperature reaches T_{deb} , is defined to be the end of the heat wave period. The third threshold (T_{int} , at 95th percentile) is used to identify moments of disruption within the heat wave period: in case the mean daily temperature within the defined heat wave period falls below T_{deb} , but stays above T_{int} for less than three consecutive days, it can be seen as a disruption of the same heat wave.

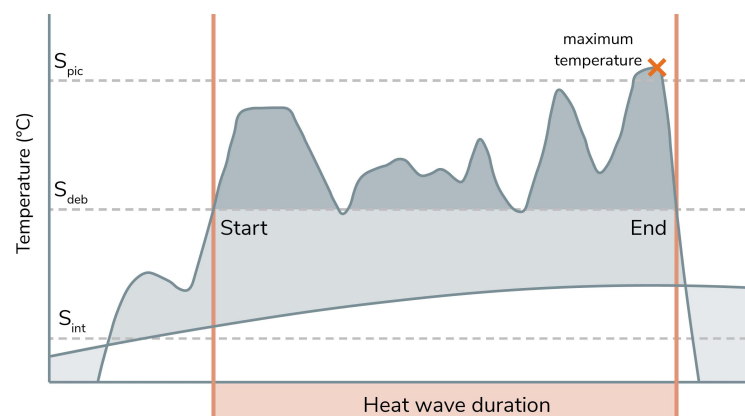


Figure 26: Heat wave identification using daily mean temperature as an indicator. Heat waves are defined by temperatures surpassing the S_{pic} threshold (99.5th percentile), with the duration determined by the start and end moments based on the S_{deb} threshold (97.5th percentile). Interruptions within the heat wave occur when temperatures fall between the S_{deb} and S_{int} thresholds (95th percentile). adapted from: Ouzeau et al. (2016)

Following the described method, a Python script has been set up to identify the three threshold temperatures for heat waves in Munich. The input is historical weather data from the “Deutsche Wetterdienst” archive and includes daily measurements of the daily mean temperatures from the period of 1992 until 2021 (Deutscher Wetterdienst, n.d.-b). Like this, $T_{pic} = 24.9$ °C, $T_{deb} = 22.6$ °C and $T_{int} = 21.1$ °C define the local thresholds of heat waves in Munich.

The next step of identifying a time period, exceeding the thresholds, could be done in an automated process (Ouzeau et al., 2016). However, it has been chosen to manually detect the time period used for the simulation, based on the calculated thresholds, which is sufficient for the following analysis. In the summer of 2015 two heat waves, from the 04th-09th of August and from the 28th of August until the 01st of September, have been detected through the manual screening of the maximum temperatures in the warmest summer months (Visual Crossing Corporation, n.d.). It has been decided to include data from two heat waves, that happened shortly after each other, as it could be interesting to see if the first heat wave also influences the results of the second heat wave. To also include pre and post heat wave conditions (each 7 days), finally weather data from the 27.08.2015 – 09.09.2015 has been used.

It is found to be difficult to find weather data that includes sufficient information on solar radiation data: Most of the commonly available weather data sources only include global solar radiation and not diffuse and normal solar radiation. Thus, for the development of a functioning EPW file, solar radiation data for the same time period is downloaded separately (Solcast, n.d.) The resulting weather file is an EPW file of Munich, containing AMY data of two heat wave periods that happened in 2015.

4.3 Definition of case study

To evaluate the proposed framework, a case study was carried out in Munich. Despite not being commonly associated with heat waves, Munich, located in the South German state of Bavaria, was chosen for several reasons: located in Central Europe, the city experiences a “Temperate oceanic” climate, “(...) typical of west coasts in higher middle latitudes of continents, generally featuring cool summers and mild winters (for their latitude), with a relatively narrow annual temperature range and few extremes of temperature” (SKYbrary Aviation Safety, n.d.). With an average temperate climate and cool summers, the focus is primarily on providing sufficient heating in the colder winter condition. Currently, mechanical cooling systems and exterior shading options are not widely used, especially not in residential buildings.

However, Munich's climate is projected to change, becoming more similar to Milan's current climate (Crowther Lab, ETH Zurich, n.d.): the warmest month is predicted to experience an increase of daily maximum temperature of 4.6°C. While heating will still be necessary during winters, the warmer summer conditions require further investigation and preparation. Therefore, the chosen case study is focuses on a representative residential building archetype, located in Munich's "Maxvorstadt" area. The Maxvorstadt was planned and constructed as the first expansion of the inner city between 1825 and 1900 (Portal München Betriebs GmbH & Co. KG, n.d.). The rectangular street pattern divides the area into large residential building blocks, which represent a typical urban pattern of inner city urban living in Germany.

In focus is an apartment in the third floor of a six storey building. Accessed from the courtyard side, the living spaces are facing the street, which is the same for all the surrounding apartments. Thus, the case study is representative for the building type of a residential block from the 19th century in Munich.



Figure 27: Bird's-eye view of the "Maxvorstadt" district in Munich, showcasing the distinct urban plan characterized by a repetitive pattern of residential buildings. source: (Hallo München, 2021)

4.3.1 Base case simulation set-up

The case study focuses on a single thermal zone, representing the living area within the apartment. For the further analysis, a building performance model was created using a combination of Grasshopper (version 2021-Apr-22), Rhinoceros 3D and Ladybug Tools, with EnergyPLUS as the simulation engine. With Grasshopper as the interface, the geometry is set up parametrically. The model aims to describe the current state scenario, with the following parameters as simulation input:

Table 4: Simulation parameters of the case study building in its current state (definition of base case scenario). source: own

location	building location	weather station location	terrain
	Munich, Maxvorstadt 48.15, 11.57	Munich, airport 48.35, 11.78	"urban"
orientation	orientation		
	South-East -45°C		
geometry and surfaces	dimensions	room height	surfaces
	10 x 5 m	2.80m	walls: 3 adiabatic, 1 diabatic ceiling: adiabatic floor: adiabatic
program	occupancy	electrical equipment	lighting
	4 residents occupancy schedule: hourly	5W/area schedule: based on hourly occupancy schedule	5W/area schedule: based on hourly occupancy schedule
construction	exterior wall	ceiling and floor	interior walls
	exterior finish: plaster structure: brick interior finish: plaster	structure: wooden beams insulation	finishing: plaster main construction: brick
Window properties	Window to wall ratio	U-value	g-value
	0.25	2.7 W/m ² K	0.70

HVAC	mechanical cooling	mechanical heating	ventilation
	off	on	on when exterior temperature > = 15°C interior temperature >= 26°C (Ji et al., 2022) and exterior temperature < 2°C< interior temperature (Sun et al., 2020)
infiltration	air flow per square meter of exterior facade		
	0.0006 m ³ /m ²		

The primary construction can be assumed to be brick, with a painted plaster layer on both sides (Prof. Dr.-Ing. Doris Haas-Arndt et al., n.d.). Therefore, the material properties are defined as in Table 5. The following discussions options for potential façade retrofits and their corresponding parameters for further analysis.

Table 5: Material properties of exterior wall of case study construction. Properties in alignment with EnergyPLUS material property input. source: own

	thickness (m)	specific heat (J/kgK)	thermal conductivity (W/mK)	density (kg/m ³)	roughness	thermal absorptance	solar absorptance	visible absorptance
brick	0.365	840	0.5	1000	medium rough	0.9 (default)	0.7 (default)	0.9 (default)
plaster (exterior/interior)	0.02	1000	0.7	1400	medium rough	0.9 (default)	0.7 (default)	0.9 (default)

4.3.2 Inputs and range of variation

With the national German construction law of energy efficiency, known as the "Energieeinsparverordnung" (EnEV), homeowners are being legally obliged to follow certain standards of the energy efficiency of the building (Bundesministerium für Wirtschaft und Klimaschutz, 2013). Since 2002 the EnEV has been frequently updated, modifying the energy classification requirements of new and existing constructions. The regulation also includes provisions for heat protection in summer, which new constructions in any case and existing constructions, as soon as a major renovation is necessary, must meet. Additionally, the "Bundesförderung für effiziente Gebäude" (BEG) provides additional funding to encourage retrofitting (Bundesministerium für Wirtschaft und Klimaschutz, 2023). Thus, any building retrofit in Germany is guided by the requirements of the EnEV and the BEG. This includes limits on the annual primary energy consumption regulating heat transmission in winter, and heat protection in summer using specified maximum thermal transmittance values for each building component.

In the case of the case study building, without insulation, the exterior wall of the is estimated to have a thermal transmittance of around 1.26 W/m²K. To meet the minimum EnEV criteria for thermal transmittance for diatomic exterior walls (0.28 W/m²K), a retrofit would most probably include the installation of insulation material.

$$U = \frac{1}{R_1 + R_2 + R_3} = \frac{1}{\frac{d_{Brick}}{\lambda_{Brick}} + 2 \times \left(\frac{d_{Plaster}}{\lambda_{Plaster}}\right)} = \frac{1}{\frac{0.365 \text{ m}}{0.5 \frac{W}{mK}} + 2 \times \left(\frac{0.02 \text{ m}}{0.7 \frac{W}{mK}}\right)} = 1.26 \frac{W}{m^2K} \quad (1)$$

Therefore, insulation material is modelled with the following properties (Table 6). Based on the findings of the literature review (Chapter 2.4.3), only externally added insulation has been considered.

Table 6: Material properties of added insulation. Properties in alignment with EnergyPLUS material property input. source: own

	thickness (m)	specific heat (J/kgK)	thermal conductivity (W/mK)	density (kg/m3)	roughness	thermal absorptance	solar absorptance	visible absorptance
insulation	0.2	800	0.05	40	medium rough	0.9 (default)	0.7 (default)	0.9 (default)

To mitigate overheating risk in summer, the EnEV establishes standards for the solar heat gain coefficient (g-value) as well as for the maximal thermal transmittance (U-value) of glazing in residential buildings. When using exterior shading options, the maximum allowed g-value for the glazing is 0.60, whereas without shading, it is 0.35. The maximum permissible U-value of the glazing in residential buildings is 1.3 W/m²K in case they are supposedly heated to above 19°C in winter. Since the assumed double-glazing without shading in the case study building fails to meet both requirements, the windows would need to be replaced in any retrofit scenario.

Evaluating the current state of the case study building and potential retrofit options, certain parameters were assessed for their predicted impact on thermal indoor conditions and the building's thermal resilience during heat waves. Elements/properties that are less likely to be changed during retrofitting (like the window-to-wall ratio etc.) were excluded from the analysis. Similarly, properties or elements that not described numerically in EnergyPLUS, such as the material's property "roughness", varying from "very smooth" to "very rough", are also excluded.

Seven relevant parameters were selected for the sensitivity analysis, as shown in Table 7. The infiltration is chosen as a variable strongly influencing the convective heat flow through the exterior wall. As in discussed in Chapter 2.2, the airtightness of a façade thus has a large impact on the thermal comfort indoors. The specific heat of the structural wall as well as of the interior finish is included as variables analysing the required heat storage capacities of the wall. During the conductive heat flow through the exterior wall, materials with a higher specific heat count as a "heat buffer" – more energy is needed to increase their temperature, which makes them store heat and release it slowly. Thus, this is of interest for the massive, structural part of the wall, to understand the required thermal mass and the desired time lag in thermal response to the outside environment. Similarly, also for the interior layer, as here it is important to consider the time and amount of energy transferred to the interior space by convection and radiation. Additionally, the thermal conductivity of the insulation is included. The insulation with significantly lower thermal conductivity values reduces the conductive heat flow through the exterior wall, which makes it an important variable to consider. And lastly, the glazing U- and g-value: the U-value of the glazing can substantially decrease the heat flow between the exterior and interior. A lower U-value means a higher resistance to thermal conductivity, which results in an improved level of thermal insulation. With high solar radiation in summer, the g-value restricts the percentage of the incoming solar heat gain through transparent surfaces. Hence both the g-value and the U-value of the glazing are important to consider.

Reasonable and realistic ranges have been assigned to each variable, considering relevant regulations and material properties. For the variable “air flow per square meter of exterior façade” the range is specified through the EnergyPLUS input variance for the same (0.0001 for a “tight” building, 0.0006 for a “leaky” building). The range of the U- and g-value is determined by the EnEV requirements. For the specific heat (both for the interior finish and the structural part of the exterior wall), thermal conductivity of the added insulation and solar absorptance of the exterior finishing, the values are based on a realistic range of common building materials’ properties (Engineering ToolBox, 2001; Lawrence Berkeley National Lab, 2019).

Throughout the analysis, the simulation input for **geometry, location, orientation, simulation period, HVAC system, occupancy and internal gains**, and **other material properties** are kept constant (in correspondence with the base case scenario, discussed in Chapter 4.2.1).

Table 7: Range and distribution of facade variables for retrofit options source: own

	infiltration	structural wall	exterior insulation	exterior finish	interior finish	glazing	glazing
	air flow per square meter of exterior facade (m ³ /m ²)	specific heat (J/kgK)	thermal conductivity (W/mK)	solar absorptance	specific heat (J/kgK)	u-value (W/m ² K)	g-value
range	0.0001 - 0.0006	400 - 1500	0.03 - 0.1	0.2 - 0.9	400 - 1500	0.6 - 1.3	0.1 - 0.8
distribution	uniform	uniform	uniform	uniform	uniform	uniform	uniform

4.4 Sensitivity analysis

Sensitivity analyses get increased attention in the building sector as a tool of supporting design decisions both in the early and later stages of design projects (Hopfe, 2009; Struck, 2012; Tian, 2013). Based on the detailed analysis of the building performance with varying input parameters, the specific importance of each input parameter on the output can be determined. In global sensitivity analysis also the inputs’ interactions are explored (Loonen & Hensen, 2013). Hereby, the output, the sensitivity is calculated towards, can range from the energy demand (Goffart & Woloszyn, 2021; Hopfe & Hensen, 2011), thermal comfort (Burhenne & Herkel, 2013; Tian & de Wilde, 2011), or carbon emissions (Chen & Tsay, 2022) with the corresponding application in building envelope optimization (Capozzoli et al., 2013; Raji et al., 2016), layout/geometry design (Hemsath & Alagheband Bandhosseini, 2015; Østergård et al., 2017), building services engineering (Lauss et al., 2022) etc. In summary, sensitivity analyses provide insights into the relationship between input parameters and desired outcome, which makes them a valuable tool for decision-making frameworks in the field of building design and performance.

The process of a sensitivity analysis is based on a principle, which was first mentioned by biologist Robert Rosen (1991) (Figure 28). A numerical model is created by shaping a “formal system” from a “natural system”. Rules are established, capturing the “natural system” and representing them in the modelled

version (Rosen, 1991; Saltelli et al., 2008). The model, the “formal system”, therefore can describe various processes, with the only requirement of numerical input to be able to calculate the output.

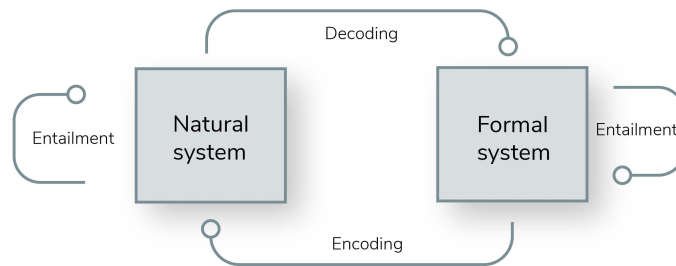


Figure 28: Illustration of the simplified modelling process where numerical models are used to simulate complex natural systems. These models aim to reproduce the processes and behaviour observed in the natural system, creating a parallel representation of each other. adapted from: Rosen (1991)

There are “diagnostic” and “prognostic” sensitivity analysis. The distinction is “(...) between models used to understand a law and models used to predict the behaviour of a system given a supposedly understood law” (Saltelli et al., 2008, p. 5). Models can either be based on speculations or based on already precise predictions. However, in both cases, the actual uncertainty analysis happens by “running” or “computing” the model for multiple “vectors” (Fig. 29). The vectors are a combination of sample values per model input parameter (α , β , γ , etc.) within a set range (Saltelli et al., 2008). Thus, the input array is defined by the manually set range of each parameter, the number of samples and the number of input parameters. Running the model with one row of the input array at a time results in the one-dimensional output array. The last step is to evaluate the model behaviour due to input and output and thus calculate the sensitivities per parameter.

This also explains why a larger input array (a larger sample size) gives higher accuracy. However, the number of samples needed to sufficiently calculate the impact of the parameters depends on the chosen method, the number of inputs, the complexity of the model, and the bounds of the parameters.

For the sampling as well as the evaluation process different established methods are available. They are accessible through Python libraries like SALib (Herman & Usher, 2017; Iwanaga et al., 2022), which include the different sensitivity analysis algorithms. The model itself as well as the input and output parameters, plus the variable ranges to be pre-defined. Hereby, the model can be a mathematical equation or, like in the case of this thesis, an externally accessed simulation/etc.

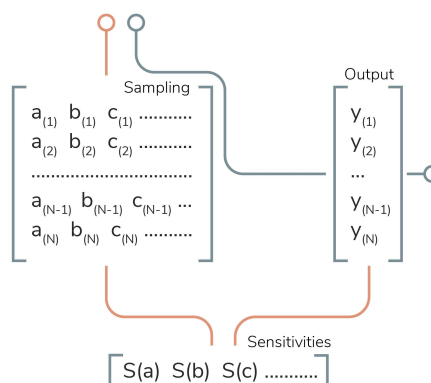


Figure 29: Illustration of the schematic methodology for sensitivity analysis. Variable combinations are sampled to create an input array, where each row represents a unique combination. Numerical output is calculated for each combination, and the sensitivities of variables are derived based on the variance of the output when changing the input. adapted from: Saltelli et al. (2008)

4.4.1 The Sobol method

For the objectives of the proposed framework, the so-called “Sobol” (Sobol, 1993) method is chosen. The Sobol method has been proven to be valid for sensitivity analyses for building performance (Chen & Tsay, 2022; Jin & Overend, 2014). It is a variance-based approach that assesses the importance of input variables calculating their impact on the variance of the output. The Sobol method computes three types of sensitivities: the direct (S_1), the indirect (S_2) and the total (S_T). The S_T consists of both, the S_1 and S_2 sensitivities, which means it takes into account direct influences of each variable on the output and possible interactions of variables and their effect on the output. E.g., the output of $S_1 = 0.2$ would mean that by only varying this specific variable, the output would be varied by 20%. The analysis of the S_2 output is more complex and requires an in-depth analysis. In principle, it can be said that a large S_2 value suggests a significant importance of interaction between the variables on the variance of the output. Lower S_2 values suggests less impact of the variable interactions on the model outcome. As the S_T sensitivities indirectly also provide insight on the variable S_2 sensitivities, the focus of the further analysis, is on the S_1 and S_T sensitivities.

The sensitivity analysis has been performed in Python, version 3.10.7, launched in PyCharm (2022.2.1). Next to the SALib library (1.4.7) (Herman & Usher, 2017; Iwanaga et al., 2022) for the sampling and evaluation of the sensitivity analysis, also the Eppy library (0.5.63) is used. With Eppy, it is possible to “programmatically navigate, search, and modify E+ idf files” (Santosh, 2022, p. 1), which makes EnergyPLUS simulation files accessible and changeable through Python. Furthermore, the NumPy library (1.23.4) is used for all operations of arrays (Harris et al., 2020). After running and evaluating a total 4096 simulation files and outputs, the sensitivity analysis is giving sufficient results.

The steps taken to carry out the sensitivity analysis are visualized in Figure 30:

- 1) Definition of problem: The variables are being determined by specifying the **number of variables ($D = 7$)**, giving names, bounds and distributions as in chapter 4.3.
- 2) Sample creation: The built in “**SALib.sample.sobol.sample()**” command creates the input array, based on a given **value ($N = ?$)**, generating a two-dimensional matrix with ($N \times (2D + 2)$) rows and D columns. Thus, a two-dimensional array gives a total of 4096 value combinations.
- 3) Saving and running IDF files: To create per input combination one IDF file, a “for-loop” is set up, loading the original IDF file, specifying the variables using the given value combination of the input array and saving it to a separate IDF. By giving each IDF a name based on the index of the input combination, it is made sure to not overwrite the files each time the for-loop is running. After saving the IDF file, the command “**idf.run(*the_options)**” runs the IDF file and saves the output to a separate output folder, specified before.
- 4) Calculation of the **standard effective temperature (SET)**: The output CSV files contain hourly data of the mean radiant temperature, the operative temperature, the air temperature and the relative humidity during the simulation period (1032 hrs). With that, the SET (hourly) can be calculated using the Pythermalcomfort library (Tartarini & Schiavon, 2020), version 2.7.0. Results are saved to a list, created beforehand.
- 5) Indicator array creation: A two-dimensional array is created with three columns (for the output of the indicators “resistance”, “robustness”, and “recoverability”) and rows accordingly to the sample size.

- 6) Calculation of **indicators**: With the calculated hourly SETs, the indicators are calculated and placed into the created indicator array.
- 7) Output creation: For the sensitivity analysis it is necessary to have the output data in separate lists. Therefore, the two-dimensional array is split in three lists, one for each indicator: Y1, Y2 and Y3.
- 8) Analysis of sensitivities: The in-built function “**sobol.analyze (problem, output, calc_second_order=True)**” is calculating the direct and indirect influences of the given input (**problem**) in regards to its output (**Y1/Y2/Y3**). Separate functions are used per output, as it is of interest to calculate the sensitivity per indicator (per output, but same input variables). Note, that the addition of “**calc_second_order=True**” is necessary to also receive results for the indirect impact of the variables.
- 9) Sensitivity analysis output to **CSV**: The resulting of the values for **S_T**, **S₁** and **S₂** are saved in separate **CSV files** for postprocessing and analysis.

grasshopper simulation set-up original IDF

set up problem: variables and their bounds, and distribution

```

problem = {
    'num_vars': 7,
    'names': ['structure_specific_heat', 'interior_finish_specific_heat',
              'exterior_finish_solar_absorptance', 'insulation_thermal_conductivity',
              'glazing_u_value', 'glazing_shgc_value', 'infiltration'],
    'bounds': [[400, 1500],
               [400, 1500],
               [0.2, 0.9],
               [0.03, 0.1],
               [0.6, 1.3],
               [0.1, 0.8],
               [0.0001, 0.0006]],
    'dists': ['unif', 'unif', 'unif', 'unif', 'unif', 'unif', 'unif']
}
    
```

set sample size and create samples

```

param_value = SALib.sample.sobol.sample(problem,
                                         256, calc_second_order=True)
    
```

2D array shape (sample_size, number of variables)

```

print (param_values)
[[a1 b1 c1 d1 e1 f1 g1]
 [a2 b2 c2 d2 e2 f2 g2]
 ...
 [ax bx cx dx ex fx gx]]
    
```

loop through samples; define variables save IDF, run IDFs, save outputs

```

for i in range(param_values.shape[0]):
    materials[0].Specific_Heat = param_values[i][0]
    materials[18].Solar_Absorptance = param_values[i][1]
    materials[17].Solar_Absorptance = param_values[i][2]
    materials[14].Conductivity = param_values[i][3]
    glazing_object.UFactor = param_values[i][4]
    glazing_object.Solar_Heat_Gain_Coefficient = param_values[i][5]
    infiltration[0].Flow_Rate_per_Exterior_Surface_Area = param_values[i][6]

    filename = 'test-%04d.idf' % i
    idf.saveas(output_dir_idf + '/' + filename)
    path = str('/Output_IDF/' + filename)
    output_file = 'test-%04d' % i

    def make_eplaunch_options(idf):
        ...

    idf = IDF(path, epwfile_2015)
    the_options = make_eplaunch_options(idf)
    idf.run(**the_options)
    
```

split indicators in separate lists

```

X1 = []
X2 = []
X3 = []

for i in range (sample_size):
    Y1.append(indicators[i, 0])
    Y2.append(indicators[i, 1])
    Y3.append(indicators[i, 2])
    
```

calculate sensitivity of input parameters for each of the output indicators

```

rec = sobol.analyze(problem, Y1, calc_second_order=True,
                    print_to_console=True)
res = sobol.analyze(problem, Y2, calc_second_order=True,
                    print_to_console=True)
rob = sobol.analyze(problem, Y3, calc_second_order=True,
                    print_to_console=True)
    
```

save ST, S1, S2 output to separate CSVs for further processing

```

results = [rec, res, rob]
for i, result in enumerate(results):
    total_result, first_result, second_result = result.to_df()
    
```

output CSV for each IDF including hourly data (only HW period) of:

- mean radiant temperature
- air temperature
- relative humidity

calculation of SET for each IDF hourly during HW period

```

Standard effective temperature
    
```

create empty numpy array to store output data

```

shape (sample_size, number of indicators)

indicators = np.zeros((sample_size, 3))
    
```

resulting: 2D array

```

print (indicators)
[[rec1 res1 roc1]
 [rec2 res2 roc2]
 ...
 [recx resx rocx]]
    
```

- recoveryability
- resistance
- robustness

calculate indicators per IDF and store results in numpy array

Figure 30: Procedure of Sobol sensitivity analysis source: own

4.5 Morphing of future weather data

As intended by the proposed framework methodology, the assessment accounts for future heat wave scenarios. The overall thermal resilience of the retrofit is rated based on the performance in future heat wave data of the same location. However, commonly available weather data is “actual” meteorological data (AMY) or “typical” meteorological data (TMY). Predictive future data is genuinely only available in the form of short-term forecasting models for a maximum of 16 days. However, there are methods that allow for the prediction of future weather in a long-term perspective.

Predictive future weather data is commonly “morphed” (Belcher et al., 2005). Morphing is a process that achieves to translate average weather conditions of future climate scenarios to a local level, creating weather files that can be used for simulation purposes. The algorithms produce predictive weather files based on climate prediction scenarios, such as the IPCC climate scenarios (Seneviratne et al., 2021), and a chosen EPW weather file. For the creation of predictive future weather files of Munich, the weather file generator “CCWorldWeatherGen” (Jentsch, 2017), Version 1.9, has been used. The package provides a Microsoft Excel file, which creates, based on a selected EPW file, predictive weather files for the years of 2020, 2050 and 2080.

The morphing uses the IPCC TAR model summary data of the HadCM3 experiment ensemble from the IPCC A2 scenario (explanation of IPCC narratives can be found in Chapter 2.1), which is available online in the IPCC distribution download centre (IPCC, n.d.). The A2 scenario originated from the storyline of a “very heterogeneous” world, with self-reliant countries and communities (IPCC, 2007). It is characterized by a rapid increase in the global population alongside a relatively slow progress in global economic and technological advancements, as described in the IPCC 2007 report (IPCC, 2007). It can be compared to the more recent SSP3 scenario, which features a resurgence of nationalism and a greater emphasis on domestic and regional priorities, as outlined in the IPCC 2021 report (IPCC, 2021). The resulting carbon emissions in future are assumed to be significantly higher than in the SSP1 (sustainable development) or in the SSP2 narrative, which is characterised by no drastic shift from historical patterns (IPCC, 2021). The IPCC assumes for the SSP3 narrative an estimated long-term increase of the global temperature of 3.6°C (compared to the SSP1 of 1.4°C; SSP2 of 2.7°C) (IPCC, 2021).

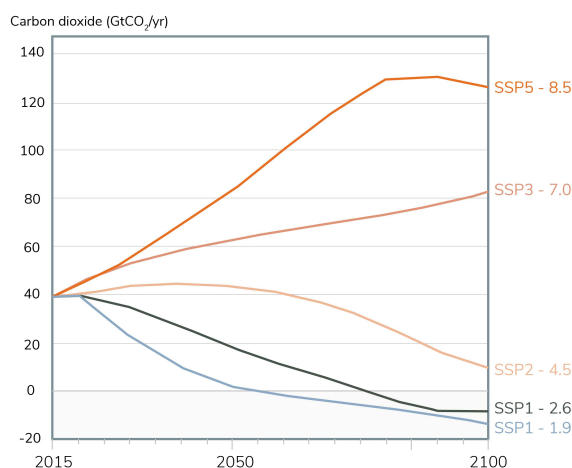


Figure 31: Predicted future CO₂ emissions considering annual predicted anthropogenic (human-caused) emissions over the period from 2015 until 2100. Shown by the five narratives SSP1-1.9/2.6, SSP2-4.5, SSP3-7.0, SSP5-8.5 adapted from: (IPCC, 2021)

With the input of the EPW simulation file, containing real weather data of two heat waves of 2015, the morphing algorithm creates predictive weather file for the city of Munich in the years of 2050 and 2080, based on the A2 scenario (comparable to the SSP3 narrative) of the IPCC report (IPCC, 2007, 2021).



Results

- 5.1 Sensitivities of variables
- 5.2 Output performance distribution
- 5.3 Identification of best performing scenario
- 5.4 Variable values comparison
- 5.5 Final rating of design cases
- 5.6 Discussion
- 5.7 Conclusion

The following section describes the results of the research. The first four subchapters analyse the outcomes of the sensitivity analysis, while the fifth subchapter postprocesses the results and assesses the chosen scenarios with future weather data.

5.1 Sensitivities of variables

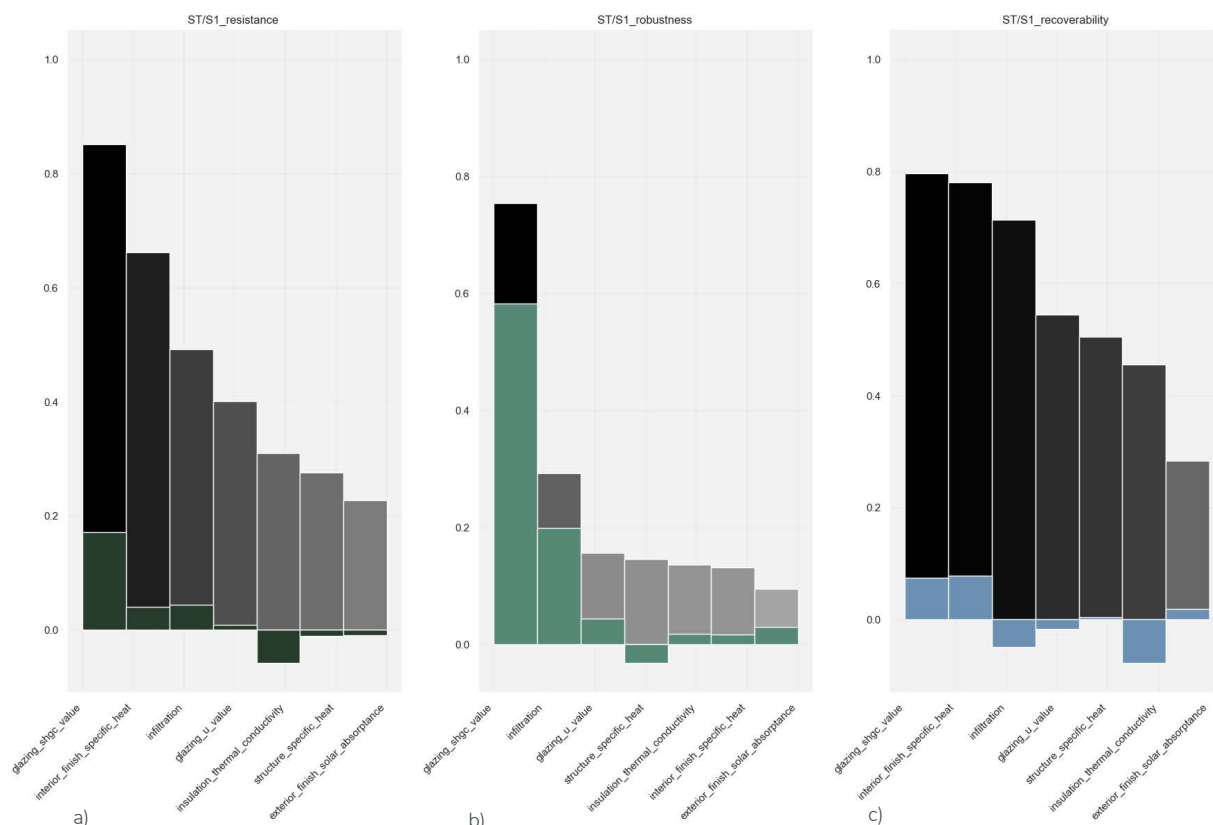


Figure 32: Result of the Sobol' sensitivity analysis. Input variables on the x-axis with corresponding Sobol's total indices, S_T (greyscale) and first order indices, S_1 , in front (in highlight colour). a) results for the resistance index, b) for the robustness and c) for the recoverability. source: own

The results of the Sobol's total indices (S_T) as well as Sobol's first order indices (S_1) are illustrated for each of the resistance indicator in a histogram (Fig. 32 a): resistance, b): robustness, c): recoverability): the S_T outcome in greyscale, and the corresponding S_1 outcome in colour.

Darker shades with **larger values** of S_T demonstrate a **larger total impact**: varying their values, the output value fluctuates strongly. Additionally, those variables have **strong interactions** with other parameters (large S_2 values). Variables with a **small S_T** value (brighter shades) leave the output value relatively **consistent** despite a large variable variance. Plus, they do **not intercorrelate** a lot with other input variables (small S_2 values).

The absolute value of S_1 gives an indication for the **magnitude** of the **effect** of the variable on the **model output**, the "strength" of the effect: it calculates the proportional change of the output when changing the input value. The sign of the S_1 value on the other hand determines the **direction** of the effect of the change of the variable on the output: "Positive" means, the model output increases with a larger input value. Conversely, if the S_1 value for a parameter is negative, it means that increasing the value of that parameter will result in a decrease in the output of the model and the other way around.

Thus, in this case, with the desired target of the smallest values for each of the output values variables with their absolute S_1 value positive, should be kept rather small. Variables with the absolute S_1 value negative give indication for a more beneficial effect when the variable value is larger. It must be noted that the terms “large” and “small” are relative to the given range of the parameter and only include values within the minimum and maximum value.

For the recoverability the difference between the largest S_T and the smallest S_T is 0.513, for resistance that is 0.624 and for the robustness that is 0.660. As additionally for the output of the recoverability all the S_T values are comparatively high (strong dark shade), the results show a similarly high impact of the variables on the recoverability. The opposite is the case for the robustness: The large difference between the high S_T values and the low S_T values (between the dark coloured shade and light-coloured shades) shows the larger contrast between variables with strong impact and variables with very low impact on the index of robustness.

The g-value of the glazing (incl. effect of possible exterior shading) is having the strongest effect on all the three indicators. On the resistance and especially on the robustness a change of the g-value variable has a strong total impact ($S_T(\text{resistance}) = 0.851$, $S_T(\text{robustness}) = 0.755$), but also a strong direct effect ($S_1(\text{resistance}) = 0.172$, $S_1(\text{robustness}) = 0.583$). The S_1 shows for the three indicators a positive correlation of the variable of the glazing g-value to the model output. Thus, it indicates a bias towards low g-values for low indicator indices.

The specific heat of the interior finishing has a similar total ($S_T = 0.781$) and a slightly larger direct impact ($S_1 = 0.078$) on the recoverability than the g-value. The specific heat of the interior finish is therefore equally important for the output of the recoverability index than the g-value. On the resistance the specific heat of the interior finish has a slightly smaller total impact with an S_T of 0.662. For the robustness on the other hand the low S_T as well as the low S_1 imply that the specific heat has very little impact.

The infiltration variable has the largest effect on the recoverability ($S_T = 0.714$), significantly less on the resistance ($S_T = 0.492$) and on the robustness ($S_T = 0.293$). The direct impact on the robustness is the largest with an of $S_1 = 0.199$, while for the recoverability and the resistance it is certainly less with $S_1(\text{recoverability}) = -0.050$ and $S_1(\text{resistance}) = 0.045$. It will be noted that the correlation is positive for both the resistance and the robustness, however not for the recoverability.

The U-value of the glazing has comparatively only a very small direct impact on both recoverability and the resistance with the $S_1(\text{recoverability})$ at -0.017 and the $S_1(\text{resistance})$ at 0.009 , with slightly larger values for the robustness with $S_1 = 0.044$.

The specific heat of the structural wall has very limited impact on each of the outputs (S_T the largest for recoverability with a value of 0.505). The additional very small direct impact of $S_1(\text{recoverability}) = 0.005$ indicates, that the specific heat of the structural wall is only enhancing the recoverability when combined with other properties (same can be said about the resistance and the robustness).

The thermal conductivity is having the largest impact on the recoverability with a total S_T of 0.456 and a S_1 of -0.077 . While the negative sign implies a negative correlation for the thermal conductivity of the insulation on the recoverability, and on the resistance ($S_1 = -0.058$), the correlation is positive for the robustness ($S_1 = 0.018$).

The solar absorptance is within the range of variables the one with the lowest impact on all the three indicators ($S_T(\text{resistance}) = 0.227$; $S_T(\text{robustness}) = 0.095$; $S_T(\text{recoverability}) = 0.284$).

To summarize, the most important variables to consider are the glazing g-value, infiltration, the specific heat of the interior layer and to a lesser extend the glazing U-value and the thermal conductivity of the insulation. Lower g- and U-values of the glazing correlate for all the outputs with an increased performance (lower output values). Whereas for the three remaining the correlation differs per output.

5.2 Output performance distribution

The plotted frequency distribution of the output indices (Fig. 33) for the defined resilience indicators of resistance (Fig. 33a), robustness (Fig. 33b) and recoverability (Fig. 33c), shows a large output range of the separate indicators.

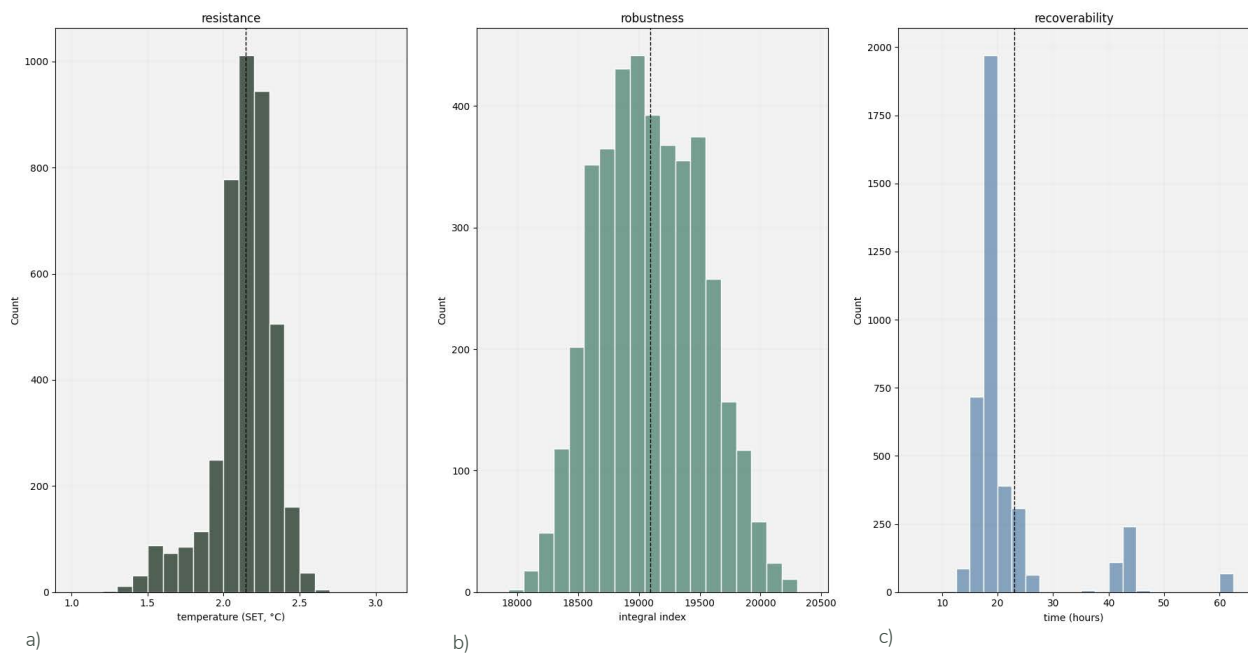


Figure 33: Frequency distribution of the resistance (a), robustness (b), and recoverability (c) output indices on the x-axis; frequency count on the y-axis; mean per index as black dashed line. Source: own

The resistance, measured in the temperature difference between the SET at the start of the heat wave and the comfort threshold of 24°C (SET), ranges from a minimum of 1.26 °C and 2.66 °C. The mean of 2.146 °C (SET) and the median of 2.16°C show the slight skewness of the distribution to the left. Although this would indicate a higher percentage of the input combinations shows a more positive result, only two combination variations have an output of 1.26°C. After which the output values are increasing notable.

To measure the robustness, the integral index, the integral of the SET over time, depicts the unmet hours of thermal comfort including its severity. The range here is from 17970.15 to 20459.30. With a mean of 19094.08 and median almost identical (19000), the distribution of the output values is almost symmetrical. With a significantly smaller frequency, the lower output values are increasing rapidly.

The recoverability, measuring the time in hours until the thermal zone is reaching the comfort threshold at 24°C SET again, ranges from 12 to 84 hours. Note, that the three concentrations of counts appear due to the fact that the recoverability is measured in hours. Since it is obvious that most frequent output values occur at $12/24 \times x$ hours, it can be assumed that the recovery happens after x days. While the best scenario is thus a recovery after 12 hours (e.g., after cooling down during the night after the peak of the heat wave), the worst-case scenario shows a recovery after 3.5 days ($(24hrs \times 3) + 12hrs = 84hrs$). The

distribution shows a large difference between the mean (23.02 hours) and the median (19 hours). 50% of the samples are resulting in a recoverability of less than 19 hours.

5.3 Identification of best performing scenarios

To further identify the scenario with the best overall performance, an input variation must be found with sufficient results for each of the indicators. For this reason, the three indicator indices must be standardized and made comparable. Thus, the sample values are compared regarding their standard deviation and the mean of each indicator. The computed z-factor measures the distance of each point in numbers of standard deviations to the mean of the population values. The “Kernel Density Estimate” (KDE) (Figs. 34) shows the outcome of the distribution of the z-factors for each indicator (on the y-axis the estimated probability density for each value of the z-factor). The integral between x-axis and graph gives a total of 1.

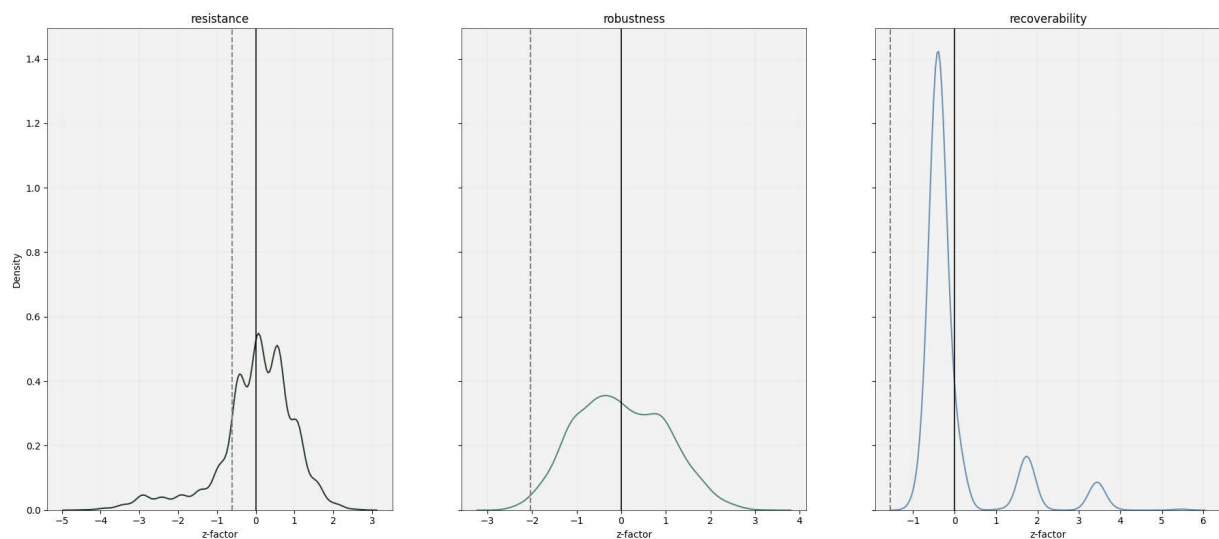


Figure 34: Kernel-density estimate for the z-factor for each indicator, the x-axis: distance to the mean in number of standard deviations solid line: mean of each output distribution; dashed line: 5th percentile. source: own

A percentile-based threshold can be calculated based on a given percentage or confidence level. The condition of having each output value within the calculated percentile, pre-selects input variations to consider. From input variations with results within the 5th percentile (within the top 5% values; illustrated by the dashed line in the plot) of each performance indicator the total mean of output values can be calculated. The scenario with the lowest mean value is chosen as the scenario with the largest potential of the best overall performance. Note that even though the previous steps of the calculation of the percentile could be done with the actual outcome indices values, however, to be able to calculate the mean per indicator combination, the standardization is necessary – here done by using the z-factor. The calculation is resulting in two possible input variations, falling within the selection of output values within the top 5% of each indicator.

Additionally, to the overall best performing scenarios, also the best performing ones per indicator can be derived. Within the sample size of 4096 possible input variations, per indicator, the five best performing ones are selected to be further analysed.

Plotting both the variable values of the best performing scenarios per resilience indicator, the relations between the indicator values become visible (Fig. 35). It becomes obvious, that the most ideal ones for the separate indicators, show less promising results for the other two indicators.

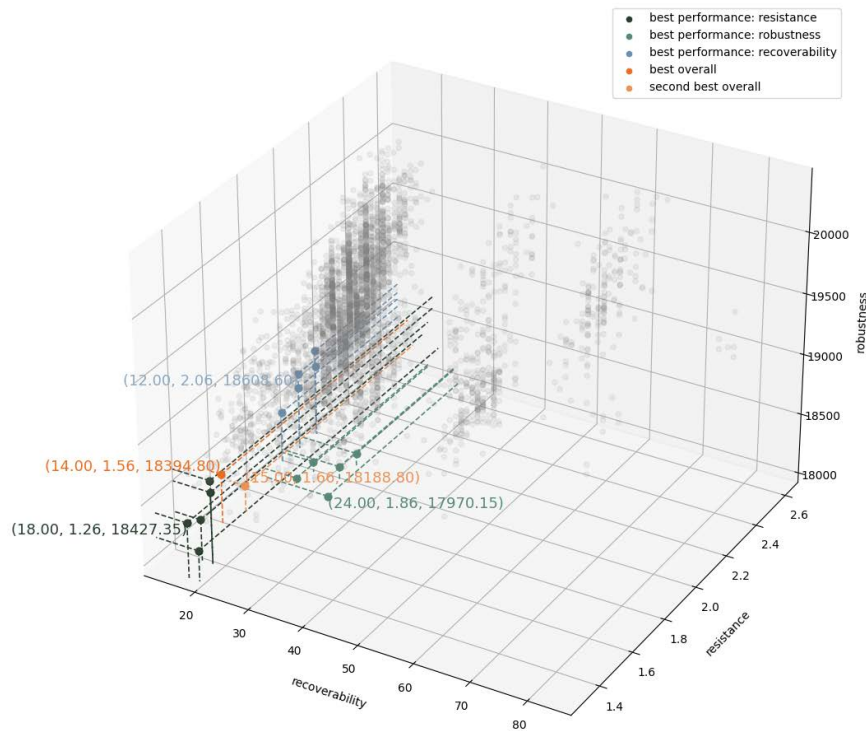


Figure 35: Comparison of performance outcome with the recoverability on the x-axis, the resistance on the y-axis and the robustness on the z-axis: most resistant scenarios in dark green, most robust in green, and scenarios with the shortest time of recovery blue; scenarios with the assumed best overall performance in orange. source: own

To conclude: the scenarios, which show the most promising results for one resilience indicators have reduced performance regarding the other two indices. The scenario with the assumed best overall performance show a compromise between the best performing scenarios.

5.4 Variable values comparison

A heatmap plot for the five best- and worst-performing scenarios per indicator shows the correlation between the actual input values and the calculated output values (Fig. 36). Hereby, the variable of the specific heat of the structural component of the wall, as well as the solar absorptance of the exterior finishing not considered. Previous results prove their little impact on the output values.

The values of the window's **g-value** for each of the five best-performing ones per indicator are equally low. They range only between 0.1 and 0.2, with 0.1 being the lowest possible g-value of the initial given range. Accordingly, for the five worst-performing ones per indicator, the g-value ranges between 0.64 and 0.78, reaching almost the upper bound of the given range of 0.8.

The initially constrained range of input values for the glazing **U-values** accounts for their limited variability across the 30 scenarios. Across all indicator outputs of the best-performing scenarios, almost all values surpass $1.1 \text{ W/m}^2\text{K}$. This indicates a consistent tendency towards higher values within the given range of $0.6\text{--}1.3 \text{ W/m}^2\text{K}$ as possible values of the glazing U-value. Equally, the mean of $0.84 \text{ W/m}^2\text{K}$ within the 15 worst-performing scenarios, suggests a tendency of lower thermal conductivity worsening the performance.

For the remaining three input variables of the specific heat of the interior finish, the infiltration and the thermal conductivity, no clear tendencies are apparent throughout the 15 scenarios of the best and worst performing scenarios.

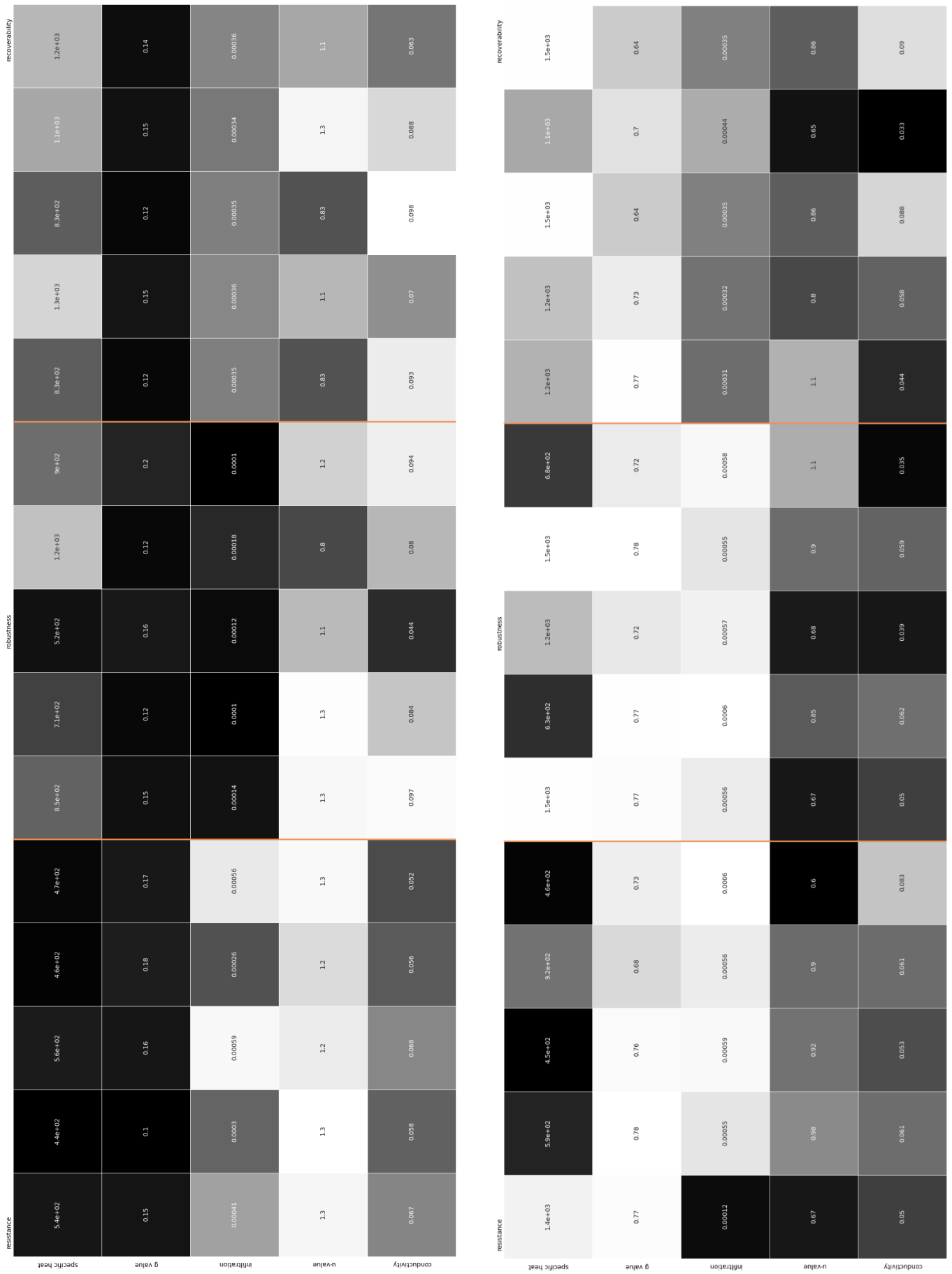


Figure 36: Heat map of variable values (horizontal) and best- (a) and worst- (b) performing variable combinations (one scenario design in one vertical column) of the best five performing ones of resistance (left), robustness (centre) and recoverability (right)
input variables: specific heat of interior finish, g-value of window, infiltration, U-value of glazing and thermal conductivity of insulation
source: own

Among the top five performing scenarios in terms of resistance, the average **specific heat** value is 494 J/kgK. In contrast, the worst-performing scenarios have an average of 764 J/kgK for this variable. This confirms the correlation between lower specific heat values and lower output values for the resistance indicator. For the "robustness" indicator, the best-performing scenarios have an average of 836 J/kgK, while the worst-performing ones have a higher average of 1102 J/kgK. In the case of the results for the recoverability, the mean value for the best-performing scenarios is 1052 J/kgK, whereas, for the worst-performing ones, it is 1300 J/kgK. Considering the initial range set between 400 and 1500 J/kgK, it can be generally observed that the best-performing scenarios fall within the lower and middle parts of the range. Conversely, poorer performance is observed in the upper part of the range.

Regarding the **infiltration**, the analysis indicates that better performance in terms of the façade's resistance is achieved when limiting it to values in the middle to upper range. A high level of infiltration leads to poorer performance. However, this tendency is not consistently confirmed when combining low infiltration with low glazing U-values and high specific heat values (see the first one of the worst-performing ones). For the robustness indicator, a clear trend demonstrates lower infiltration values corresponding to better performance, with higher infiltration values corresponding to poorer performance. In terms of recoverability, it appears that infiltration becomes a significant variable only when combined with changes in other input variables. Both the top-performing and worst-performing scenarios show values around the midpoint of the given input range (0.0003), with identical averages of 0.00035.

When comparing the **thermal conductivity** values, it appears that lower values have a slight negative impact on both the robustness and recoverability indicators. Conversely, higher values, closer to the upper limit of the specified range, seem to have a positive effect. In terms of the resistance indicator, both the top performing, and worst-performing scenarios show average values that fall within the middle range of the given input range. The average for the top five scenarios is at 0.050 W/mK, with the average of the worst-performing scenarios just slightly higher at 0.053 W/mK.

As already concluded from the analysis of the variable sensitivities, it seems that the values for the specific heat of the interior finish, the infiltration, and the thermal conductivity of the insulation are opposing between the optimized scenarios per indicator. However, for the two scenarios with the assumed best overall performance, it can be noted that their values for the specific heat and for the infiltration are in a similar range (Fig. 37). Only the value of the thermal conductivity seems to change.

The five most resistant scenarios show generally low specific heat values. For both the most robust and the ones with the best recoverability, the specific heat is generally higher. The infiltration is generally on the lower level for the most robust scenarios, in the middle range for enhanced recoverability and in the upper range for the most resistant options. Also, for thermal conductivity, the most resistant scenarios (with generally lower values) are in contrast to the most robust option as well as the best-performing scenarios in recoverability (with generally larger values). Thus, the low thermal conductivity of the insulation seems to only improve the performance when combined with a low specific heat of the interior layer, improving the resistance.

In short: the variable values match the predicted correlations of Chapter 5.1. Within the five variables with relevant impact: the tendency to achieve smaller output values goes for the glazing g- and U-value to smaller values, equally for all three performance indicators. Whereas, for the specific heat of the interior layer, the thermal conductivity of the insulation and the infiltration different correlations are detected within the different performance indicators. Notably is that the contrast is especially between the values for the most resistant scenarios and those enhancing robustness and recoverability.

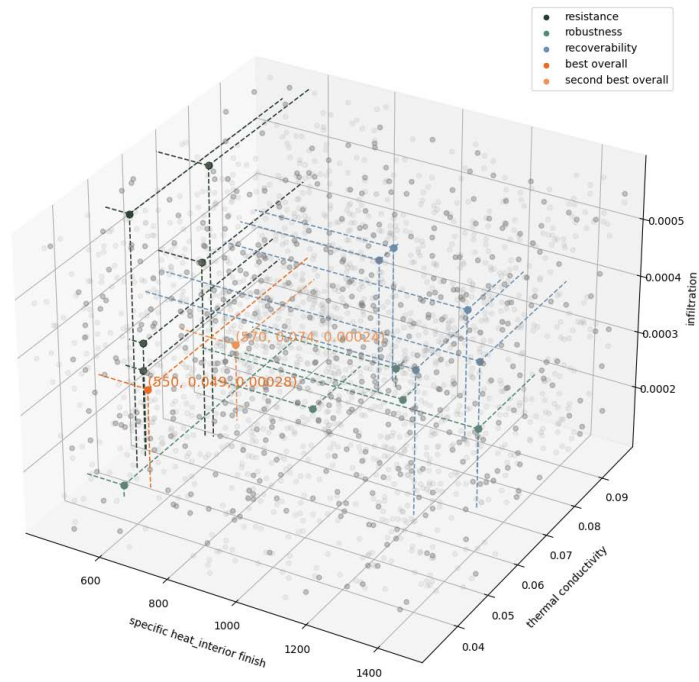


Figure 37: 3D plot of the most contradicting variables: the specific heat of the interior finishing (x-axis), the thermal conductivity of the insulation (y-axis) and the infiltration (z-axis) with the top five performing scenarios per indicator (each scatter illustrates one scenario) with the best performing ones of the resistance (dark green), robustness (green) and recoverability (light blue); overall best performance in dark orange, second best overall performance in light orange
source: own

Accordingly, design cases for the further analysis are developed. The variables with a consistent tendency throughout all the top performing scenarios (U-value, g-value), as well as the variables with little impact (specific heat of structural wall, solar absorptance of the exterior finish) has been kept constant for all the case designs.

Table 8: Material properties of design cases as per research results
source: own

	infiltration	structural wall	exterior insulation	exterior finish	interior finish	glazing	glazing
	air flow per square meter of exterior facade (m ³ /m ²)	specific heat (J/kgK)	thermal conductivity (W/mK)	solar absorptance	specific heat (J/kgK)	u-value W/m ² K	g-value
"res design case" best performance in resistance	0.00041	840	0.067	0.7	537	1.1	0.15
"rob design case" best performance in robustness	0.00014	840	0.097	0.7	851	1.1	0.15
"rec design case" best performance in recoverability	0.00035	840	0.093	0.7	828	1.1	0.15
"top design case" overall best performance	0.00028	840	0.049	0.7	550	1.1	0.15
base case	0.00060	840	n.a.	0.7	1000	2.7	0.6

The U- and g-value of the design cases is established by calculating the average over all 15 best performing scenarios. The specific heat of the structural wall as well as the solar absorptance of the exterior finish remain unchanged.

For the specific heat of the interior finish, the infiltration and the thermal conductivity of the insulation, value have been set according to the best performing scenario per indicator. Table 8 shows the developed design cases. Note that all other simulation parameters are equal to the base case and kept as described in chapter 4.3.1 and 4.3.2.

5.5 Index evaluation and final rating of design cases

For the final analysis, the design cases, as discussed in chapter 5.4, are input for a final run of simulations. From the simulation output, again, the resilience indicators are calculated. However, this time, additionally to AMY heat wave weather data of 2015, for the calculation of the adaptive capacity, predictive data of 2050 and 2080 is used.

Results for the five scenarios, assuming conditions as described above are the following (Table 9). Note that for the overall performance, the indices are normalized, using the formula:

$$x_{normalized} = \frac{(x - x_{minimum})}{range\ of\ x} \quad (2)$$

This means that the range of the values per index and per year of analysis are normalized on a scale from 0 to 1. The lower the value, the lower the corresponding index value of the indices, and the better the performance. For the adaptive capacity, the normalized performance rating of the design case of the three analysis years is added up and divided by the number of years considered in the analysis. The following formula is proposed:

$$adaptive\ capacity = \frac{\sum_{first\ year\ of\ analysis}^{last\ year\ of\ analysis} normalized\ case\ performance}{number\ of\ analysis\ years} \quad (3)$$

Table 9: Index calculation for design cases with unrestricted ventilation including calculation with predictive weather data. Indices are normalized and cumulated, before the FRI is derived. source: own

		resistance performance	robustness performance	recoverability performance	normalized	normalized	normalized	overall performance	adaptive capacity	total FRI
2015	base case	4.96	19400.30	15	1.00	1.00	0.43	2.43	1.97	4.40
	top case	3.86	19003.69	14	0.39	0.56	0.17	1.12	1.39	2.51
	res case	3.16	19241.25	19	0.00	0.82	0.58	1.41	1.13	2.54
	rob case	4.06	18493.80	17	0.50	0.00	0.42	0.92	1.75	2.67
	rec case	3.16	18961.95	12	0.00	0.52	0.00	0.52	1.12	1.64
	combined case	3.16	18493.80	12	0.00	0.00	0.00	0.00	1.15	1.15
2050	base case	9.46	27914.10	88	1.00	1.00	1.00	3.00		
	top case	8.56	27696.20	88	0.18	0.53	1.00	1.72		
	res case	8.66	27445.75	40	0.27	0.00	0.00	0.27		
	rob case	8.36	27825.25	65	0.00	0.81	0.52	1.33		
	rec case	8.56	27642.70	88	0.18	0.42	1.00	1.60		
	combined case	8.66	27825.25	88	0.27	0.81	1.00	2.08		
2080	base case	11.56	28282.45	60	0.47	0.00	0.00	0.47		
	top case	10.76	29524.55	82	0.05	0.97	0.31	1.34		
	res case	10.76	29553.60	107	0.05	0.99	0.67	1.71		
	rob case	12.56	29565.40	130	1.00	1.00	1.00	3.00		
	rec case	10.66	29472.40	82	0.00	0.93	0.31	1.24		
	combined case	10.76	29565.40	82	0.05	1.00	0.31	1.37		

To simplify the analysis, the design cases in this study have been given specific names. The initial state is referred to as the "base case," while the design case assumed to have the best overall performance is called the "top case." The retrofit option with the highest resistance is called the "res case," and "rob" is short for "robustness." Similarly, "rec" represents "recoverability." A fifth design case, known as the "combined case," has been introduced, assuming optimization based on each resilience stage during the disruption period. Theoretically, the "combined case" combines the resistance performance of the "res case," the robustness of the "rob case," and the recoverability of the "rec case."

In the 2015 scenario, the output shows the widest range. Here, the results demonstrate, as assumed, that the design cases perform the best in terms of the specific index they are optimized for. This means, the normalized resistance index is 0 for the "res case," the robustness index is 0 for the "rob case," and the recoverability index is 0 for the "rec case." The design cases significantly improve the resistance and robustness performances compared to the base case scenario. In terms of resistance, this corresponds to an improvement of 1.8°C compared to the base case. However, the recoverability of the base case is enhanced by the "res design" but worsened in the "rec design," with the "res case" reducing recoverability by four hours, resulting in a recovery time of 19 hours.

In both, the 2050 and 2080 scenario, the results show smaller differences. For example, in the 2050 heat wave scenario, the "res" design only improves the resistance performance of the base case by 0.8°C, while recoverability remains unchanged. In the 2080 scenario, only the façade's resistance improves, while both robustness and recoverability decline with any retrofit option.

Regarding adaptive capacity, the "combined case" performs the best, followed by the "rec case," making them the top-performing scenarios overall. Conversely, the base case receives the lowest rating, with an FRI (Final Resilience Index) of 4.40. This indicates that the design cases enhance the performance of the base case in each disruption period. Thus, the "combined" or "rec" design case would be considered the most effective scenario based on performance.

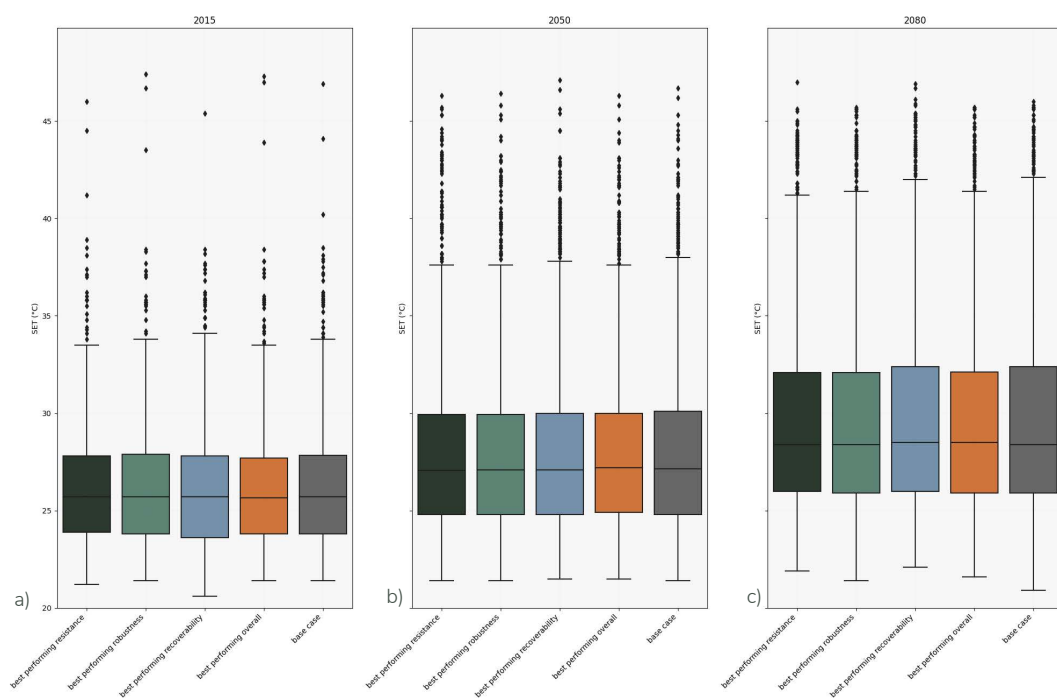


Figure 38: Boxplot of the SET hourly data with unrestricted ventilation during the simulation period per design scenario (dark green: "res" case; green: "rob" case; blue: "rec" case; orange; "top" case; grey: base case) and year a) 2015; b) 2050; c) 2080. source: own

A box plot of the SET over the whole simulation period however shows a distribution with almost no changes within the base case scenario and the four design cases (Fig. 38).

The assumption has been made that the effect of an originally constant parameter overshadows the effect of the chosen design parameters. And indeed, when changing the conditions of the natural ventilation, thus the opening/closing schedule of the windows, the results change significantly.

In addition to the requirement of the minimum indoor temperature of 26°C and a minimum difference to the exterior temperature of 2°C (lower than indoors), the minimum exterior temperature is set to 15 and then to the extreme case of 25°C.

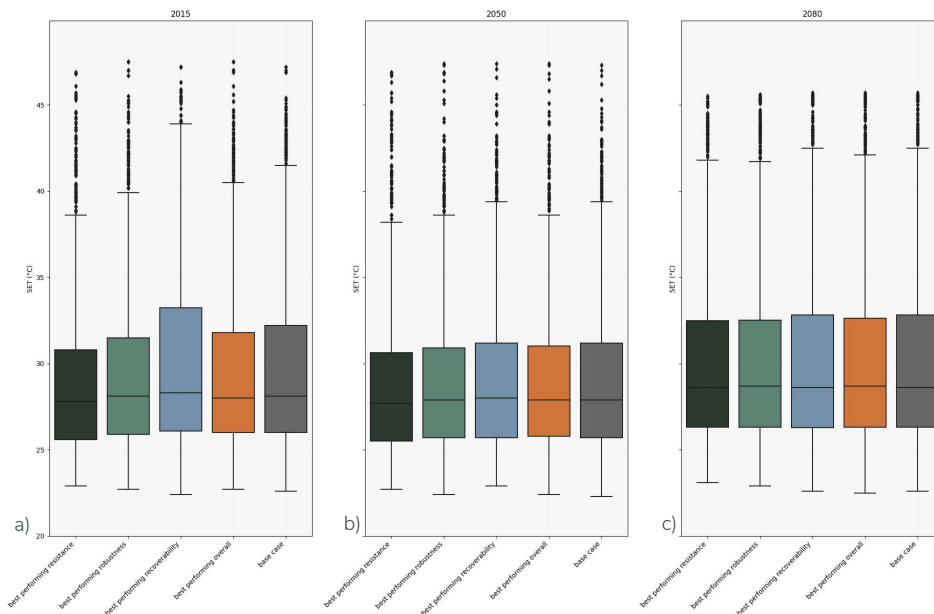


Figure 39: Boxplot of the SET hourly data with ventilation requirements (exterior temperature min. 15 degrees) during the simulation period per design scenario (dark green: "res" case; green: "rob" case; blue: "rec" case; orange; "perf" case; grey: base case) and year a) 2015; b) 2050; c) 2080. source: own

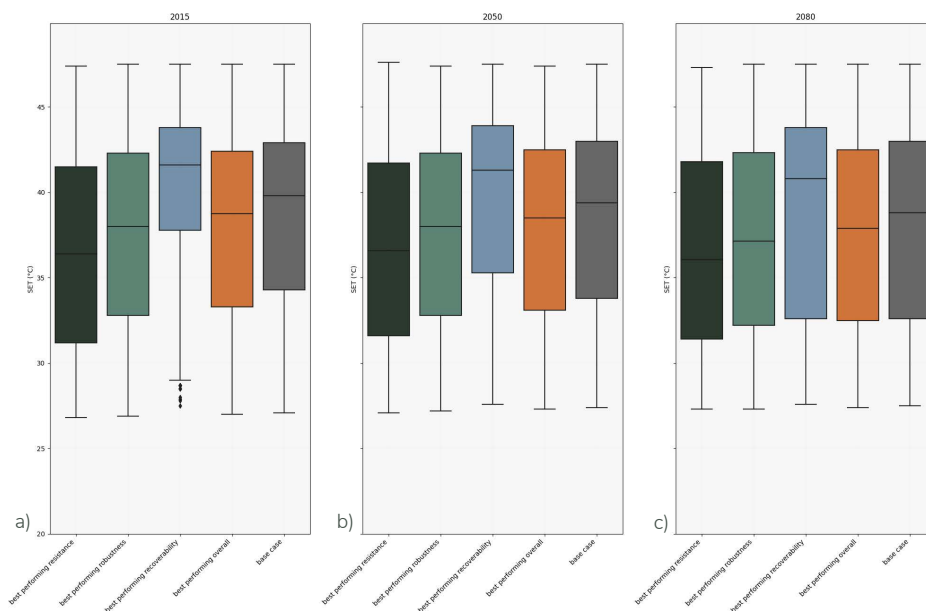


Figure 40: Boxplot of the SET hourly data during the simulation period with ventilation requirement (exterior temperature min. 25 degrees) per design scenario (dark green: "res" case; green: "rob" case; blue: "rec" case; orange; "perf" case; grey: base case) and year a) 2015; b) 2050; c) 2080. source: own

Still, when considering the ventilation requirement of a minimum exterior temperature of 15 °C, the hourly SET data from the simulation period shows only slight fluctuation between the different design cases, also compared to the base case scenario (Fig. 39). Whereas, when the ventilation requirement is increased to

the minimal exterior temperature of 25 °C, the medians of the resulting SET data for each of the design cases vary considerably, with, compared to the scenario at Figure 38, a general, significant increase.

The impact of the design cases scarcely visible when windows are generally opened during the day (scenario Fig. 38). When those become more apparent in scenario visualized in Figure 40, it becomes obvious that the design case optimized for its performance of the resistance indicator, generally performs the best in terms of daily indoor temperatures. On the other hand, when the retrofit scenario focuses on improving the recoverability indicator, the indoor SET values tend to increase, in case of decreased ventilation and infiltration.

Using the Future Resilience Index (FRI) as an evaluation method for the design cases with restricted ventilation (exterior temperature min. 25°C), the differences are not as evident (Table 10). However, it reveals that the "rec case" leads to a decline in performance (FRI of 4.22 compared to the base case performance of 2.10). It also demonstrates the improved performance of the "res case" with an FRI decrease from 2.10 (base case) to 1.92 (res case), although the improvement may not be as evident as observed in the SET data comparison.

Furthermore, when considering the performance per index, it appears that the design cases do not consistently achieve improvements in the façade's current state. The normalized indices seem to display a larger difference than the actual given performance output. In case of the resistance, the performance of the base case scenario is only slightly improved in the 2080 heat wave scenario. The robustness is in none of the cases improved, whereas the recoverability only shows a slight improvement in the 2080 scenario, and in the 2015 scenario for the "top", "res" and "rob" case.

Table 10: Index calculation for design cases with restricted ventilation (exterior temperature min. 25 degrees) including calculation with predictive weather data. Indices are normalized and cumulated, before the FRI is derived. source: own

		resistance performance	robustness performance	recoverability performance	normalized	normalized	normalized	overall performance	adaptive capacity	total FRI
2015	base case	10.06	36375.15	123	0.00	0.00	0.86	0.86	1.24	2.10
	top case	10.96	38452.1	98	0.56	0.59	0.00	1.16	1.44	2.59
	res case	10.46	37312.45	112	0.25	0.27	0.48	1.00	0.92	1.92
	rob case	11.66	37747.15	98	1.00	0.39	0.00	1.39	1.75	3.14
	rec case	10.66	39875.05	127	0.38	1.00	1.00	2.38	1.85	4.22
	combined case	10.46	37747.15	127	0.25	0.39	1.00	1.64	1.22	2.86
2050	base case	13.66	38773.1	170	0.00	0.59	1.00	1.59		
	top case	13.96	37052.1	170	0.50	0.00	1.00	1.50		
	res case	13.76	37943.55	170	0.17	0.31	1.00	1.47		
	rob case	14.26	38289.35	170	1.00	0.43	1.00	2.43		
	rec case	13.76	39954.3	170	0.17	1.00	1.00	2.17		
	combined case	13.76	38289.35	170	0.17	0.43	1.00	1.59		
2080	base case	16.16	37148	83	0.25	0.00	1.00	1.25		
	top case	16.46	38421.25	81	1.00	0.66	0.00	1.66		
	res case	16.06	37691.45	81	0.00	0.28	0.00	0.28		
	rob case	16.46	37990.3	81	1.00	0.43	0.00	1.43		
	rec case	16.06	39090.25	81	0.00	1.00	0.00	1.00		
	combined case	16.06	37990.3	81	0.00	0.43	0.00	0.43		

In summary, the "res" retrofit option shows promising results in terms of the improvement of the indoor SET during the heat wave simulation period for the current climate and in future. However, these

improvements are observed primarily when ventilation is restricted for exterior temperatures below 25 degrees, leading to excessively high interior SET values. Even with the implementation of retrofits, the median SET data remains above 35 degrees in all cases. When comparing the analysis outcomes based on the proposed indices, the differences between the results are minimal. It becomes evident that the use of predicted future weather data nearly eliminates the variability between the different index outcomes.

5.6 Discussion of research results

The research proposes a methodology to enhance the design process of retrofit options improving building thermal resilience to current and future heat waves. Studying the impacts of seven selected façade retrofit variables on developed resilience indicators, a sensitivity analysis is conducted on a case study example in Munich. Based on the results, potential retrofit options can be designed and evaluated in terms of their effectiveness in enhancing building thermal resilience to heat waves.

From the sensitivity analysis, it can be concluded that certain parameters have an equally strong impact on all three performance indicators. However, it is important to note that the correlation between variables may differ. Thus, the variables can be categorized into parameters with minimal impact (and therefore neglected in further analysis), variables with strong impact, and variables with significant impact but contradictory correlation across the different performance indices.

The façade characteristic that consistently improves the building's thermal resilience to heat waves in the case study location is the solar heat gain coefficient (g-value) of the glazing. A strong correlation of low g-value (0.12-0.15) expresses the necessity of exterior sun shading for achieving the best performance in each stage. A lower g-value of the window reduces the solar heat gain through transparent surfaces, which highlights the importance of solar radiation as a key influencer of thermal comfort in extreme heat periods.

Lowering the thermal transmittance (U-value) of the glazing also positively impacts the façade's performance in each resilience stage. A lower U-value reduces conductive heat transfer from the exterior to the interior, thereby decreasing heat gain through the window. This influences the resistance (as the interior space not heating up as much in first the place), the robustness (the "peak" gets reduced) and the recoverability (the reduced "peak" of indoor temperature is also faster equalized).

Both, a change of the specific heat of the structure, as well as the solar absorptance of the exterior finish only have minimal effect on each of the indices, in each of the resilience stages. Surprisingly, the specific heat of the interior layer has a more significant influence on the performance than variance in the specific heat of the structural part of the wall. This could be explained by the fact that the radiation from the interior walls has a strong influence on thermal comfort in extreme heat periods. The heat "buffer" of the interior finish becomes more important than the reduced conductive heat transfer within the exterior wall during the day.

Regarding the solar absorptance of the exterior finish, it appears that reducing heat flow through lower thermal conductivity is more crucial than reducing heat gain through lower solar absorptance of the exterior finish. Thus, the results of the literature review concerning the positive effect of the surface albedo (as contrary to the solar absorptance) (Sun et al., 2020, 2021; C. Zhang et al., 2021) cannot be proven for the location of Munich.

The thermal conductivity and the specific heat of the interior finish, as well as the infiltration rate, show contrasting correlations between the most resistant retrofit option and the robustness and recoverability resilience stages. When optimized for the façade's resistance, the results of the most resistant retrofit option show the tendency of a lower thermal conductivity of the added insulation and lower specific heat of the interior finish, compared to other design cases. With a higher thermal resistance, the added insulation results in a slower heat transfer during the day, and thus prevents the interior space from overheating at the start of the heat wave. Additionally, the lower specific heat of the interior finish facilitates rapid heat dissipation from the interior to the exterior, preventing thermal energy storage in the wall and the "build-up" of heat during the early stages of the heat wave.

In contrast, the results of the retrofit with the best performance at the end of the disruptive period, show comparatively higher values for the thermal conductivity and for the specific heat of the interior layer. The high specific heat of the interior finish acts as a heat buffer during the day, reducing peak interior temperatures. The low thermal conductivity of the added insulation improves the release of heat to the outside.

To enhance the building's robustness to heat waves, additionally to a comparatively high specific heat of the interior finish and low thermal conductivity, a significantly lower infiltration rate seems to be beneficial. The airflow from the warmer exterior to the interior during the day is reduced, which leads to a reduction of inside temperatures and thus to an improvement of the robustness. However, it seems that the heat buffer only works when there is the possibility of night-time ventilation. In cases of restricted night-time ventilation, the stored heat of the interior finish, which is released during the night, is trapped in the interior space, and eventually worsens the performance, resulting in higher temperatures the following morning.

Overall, each of the resilience stages shows different results for the ideal design of a facade retrofit. Especially, it seems that enhancing the façade's resistance to heat waves contradicts the improvement of the façade's robustness and recoverability. Consequently, the retrofit option assumed to perform the best demonstrates intermediate variable values between the resistance-optimized scenario (lower thermal conductivity, lower specific heat) and the robustness-optimized scenario (low infiltration). However, the theoretical "combined" design case captures the potential of retrofitting the facade to be responsive to resilience stages. It adapts its properties to the most resistant design during the initial disruption period, when outside temperatures are increasing, and transitions to properties aligned with optimized robustness and recoverability as these become increasingly important during the heat wave period. This allows for higher specific heat and higher thermal conductivity, facilitating improved recoverability. The façade's properties would "respond" to the requirements of a façade design enhancing building thermal resilience.

When evaluating the developed design cases for the retrofit of a residential case study building in Munich, it becomes evident that the aspect of ventilation needs careful consideration. With unrestricted ventilation during the night, the nighttime recovery effectively counteracts the impact of façade interventions. In the climate of Munich, even during heat waves, the temperatures during the night are low enough to recover the increased daytime temperatures. This aligns with the findings of the literature study, which highlight the importance of nighttime ventilation in combination with discussed façade retrofits (Ji et al., 2022; Schünemann et al., 2022; Sun et al., 2020, 2021). However, this highlights the significance of the developed resilience index, which captures specifically the thermal comfort of occupants during heat wave periods rather than solely capturing the overall risk of overheating.

With restricted night-time ventilation, the resistance of the façade retrofit to extreme temperatures becomes more important. Even though the interior space is overheating regardless of the applied retrofit, the best-performing scenario optimized for the resistance appears to improve the performance. This implies that the goal of the most resistant retrofit of minimizing the temperature increase at the start of the heat wave (during the day) is achieved.

It must be acknowledged that there is room for further improvement in the evaluation method used. The developed indices show promising results as design indicators. The developed design cases meet the assumed improvement of performance, especially visible in the 2015 scenario, thus the indices effectively capture the façade's performance at different stages of the heat wave period. However, the method needs to investigate in more detail the consideration of future weather data. The façade's performance in the 2050/2080 heat wave scenario requires more sensitive indices, as otherwise, the climate conditions seem to overshadow the changes in performance. Especially the "robustness" index needs refinement: the index results do not align with the outcome of the overall SET during the whole simulation period.

The normalization of the indices allows for comparability but requires careful consideration of the range of data and their impact but has been simplified in the progress of this thesis. E.g., six considered design cases, show only limited variety in the output index, thus, the impact on the output, with the minimum of "0" and the maximum of "1" is too strong to reflect the actual difference in performance.

In general, the identified resilience indicators with their corresponding, proposed resilience indices are a valuable tool to improve the design process of retrofits, by enhancing decision-making for improved building thermal resilience during heat waves.

For easier application, further development of the evaluation could also include performance classifications. Commonly used in assessing energy efficiency of buildings (Bundesministerium für Wirtschaft und Klimaschutz, 2013; Rajagopalan & Leung Tony, 2012), it has been proposed for the assessment of the thermal resilience performance of retrofits (Homaei & Hamdy, 2021a; Ji et al., 2022). Applied to the proposed metric, the classifications "A/B/C" etc. would simplify ratings for the overall performance, but also for the façade's resistance, robustness, and recoverability. The classification system, when based on empirical data of multiple scenarios, would give clear indications, also when only one single scenario is evaluated.

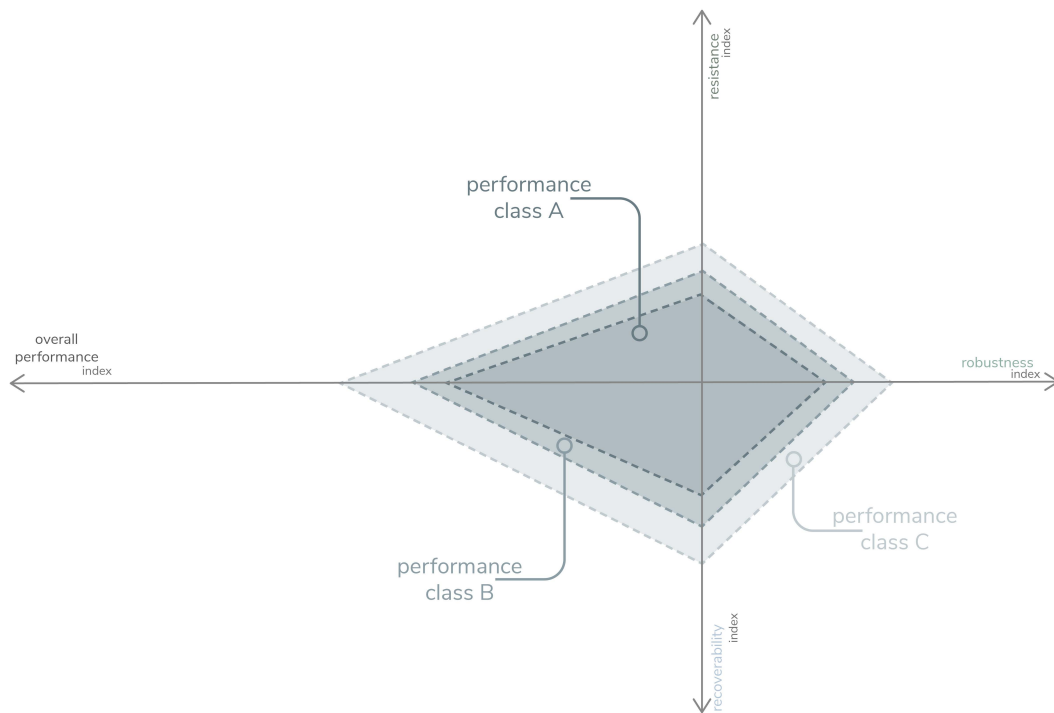


Figure 41: Empirical-based classification scheme "A/B/C" proposed for the overall thermal resilience performance of facades, considering their resistance, robustness, and recoverability. source: own

5.7 Conclusion


When concluding on the proposed framework for the enhancement of decision-making in the design process of façade retrofits for improved thermal resilience of a residential case study building in Munich, two aspects need to be considered: First, the workflow methodology, which includes the proposed strategy of four resilience indicators as resilience indices, corresponding to four stages of the disruption of a heat wave. And second, the final retrofit design for the chosen case study location.

Resistance, robustness, recoverability, and adaptive capacity are proposed as design indicators for retrofit options. They not only guide the decision-making, but they also finally evaluate the façade's performance during heat waves. It can be concluded that the proposed framework is applicable as a tool for the decision-making process during the design of retrofits for enhanced thermal resilience, effectively improving the façade's performance of the specified resilience stage. As the only constraint the ventilation parameter requires more careful consideration. The framework can be adjusted, and the resulting design can be optimized for overall performance, or in terms of one specific characteristic. However, the application of the indices as an evaluation tool for the overall performance needs further investigation, especially in terms of the consideration of future climate scenarios. The same can be said about the formulation of an overall index: the calculation, including the four separate indices needs to be further refined.

For the ideal retrofit design of the location of Munich, certain recommendations can be given. The retrofit design should almost certainly include added external shading devices (lower solar heat gain coefficient/g-value). Additionally, the replacement of the low-performing windows with those with lower thermal

transmittance (U-value), is necessary to align with building requirements for the building's energy efficiency (German EnEV regulation). Both interventions reduce the heat gain during extreme heat periods, the lower g-value significantly, and the lower U-value markedly.

It is important to note that the design for enhancing the façade's resistance conflicts with the design for enhancing the façade's robustness and recoverability. The decision-making during the design process for any other property than the g- and U-value of the windows of the retrofit façade, thus strongly depends on individual requirements: e.g., the given ventilation schedule, as well as the specific programme to design for. In scenarios where night-time ventilation is restricted with the windows closed during the night, the façade's resistance performance should be given the largest attention – then it is especially crucial to keep the heat out during the day. When windows can be opened during the night, the retrofit design should additionally improve robustness and recoverability. To improve robustness, the incoming convective heat flow should be decreased during the day by decreasing the infiltration rate significantly. For improved recoverability, heat buffer is required that stores any transferred heat, and only slowly releases the heat during the night, where ventilation reduces the heat load. Thus, the combination of enhanced resistance, robustness and recoverability concludes on the best performing retrofit option for the location of Munich.



Materialisation and design

- 6.1 Materialisation of parameter values
- 6.2 Resilience performance evaluation of retrofit

6.1 Materialisation of parameter values

It is concluded that the ideal retrofit design in terms of its performance improving the building's thermal resilience for a residential building in Munich (with natural ventilation unrestricted during the night) considers the most important parameters of all three separate indicator designs. As discussed in Chapter 5.6, the primary factor for a resistant design is added insulation, to reduce the conducted heat through the exterior wall. To improve the façade's robustness, the airtightness should be reduced, to lower the convective heat flow. For improved recoverability, the most crucial aspect is the addition of an interior layer with high specific heat properties. The resulting heat buffer helps to reduce the peak load and improves the possibility of releasing heat during the night. Note that the following materialisation is specifically designed for a living area, with estimated minimal occupancy during the night.

The insulation of the most resistant retrofit option has a thermal conductivity of 0.069 W/mK and a set thickness of 20cm, with a resulting required thermal resistance (R) of 2.9 m²K/W. To reach the same R with a reduced thickness of 14 cm (example value), a thermal conductivity of 0.043 W/mK is needed.

Table 11: Derivation of design values for reduced thickness insulation while meeting thermal resistance requirements. source: own

	insulation thickness	insulation thermal transmittance	insulation thermal resistance
given	$d = 200\text{mm} = 0.2\text{m}$	$\lambda = 0.069 \frac{\text{W}}{\text{mK}}$	$R = \frac{d}{\lambda} = \frac{0.2\text{m}}{0.069 \frac{\text{W}}{\text{mK}}} = 2.9 \frac{\text{m}^2\text{K}}{\text{W}}$
designed	$d = 140\text{mm} = 0.140\text{m}$	$\lambda = \frac{d}{R} = \frac{0.14\text{m}}{2.9 \frac{\text{m}^2\text{K}}{\text{W}}} = 0.043 \frac{\text{W}}{\text{mK}}$	$R = 2.9 \frac{\text{m}^2\text{K}}{\text{W}}$

To improve recoverability, it had been found that the required thermal conductivity and the specific heat conflict the requirements for the improvement of resistance. However, for the recoverability the increase of specific heat of the interior layer, to create a thermal buffer during the daytime, can be identified as the key aspect. This results in a slow heat release during the night, which reduces the peak and therefore the recovery time due to night-time ventilation.

To address the contrasting requirements of improving both, resistance and recoverability, a phase change plasterboard is proposed. The material absorbs the transferred heat during the day and liquifies. But due to the energy needed during the phase change, the resulting temperature of the board almost stays the same. When the ambient temperature decreases, the PCM undergoes the reverse phase transition, releasing the stored heat energy back into its surroundings. The phase change material solidifies or condenses. During this process, it releases the latent heat it had previously absorbed. The specific heat is proven to be lower in the liquid state, than in the solid state (Jansone et al., 2018) – responding to the requirements of the enhanced resistance and recoverability of a thermally resilient retrofit. The “KNAUF Comfortboard” (Knauf, 2014) thus promises to reduce the peak indoor temperature, and improve night-time recovery (when (natural) ventilation is guaranteed).

Furthermore, the window g-value is reduced by exterior Venetian blinds. The assumed occupancy schedule allows for reducing the view quality during the day. Thus, the Venetian blinds can be closed during the day, which reduces the g-value significantly. Furthermore, the windows, with an assumed U-value of 2.7 W/m²K (renovated in the 1990s), are replaced with windows, reaching a double-glazing standard U-value of 1.1 W/m²K.

The installation of the windows with advanced sealing techniques, as well as the overall coverage of the façade leads to improved airtightness, enhancing the façade's robustness. The infiltration rate of the ideal robustness retrofit (0.00014) is assumed to be achieved.

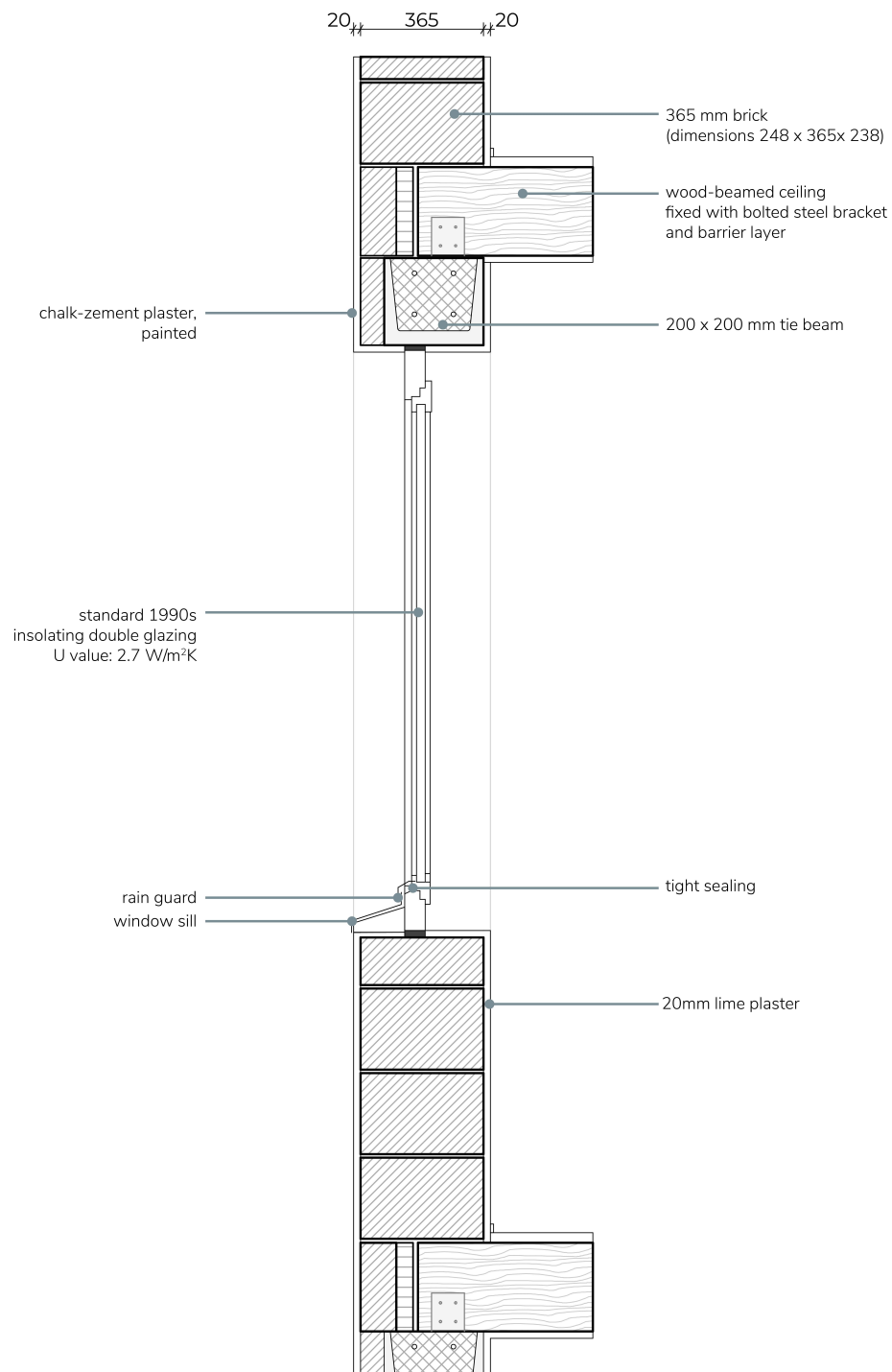


Figure 42: Section in 1:20 of case study façade in its current state.

The current construction of the exterior wall has a total U-value of 1.26 W/m²K. For the present standard of a maximum of 0.24 W/m²K (Bundesministerium für Wirtschaft und Klimaschutz, 2013), the exterior wall construction with solely bricks and plaster does not meet the requirements. Thus, a retrofit would not only improve the thermal resilience of the façade during heat waves, but also the energy efficiency requirements in the heating dominated climate of Munich.

$$U = \frac{1}{R_1 + R_2 + R_3} = \frac{1}{\frac{d_{Brick}}{\lambda_{Brick}} + 2 \times \left(\frac{d_{Plaster}}{\lambda_{Plaster}}\right)} = \frac{1}{\frac{0.365 \text{ m}}{0.5 \frac{W}{mK}} + 2 \times \left(\frac{0.02 \text{ m}}{0.7 \frac{W}{mK}}\right)} = 1.26 \frac{W}{m^2K} \quad (4)$$

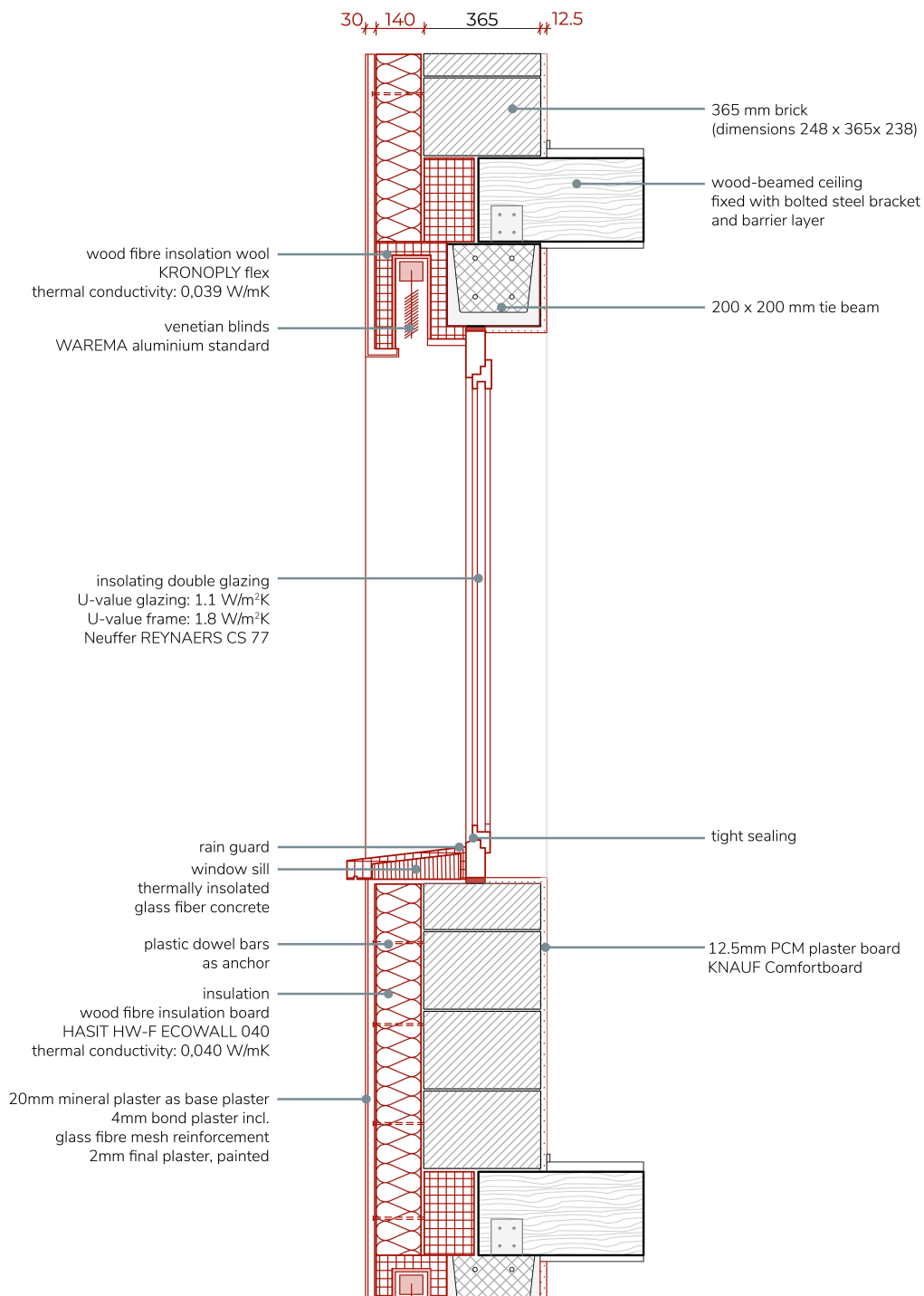


Figure 43: Section in 1:20 of case study façade retrofit proposal with retrofitted elements in red, source: own

The resulting exterior wall after retrofitting, has a U value of 0.23 W/m²K, which surpasses the conditions of the EnEV of a maximum of 0.24 W/m²K (Bundesministerium für Wirtschaft und Klimaschutz, 2013).

$$R = R_1 + R_2 + R_3 + R_4 = \frac{d_{PCM\ board}}{\lambda_{PCM\ board}} + \frac{d_{Brick}}{\lambda_{Brick}} + \frac{d_{insulation}}{\lambda_{isolation}} + \frac{d_{plaster}}{\lambda_{Plaster}} = \frac{0.0125\ m}{0.18\ \frac{W}{mK}} + \frac{0.365\ m}{0.5\ \frac{W}{mK}} + \frac{0.14\ m}{0.040\ \frac{W}{mK}} + \frac{0.02\ m}{0.7\ \frac{W}{mK}} = 4.34\ \frac{W}{mK} \quad (5)$$

$$U_{design_case} = \frac{1}{R_{total}} = \frac{1}{4.34\ \frac{W}{mK}} = 0.23\ \frac{W}{m^2K} \quad (6)$$

6.2 Materialisation of parameter values

Figure 44 visualizes the results of the evaluation of the performance of the retrofit proposal (solid line) compared to the façade's performance in its current state (dotted line) throughout the analysed heat wave scenarios of 2015 (dark red), 2050 (red) and 2080 (light red).



Figure 44: Thermal resilience indices performance of retrofit proposal (solid line) compared to base case (dotted line) in 2015 (dark red), 2050 (red) and 2080 (light red)
source: own

With the area within the output of the performance indices reducing with the applied retrofit, it can be observed that the overall thermal resilience performance of the façade during a heat wave is indeed improved. It is obvious that the retrofit especially improves the façade's resistance. Throughout the heat wave scenarios of 2015, 2050 and 2080, the retrofit seems to be the more resistant design. Also, the robustness is improved in the heat wave scenario of 2015 and 2050. Only in the scenario of 2080, the robustness seems to remain the same with the applied retrofit. The recoverability does not appear to be improved. In the heat wave scenario of 2015, there is a slight increase in the recovery time, in 2080 it is comparable to the performance of the base case, whereas in the heat wave scenario of 2050, the performance is significantly decreased. It has been concluded for the design of the retrofit that the added

thermal insulation is contra-productive for the recoverability of the façade. This is confirmed through the evaluation of the retrofit. For now, the specific heat of the interior finishing is simplified and kept constant at a value of 828 J/kgK, as in the simulation output. However, it can be assumed that the recoverability performance should again be improved when properly modelling the phase change plasterboard. This also emphasizes the need for responsive building materials, that can adapt to the changing requirements of the building envelope to on one hand reduce the incoming thermal energy during the day, and on the other hand, increase the release the heat to the outside environment during the night (the same can be said for the contrasting needs of reducing the overheating risk during summer and the need for improved thermal insulation in winter).

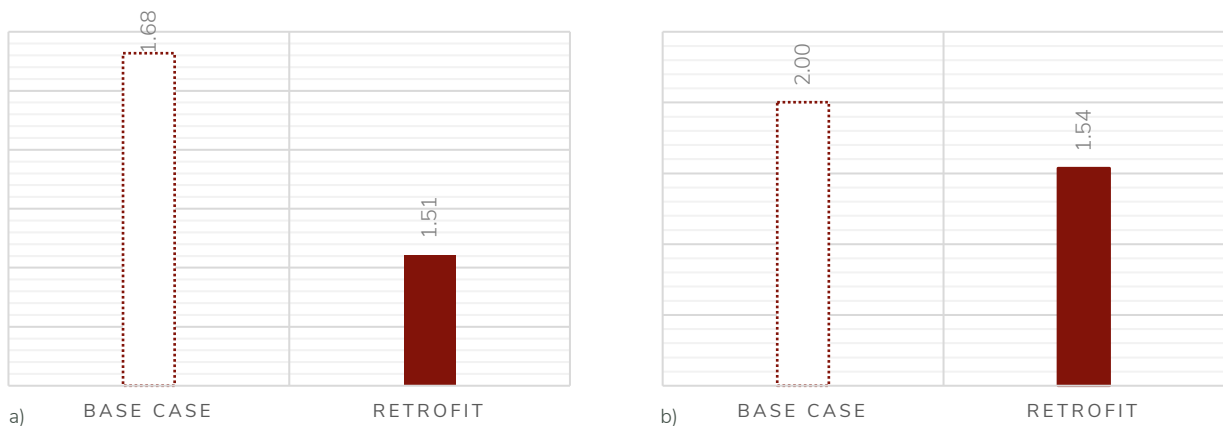


Figure 45: Performance of facade's current state (base case in dotted line) and retrofit (solid) in regard of
a) the adaptive capacity and b) the FRI
source: own

It is obvious that the future heat wave conditions decrease the thermal performance of both, the current state façade, and the retrofit proposal. The retrofit shows a significantly improved thermal resilience in current (2015) extreme heat conditions. However, based on the evaluation of the performance in future heat wave conditions, it can be assumed that the impact of the outdoor heat conditions on the indoor thermal comfort becomes substantially larger and thus decreases the potential for improvement. Still, comparing the adaptive capacity of the base case and the retrofit (Fig. 45a), it can be concluded that with a reduced adaptive capacity the retrofit improves the performance of the façade in terms of its long-term performance, considering the overall performance with the 2015, 2050 and 2080 heat wave data. Overall, this results in an improved FRI of 1.54 (Fig. 45b).

To summarize, it can be said that the overall thermal resilience of the case study façade of a residential building block in Munich is improved through the applied retrofit design. This concludes the proposed framework as a valid decision-making tool for retrofits to enhance decision-making for retrofit design, improving building thermal resilience. Potential development could further analyse future heat wave conditions and their impact on the applied methodology.



Conclusion and outlook

- 7.1 Conclusion
- 7.2 Limitations of research
- 7.3 Future challenges

7.1 Conclusion

This research aims to answer the question: "How can we evaluate the influence of façades on building thermal resilience during heat waves?". To conclude on the main research question, the following presents findings related to the raised sub-questions:

How do future climate related heat waves change building requirements for façade constructions?

The observed increase in mortality and morbidity during heat wave periods highlights a significant shortcoming in the current design practise, which fails to consider the impact of temperature extremes. The predicted increased intensity, frequency and magnitude of future heat waves requires the reevaluation of building requirements. Present building standards primarily assess performance under typical weather conditions, resulting in disrupted or compromised indoor thermal comfort during extreme heat periods. There is an urgent need to focus on the building skin with its key role between the exterior and indoor environment, mitigating risks for the occupants during heat waves. Façade design must account for local heat wave hazards, including their frequency, duration, and magnitude specific to the chosen location. It is essential to adapt building requirements to establish façade design that can enhance thermal resilient buildings, providing adequate thermal conditions in extreme heat periods; applied to new as well as existing constructions.

To achieve the same, the development of a thermal comfort metric capable of capturing occupants' perception of heat and evaluating their estimated heat hazard level, is crucial. Within the common thermal comfort metrics, e.g., the PMV, the adaptive thermal comfort model, SET etc., the SET has been identified to sufficiently display the thermal perception of occupants under extreme heat. However, to comprehensively reflect the occupant's thermal comfort during heat waves, an additional level of detail is required: e.g., the time of exposure to a certain hazard level of heat or the night-time temperatures.

How is the influence of façade on building thermal resilience to extreme heat assessed?

What are commonly used metrics?

Assessment methodologies for evaluating thermal resilience on building or façade level during heat waves have been analysed. Each proposal follows a similar procedure, starting with the establishment of their individual resilience terminology. Resilience criteria are then formulated, expressing the building's/façade's abilities to meet resilient conditions. Based on these criteria, resilience indicators are defined, which can be quantified through adjusted thermal comfort measurements.

Although there is no universally used metric, it needs to be noted that there are similarities within the assessed proposals and their definitions used. Qualitative assessment methods base their analysis on the required criteria of durability or adaptability. Whereas most of the quantitative methods refer in their resilience definition to four stages of the disruptive period: vulnerability as the pre-condition, resistance to shocks, robustness during the disruptive phase and recoverability or speed of returning to pre-shock conditions.

While multiple resilience indicators are defined, each assessed metric focuses on the measurement of one thermal resilience index. Those typically include the measurement of standard thermal comfort metrics and the additional measurement of the exceedance time and severity above a certain threshold. The resulting indices (WSETH, WUMTP, UHD, SEUHD, PMVEH and TDH) effectively reflect indoor thermal comfort during heat waves.

How could current assessment methodologies of building thermal resilience be improved?

The reviewed assessment methodologies adequately assess occupant thermal comfort during heat waves. However, they could be improved in terms of their depth of analysis specifically of the façade's influence on the thermal resilience of the building. Although the reviewed metrics show a comprehensive definition of terminology, they lack detail in translating the same to indices to quantify. The identified criteria for a resilient façade response are not fully applied on the proposed assessment of resilience performance, resulting in a reduction of detail. The resulting index primarily serves as an indicator of overall overheating risk.

To improve reviewed metrics, it is proposed to incorporate all the identified resilience indicators into a "multi-levelled" resilience metric. The metric aims to capture the façade's performance in terms of resistance, robustness, recoverability, and adaptive capacity to extreme heat in several indices, potentially combining them to one overall thermal resilience index. This approach allows the user to customize the assessment focus based on specific criteria. Additionally, the proposal suggests analysing the long-term performance of façade designs, evaluating the adaptive capacity of resilient systems, to be "prepared for" future challenges.

It can be concluded that the introduction of a multi-levelled resilience index improves decision-making during the design process of thermal resilient retrofits by providing clear indications of the façade parameters that should be in focus. Evaluating the performance based on the facade's resistance, robustness, and recoverability also reveals the contradictory parameter values required to achieve the building's resilience criteria across different stages of the disruptive periods. This highlights an important realization.

However, further research is needed to explore the inclusion of predictive weather data in the evaluation index. For now, the innovation lies in the concept of including predictive weather data into the overall methodology, which has not been proposed before.

What are relevant façade parameters to be considered for retrofitting improving occupants' thermal comfort during extreme heat events?

The design of a thermal resilient retrofit involves considering relevant façade parameters that impact the heat flow through the building's exterior envelope. During heat waves, the focus is to either prevent heat from entering the interior space or enhance the release of heat from overheated interior spaces to the external environment.

Through a literature review, key façade properties influencing the general heat flow within and through the exterior wall have been identified. While there are several other façade properties that affect thermal performance, the most significant ones for further analysis have been determined: The thermal conductivity, expressing the materials thermal transmittance resistance in terms of the conductive heat flow. The specific heat, as a material's property indicating the material's capacity to absorb and store heat. Thus, the specific heat of façade materials describes the heat storage capacity and the temperature regulation during the day and night – a higher specific heat can therefore prevent temperature peaks, by having a slower thermal response. The air tightness of a façade with the corresponding rate of infiltration can be identified as the façade property with a key influence on the convective heat flow. It regulates how much heat can be transferred by incoming and outgoing air flow through construction gaps, cracks etc. As a façade property with a key influence on the radiative heat flow, the window's solar heat gain coefficient (g-value) needs to be considered. Giving insight on the fraction of total solar radiation, both, directly transmitted, and indirectly transmitted by being first absorbed by the window surface, and then reemitted

into the interior space. Thus, the exterior surface albedo, as a measurement of the surface's reflectivity, it also provides insight on the amount of solar radiation absorbed by the wall.

An analysis of a typical living space in a German residential urban block in Munich indicates that the glazing's solar heat gain coefficient (g-value) has the strongest influence on occupant thermal comfort during heat waves. The specific heat becomes important for the choice of the interior finish layer of the exterior wall. Also, the infiltration rate can be identified to have a significant influence on thermal environment indoors. The thermal conductivity of exterior insulation and the thermal transmittance of the window have less impact, with the specific heat of the structural layer and the solar absorptance of the exterior finish with surprisingly almost no impact.

It is important to note that these findings are specific to the analysed case study and the local climatic zone. The dependency of results on construction and environmental specific conditions should be highlighted.

What are the most important façade parameters influencing resilience indicators?

The analysis conducted on the case study building concludes on specific façade parameters with a key influence on the building's abilities during each phase of disruption. Also here, the conclusions are limited to the location and construction of the case study building in Munich.

In general, the window's g-value can be identified as a crucial parameter to consider for improved performance throughout the whole heat wave period. The reduction of incoming heat flow through the transparent window surfaces gives a clear indication for the need of external sun shading. Enhancing the façade's resistance to extreme outdoor temperatures primarily relies on reducing its thermal conductivity. This emphasizes the need for additional insulation to decrease conductive heat flow during the day. To increase the façade's robustness, increasing the airtightness of the exterior wall is recommended. This results in a decreased convective heat flow which has a strong influence on the overheating severity. For effective recovery the specific heat of the internal surface finish shows to be crucial. With the limitation of unrestricted ventilation, a higher specific heat is beneficial for night-time recovery. Increasing the "heat buffer" of the façade, results in a lower indoor temperature peak and thus in a more rapid recovery. It's important to recognize that these findings are specific to the analysed case study and may vary depending on the location and construction characteristics of different buildings. For deeper analysis and further understanding of influential factors, it is proposed to include the analysis of the interdependencies of the different facade parameters, as the combination of factors is proven to play a key role to improve the façade's resilience.

An assessment framework was developed and tested on a case study building in Munich to evaluate the influence of façade design on the thermal resilience of buildings to heat waves. The framework aims to improve upon existing assessment metrics of the state-of-the-art research in several ways: It involved a detailed analysis of the thermal resilience performance, considering not only the potential for overheating but also the influence of various façade parameters during different phases of disruption. The final evaluation also includes the analysis of the long-term performance, for which predictive weather data is included.

The proposed framework can be used to improve decision-making during the design process of thermal resilient retrofits. It has been found to be a relevant addition to common resilience metrics to capture not only the overall performance, but also the influence of the intervention on separate resilience indicators. This emphasizes that resilience can be described as an iterative, cyclic process, coping with upcoming challenges, going through several stages. During those stages, different criteria need to be met, thus, different, time dependent characteristics result in a “resilient” system. Summarized in only one index, the required changes per disruptive period cannot be distinguished. In fact, the procedure of quantifying resilience per heat wave period, led to the realization of contrasting façade requirements in each of the disruptive periods. This has a crucial importance in the design of the corresponding retrofit.

The resulting design for the residential case study building in Munich, includes the installation of external sun shading, additional thermal insulation, and, in case unrestricted night-time ventilation is possible (open windows during the night), increased airtightness and the use of PCM plasterboard as the internal finishing. By considering the crucial façade parameters that optimise the performance for each of the resilience indicators, the performance of the façade is improved during the whole heat wave period.

Indeed, it can be said that the proposed framework does improve the decision-making during the design process of the retrofit scenarios. However, to achieve universal applicability, the evaluation methodology would need to be reconsidered. The evaluation based on the developed indices results in promising results, which however need some refinement. Also, chosen parameters would need to be reconsidered. E.g., for the location of Munich, with strong contrast in day- and night-time temperatures, the ventilation parameter is important to consider. Depending on climate, location and construction type, also other parameters might need to be included in the consideration.

In conclusion, this thesis contributes to the research on transitioning to a more resilient built environment, aiming to develop a methodology for providing secure and comfortable living conditions during heat waves. The research objectives address the need for a universally applicable metric to assess the influence of façade design on building's thermal resilience to extreme heat. The study concludes that quantifying thermal resilience benefits from defining multiple resilience indices. Certainly, this methodology improves decision-making during the design process of façade retrofits for an enhanced building thermal resilience.

7.2 Limitations of research

The suggested framework includes a decision-making methodology applicable to the assessment of thermal resilience in the building context. Its formulation allows for flexibility and adaptability, making it widely applicable to decision-makers. However, it is important to acknowledge certain limitations associated with the methodology.

Firstly, the process is developed specifically for the assessment of retrofit scenarios for the improvement of the building's thermal resilience during heat wave periods. It is important to note that the methodology is designed for the climate conditions prevalent in Munich, which is characterized by a heating-dominated climate. However, the framework does not include the evaluation of the proposed retrofit's performance during winter conditions. The only constraints considered are the EnEV regulations, which also account for the energy efficiency in colder winter conditions. Nonetheless, it is worth considering that since heating plays a significant role, particularly in the chosen location, an evaluation under winter conditions could potentially change the results.

Secondly, it must be noted that the heat wave weather data, derived from VisualCrossing (Visual Crossing Corporation, n.d.), is not certainly from a weather station in the centre of Munich. The historical AMY data to download from VisualCrossing is a combination of data from up to three weather stations, located in and around Munich. Thereby, VisualCrossing guarantees the most accurate reports. However, as the urban infrastructure (less greenery, asphalt surfaces, decreased wind speed etc.) contributes to the urban heat island effect, temperatures in an urban centre are generally warmer. This makes the used weather data slightly inaccurate for the chosen location.

Thirdly, the simulations do not account for the surrounding. The EnergyPLUS field "terrain" is set to "urban", which accounts for the changes in the windspeed based on the surrounding of an urban landscape. Nevertheless, the actual surrounding of the building is not included in the simulations. Thus, shadows from surrounding buildings/trees/etc. are neglected. As they would influence in which way the façade is exposed to direct sunlight, the additional consideration of the actual surrounding would more carefully include the total heat gain throughout the day.

Furthermore, the findings highlight the importance of a more thorough investigation of the ventilation parameter. While the focus of the assessment is primarily on façade interventions, the ventilation parameter is simplified and kept constant. However, it has been observed that the impact of ventilation can overshadow the effects of retrofit options on the indicator output. Therefore, it is crucial to consider the actual ventilation schedule specific to the case study. Factors such as the zone's program, occupancy, potential acoustical discomfort during the night due to traffic noise, neighbourhood safety, and other influential variables contribute to the individual natural ventilation schedule of the thermal zone. Those factors should be carefully studied and applied to the case study simulations to reach a more realistic output.

Furthermore, the chosen thermal comfort metric, the "Standard effective temperature" (SET), has been proven to be a suitable measure for assessing thermal comfort in extreme heat conditions. Previous research (Ji et al., 2022) applied it to their case study in Montreal, classified as the same climatic zone as Munich ("Cfb" of the Koppen climate zone classification). However, to ensure the applicability of the proposed method in diverse climate zones, a reassessment of the SET as the thermal comfort indicator would be necessary. The SET aims to describe the actual perception of thermal comfort, based on environmental and personal factors. As the chosen thermal comfort metric, the simulation output of the dry bulb temperature, the mean radiant temperature and the relative humidity is varying input for the SET

calculation. However, so far, the clothing insulation, body position, metabolic rate, body surface area and external work are kept as constants; based on a realistic scenario for a living area in summer conditions: typical summer clothing, minimal activity level – the body position is kept at the default: “standing”. Thus, the adaptive behaviour of the occupants is not accounted for. For more accuracy, individual personal factors of the occupants should be included.

Previous work emphasizes the importance of investigating additional thermal zones with different thresholds based on the typical activity and the programme of the space (Ji et al., 2022). Plus, the location of the apartment within the building (plus the ground floor and attic) is another parameter to consider within the assessment framework. The methodology is currently limited to the assessment of one thermal space (living area) on the third floor of a six-storey building. When including also other thermal zones, it could be accounted for the adaptive behaviour of the occupants to change their location within their flat, as well as the impact of the apartment’s location within the building.

The conducted sensitivity analysis results in the predicted impact of the variables on the indicator indices. The chosen Sobol method calculates the first- and second-order, and the total effects: the impact of the individual variables separately when combined with variables and in total. For now, the methodology proposes to discuss only the total and first-order effects. This however limits the depth of detail of the analysis. Adding the second-order effects would improve the method in the sense of also understanding the interconnections of the variables, which has been proven to be important for the analysis of retrofit options in heat wave scenarios (Ji et al., 2022; Schünemann et al., 2022; Sun et al., 2020, 2021).

And finally: the rating strategy includes the assessment of the performance in future climate conditions. The fact that the created predictive weather files are solely based on predictions of the A2 climate scenario of the IPCC (Seneviratne et al., 2021), limits the comparison to the “worst case” emission scenario.

7.3 Future challenges

The focus of this thesis is to assess the building's response to extreme heat and its resilience in such conditions, including the evaluation of future heat wave scenarios. However, it is important to note that future scenarios involve not only heat extremes but also other potential extremes such as cold snaps, floods, droughts leading to wildfires, and earthquakes. A truly "resilient" building should consider a multi-hazard approach, taking into account local risks and the building's exposure to various extremes. Therefore, the decision-making framework for enhancing resilience at the facade level should include a multi-criteria approach, rather than solely focusing on improving thermal resilience.

It also must be said that the proposed framework, as presented in this thesis, still requires refinements to create a widely accessible tool for stakeholders like façade designers, architects, or occupants. The most important one is to generate a simpler application. Potentially, the process could be simplified in form of guidelines for the design of thermal resilient retrofits, introducing well established rules, based on the climate, and other influential factors like the construction type etc. Empirical data based on climate, and other influential factors like the construction type etc. are carefully considered in such guidelines and thus make multiple steps in the proposed framework redundant. With the addition of resilience classes, which are based on overall evaluations, the framework would improve as an integrated and easily applicable metric, making both, the workflow methodology and the final assessment more practical and user-friendly during the design process.



References

- Alfraidi, Y., & Boussabaine, A. H. (2015). *Design Resilient Building Strategies In Face Of Climate Change*.
<https://doi.org/10.5281/ZENODO.1338054>
- ASHRAE. (2017a). *ANSI/ASHRAE Standard 55-2017*.
- ASHRAE. (2017b). *ASHRAE Handbook Fundamentals*. University of Cambridge.
- Attia, S., Levinson, R., Ndongo, E., Holzer, P., Berk Kazanci, O., Homaei, S., Zhang, C., Olesen, B. W., Qi, D., Hamdy, M., & Heiselberg, P. (2021). Resilient cooling of buildings to protect against heat waves and power outages: Key concepts and definition. *Energy and Buildings*, 239, 110869.
<https://doi.org/10.1016/j.enbuild.2021.110869>
- Belcher, S., Hacker, J., & Powell, D. (2005). Constructing design weather data for future climates. *Building Services Engineering Research and Technology*, 26(1), 49–61.
<https://doi.org/10.1191/0143624405bt112oa>
- Berglund, L. G. (1995). *Comfort criteria: Humidity and standards*. (Proceedings of Pan Pacific Symposium on Building and Urban Environmental Conditioning in Asia). University of Nagoya.
- Bilardo, M., Ferrara, M., & Fabrizio, E. (2019). Resilient optimal design of multi-family buildings in future climate scenarios. *E3S Web of Conferences*, 111, 06006. <https://doi.org/10.1051/e3sconf/201911106006>
- Boschma, R. (2015). Towards an Evolutionary Perspective on Regional Resilience. *Regional Studies*, 49(5), 733–751. <https://doi.org/10.1080/00343404.2014.959481>
- Bruneau, M., Chang, S. E., Eguchi, R. T., Lee, G. C., O'Rourke, T. D., Reinhorn, A. M., Shinozuka, M., Tierney, K., Wallace, W. A., & von Winterfeldt, D. (2003). A Framework to Quantitatively Assess and Enhance the Seismic Resilience of Communities. *Earthquake Spectra*, 19(4), 733–752.
<https://doi.org/10.1193/1.1623497>
- Bundesministerium für Wirtschaft und Klimaschutz. (2013). *Energieeinsparverordnung Bundesgesetzblatt*.
Bundesministerium für Wirtschaft und Klimaschutz.
https://www.bmwk.de/Redaktion/DE/Downloads/E/enev-nichtamtliche-lesefassung-zur-zweiten-verordnung-zur-aenderung-derenergieeinsparverordnung.pdf?__blob=publicationFile&v=1

- Bundesministerium für Wirtschaft und Klimaschutz. (2023). *Bundesförderung für effiziente Gebäude (BEG 5.0)*. Bundesministerium für Wirtschaft und Klimaschutz.
- Burhenne, S., & Herkel, S. (2013). Methodik zur Unsicherheitsbewertung und Sensitivitätsanalyse für thermische Gebäudesimulationen. *Bauphysik*, 35(2), 94–98. <https://doi.org/10.1002/bapi.201310052>
- Cabinet Office. (2011). *Section A: Keeping the Country Running: Natural Hazards and Infrastructure in PDF Format*.
- Capozzoli, A., Gorrino, A., & Corrado, V. (2013). A building thermal bridges sensitivity analysis. *Applied Energy*, 107, 229–243. <https://doi.org/10.1016/j.apenergy.2013.02.045>
- Chen, R., & Tsay, Y.-S. (2022). Carbon emission and thermal comfort prediction model for an office building considering the contribution rate of design parameters. *Energy Reports*, 8, 8093–8107. <https://doi.org/10.1016/j.egy.2022.06.012>
- Coumou, D., & Rahmstorf, S. (2012). A decade of weather extremes. *Nature Climate Change*, 2(7), 491–496. <https://doi.org/10.1038/nclimate1452>
- Crowther Lab, ETH Zurich. (n.d.). *Current v. Future cities*. Retrieved 27 April 2023, from <https://crowtherlab.pageflow.io/cities-of-the-future-visualizing-climate-change-to-inspire-action#213121>
- Designing Buildings Ltd. (2022, August 11). *G-value in buildings*. Designing Buildings Construction Wiki. https://www.designingbuildings.co.uk/wiki/G-value_in_buildings
- Deutscher Wetterdienst. (n.d.-a). *Hitze- und UV-Warnungen*. Retrieved 27 April 2023, from https://www.dwd.de/DE/wetter/warnungen_aktuell/kriterien/uv_hitze_warnungen.html;jsessionid=95AC0F19503B6D07A88F68EB07B3894C.live31094?nn=508722
- Deutscher Wetterdienst. (n.d.-b). *Klimadaten Deutschland—Monats- und Tageswerte (Archiv)*. Retrieved 28 April 2023, from <https://www.dwd.de/DE/leistungen/klimadatendeutschland/klarchivtagmonat.html#buehneTop>
- Encyclopædia Britannica. (n.d.). *Resilience definition*. Retrieved 25 January 2023, from <https://www.britannica.com/dictionary/resilience>

- Engineering ToolBox. (2001). *The Engineering Toolbox*. <https://www.engineeringtoolbox.com/>
- Epstein, Y., & Moran, D. S. (2006). Thermal Comfort and the Heat Stress Indices. *Industrial Health*, 44(3), 388–398. <https://doi.org/10.2486/indhealth.44.388>
- Fanger, P. O. (1970). *Thermal comfort-Analysis and applications in environmental engineering*. Danish Technical Press.
- Fischer, E. M., & Schär, C. (2010). Consistent geographical patterns of changes in high-impact European heatwaves. *Nature Geoscience*, 3(6), 398–403. <https://doi.org/10.1038/ngeo866>
- Folke, C., Carpenter, S., Elmqvist, T., Gunderson, L., Holling C.S., & Walker, B. (2002). Resilience and sustainable development: Building adaptive capacity in a world of transformations. 31(5), 437–440. <https://doi.org/10.1579/0044-7447-31.5.437>
- Friedland, C. J., & Gall, M. (2012). True Cost of Hurricanes: Case for a Comprehensive Understanding of Multihazard Building Damage. *Leadership and Management in Engineering*, 12(3), 134–146. [https://doi.org/10.1061/\(ASCE\)LM.1943-5630.0000178](https://doi.org/10.1061/(ASCE)LM.1943-5630.0000178)
- Gagge, A. P. (1937). A new physiological variable associated with sensible and insensible perspiration. *American Journal of Physiology*, 20(2), 277–287.
- Gagge, A. P., Stolwijk, J. A. J., & Hardy, J. D. (1967). Comfort and thermal sensations and associated physiological responses at various ambient temperatures. *Environmental Research*, 1(1), 1–20. [https://doi.org/10.1016/0013-9351\(67\)90002-3](https://doi.org/10.1016/0013-9351(67)90002-3)
- Goffart, J., & Woloszyn, M. (2021). EASI RBD-FAST: An efficient method of global sensitivity analysis for present and future challenges in building performance simulation. *Journal of Building Engineering*, 43, 103129. <https://doi.org/10.1016/j.jobbe.2021.103129>
- Hardy, J. D., Stolwijk, J. A. J., & Gagge, A. P. (1971). Man. Charles C. Thomas.
- Harris, C. R., Millman, K. J., van der Walt, S. J., Gommers, R., Virtanen, P., Cournapeau, D., Wieser, E., Taylor, J., Berg, S., Smith, N. J., Kern, R., Picus, M., Hoyer, S., van Kerkwijk, M. H., Brett, M., Haldane, A., del Río, J. F., Wiebe, M., Peterson, P., ... Oliphant, T. E. (2020). Array programming with NumPy. *Nature*, 585(7825), 357–362. <https://doi.org/10.1038/s41586-020-2649-2>

- Havenith, G., & Fiala, D. (2015). Thermal Indices and Thermophysiological Modeling for Heat Stress. In R. Terjung (Ed.), *Comprehensive Physiology* (1st ed., pp. 255–302). Wiley.
<https://doi.org/10.1002/cphy.c140051>
- Hemsath, T. L., & Alagheband Bandhosseini, K. (2015). Sensitivity analysis evaluating basic building geometry's effect on energy use. *Renewable Energy*, 76, 526–538.
<https://doi.org/10.1016/j.renene.2014.11.044>
- Herman, J., & Usher, W. (2017). SALib: An open-source Python library for Sensitivity Analysis. *The Journal of Open Source Software*, 2(9), 97. <https://doi.org/10.21105/joss.00097>
- H.-O. Pörtner, D.C. Roberts, E.S. Poloczanska, K. Mintenbeck, M. Tignor, A. Alegría, M. Craig, S. Langsdorf, S. Löschke, & V. Möller. (2022). *IPCC Summary for Policymakers* (Climate Change 2022: Impacts, Adaptation and Vulnerability., pp. 3–33). Cambridge University Press.
 doi:10.1017/9781009325844.001
- Holling, C. S. (1973). Resilience and Stability of Ecological Systems. *Annual Review of Ecology and Systematics*, 4(1), 1–23. <https://doi.org/10.1146/annurev.es.04.110173.000245>
- Holling, C. S. (1996). Engineering Resilience versus Ecological. In P. C. Schulze (Ed.), *Engineering within ecological constraints* (p. 4919). National Academies Press. <https://doi.org/10.17226/4919>
- Holmes, S. H., Phillips, T., & Wilson, A. (2016). Overheating and passive habitability: Indoor health and heat indices. *Building Research & Information*, 44(1), 1–19.
<https://doi.org/10.1080/09613218.2015.1033875>
- Homaei, S., & Hamdy, M. (2021a). Thermal resilient buildings: How to be quantified? A novel benchmarking framework and labelling metric. *Building and Environment*, 201, 108022.
<https://doi.org/10.1016/j.buildenv.2021.108022>
- Homaei, S., & Hamdy, M. (2021b, September 1). Developing a test framework for assessing building thermal resilience. 2021 Building Simulation Conference. <https://doi.org/10.26868/25222708.2021.30252>
- Hopfe, C. J. (2009). *Uncertainty and sensitivity analysis in building performance simulation for decision support and design optimization*. Eindhoven University of Technology.

- Hopfe, C. J., & Hensen, J. L. M. (2011). Uncertainty analysis in building performance simulation for design support. *Energy and Buildings*, 43(10), 2798–2805. <https://doi.org/10.1016/j.enbuild.2011.06.034>
- Huizenga, C., Zhang, H., Mattelaer, P., Yu, T., Arens, E., & P., L. (2006). *Window performance for human thermal comfort*.
- IEA. (2018, May). *The future of cooling*. The Future of Cooling. <https://www.iea.org/reports/the-future-of-cooling>
- IPCC. (n.d.). *HadCM3 Climate Scenario Data*. Data Distribution Center. Retrieved 21 May 2023, from https://www.ipcc-data.org/sim/gcm_clim/SRES_TAR/hadcm3_download.html
- IPCC. (2007). *Summary for Policymakers (Climate Change 2007: The Physical Science Basis. Contribution of Working Group I to the Fourth Assessment Report of the Intergovernmental Panel on Climate Change)*. Cambridge University Press.
- IPCC. (2012). *Managing the Risks of Extreme Events and Disasters to Advance Climate Change Adaptation (A Special Report of Working Groups I and II of the Intergovernmental Panel on Climate Change, p. 582 pp.)*. Cambridge University Press.
- IPCC. (2021). *Summary for Policymakers (Climate Change 2021: The Physical Science Basis. Contribution of Working Group I to the Sixth Assessment Report of the Intergovernmental Panel on Climate Change)*.
- Iwanaga, T., Usher, W., & Herman, J. (2022). Toward SALib 2.0: Advancing the accessibility and interpretability of global sensitivity analyses. *Socio-Environmental Systems Modelling*, 4, 18155. <https://doi.org/10.18174/sesmo.18155>
- Jansone, D., Dzikevics, M., & Veidenbergs, I. (2018). Determination of thermophysical properties of phase change materials using T-History method. *Energy Procedia*, 147, 488–494. <https://doi.org/10.1016/j.egypro.2018.07.057>
- Jentsch, M. F. (2017). *CCWorldWeatherGen (1.9)*.
- Ji, L., Shu, C., Laouadi, A., Lacasse, M., & Wang, L. (Leon). (2022). Quantifying improvement of building and zone level thermal resilience by cooling retrofits against summertime heat events. *Building and Environment*, 229, 109914. <https://doi.org/10.1016/j.buildenv.2022.109914>

- Jin, Q., & Overend, M. (2014). Sensitivity of façade performance on early-stage design variables. *Energy and Buildings*, 77, 457–466. <https://doi.org/10.1016/j.enbuild.2014.03.038>
- J.T. Houghton, Y. Ding, D.J. Griggs, M. Noguera, P.J. van der Linden, X. Dai, K. Maskell, & C.A. Johnson. (2001). *Climate Change 2001: The Scientific Basis Appendix I* (p. 790). CAMBRIDGE UNIVERSITY PRESS.
- Junk, J., Goergen, K., & Krein, A. (2019). Future Heat Waves in Different European Capitals Based on Climate Change Indicators. *International Journal of Environmental Research and Public Health*, 16(20), 3959. <https://doi.org/10.3390/ijerph16203959>
- Knauf. (2014). *Knauf Comfortboard Phase change plasterboard – thermal mass without the weight*.
- Koffi, B., & Koffi, E. (2008). Heat waves across Europe by the end of the 21st century: Multiregional climate simulations. *Climate Research*, 36, 153–168. <https://doi.org/10.3354/cr00734>
- Lassandro, P., & Di Turi, S. (2019). Multi-criteria and multiscale assessment of building envelope response-ability to rising heat waves. *Sustainable Cities and Society*, 51, 101755. <https://doi.org/10.1016/j.scs.2019.101755>
- Lauss, L., Meier, A., & Auer, T. (2022). Uncertainty and sensitivity analyses of operational errors in air handling units and unexpected user behavior for energy efficiency and thermal comfort. *Energy Efficiency*, 15(1), 4. <https://doi.org/10.1007/s12053-021-10013-w>
- Lawrence Berkeley National Lab. (2019). *Simulation Research*. <https://simulationresearch.lbl.gov/>
- Linden, A. C. van der, Erdtsieck, P., Kuijpers-van Gaalen, I. M., & Zeegers, A. (2013). *Building physics* (1st ed). ThiemeMeulenhoff.
- Loonen, R. C. G. M., & Hensen, J. L. M. (2013). DYNAMIC SENSITIVITY ANALYSIS FOR PERFORMANCE-BASED BUILDING DESIGN AND OPERATION. *Proceedings of BS2013: 13th Conference of International Building Performance Simulation Association*.
- Luna Navarro, A., Fidler, P., Law, A., Torres, S., & Overend, M. (2021). Building Impulse Toolkit (BIT): A novel IoT system for capturing the influence of façades on occupant perception and occupant-façade interaction. *Building and Environment*, 193, 107656. <https://doi.org/10.1016/j.buildenv.2021.107656>

- Matthews, E. C., Sattler, M., & Friedland, C. J. (2014). A critical analysis of hazard resilience measures within sustainability assessment frameworks. *Environmental Impact Assessment Review*, 49, 59–69. <https://doi.org/10.1016/j.eiar.2014.05.003>
- McMichael, A. J., & Lindgren, E. (2011). Climate change: Present and future risks to health, and necessary responses: Review: Climate change and health. *Journal of Internal Medicine*, 270(5), 401–413. <https://doi.org/10.1111/j.1365-2796.2011.02415.x>
- Meehl, G. A., & Tebaldi, C. (2004). More Intense, More Frequent, and Longer Lasting Heat Waves in the 21st Century. *Science*, 305(5686), 994–997. <https://doi.org/10.1126/science.1098704>
- Nairn, J. R., & Fawcett, R. (2013). *Defining heatwaves: Heatwave defined as a heat-impact event servicing all community and business sectors in Australia*. Centre for Australian Weather and Climate Research.
- Nicol, F. (2013). *The limits of thermal comfort: Avoiding overheating in European buildings*. London: The Chartered Institution of Building Services Engineers.
- O'Brien, W., & Bennet, I. (2016). *Simulation-based evaluation of high-rise residential building thermal resilience*. 122, 455–468.
- Østergård, T., Jensen, R. L., & Maagaard, S. E. (2017). Early Building Design: Informed decision-making by exploring multidimensional design space using sensitivity analysis. *Energy and Buildings*, 142, 8–22. <https://doi.org/10.1016/j.enbuild.2017.02.059>
- Ouzeau, G., Soubeyroux, J.-M., Schneider, M., Vautard, R., & Planton, S. (2016). Heat waves analysis over France in present and future climate: Application of a new method on the EURO-CORDEX ensemble. *Climate Services*, 4, 1–12. <https://doi.org/10.1016/j.cliser.2016.09.002>
- Ozarisoy, B. (2022). Energy effectiveness of passive cooling design strategies to reduce the impact of long-term heatwaves on occupants' thermal comfort in Europe: Climate change and mitigation. *Journal of Cleaner Production*, 330, 129675. <https://doi.org/10.1016/j.jclepro.2021.129675>
- Parsons, K. (2002). *Human Thermal Environments*.
- Pattenden, S. (2003). Mortality and temperature in Sofia and London. *Journal of Epidemiology & Community Health*, 57(8), 628–633. <https://doi.org/10.1136/jech.57.8.628>

- Patterson, M. (2022). Resilience by design: Building facades for tomorrow. In *Rethinking Building Skins* (pp. 359–375). Elsevier. <https://doi.org/10.1016/B978-0-12-822477-9.00002-4>
- Patterson, M., Kensek, K., & Noble, D. (2017). Supple Skins: Considering the Relevance, Scalability, and Design Strategies for Façade System Resilience. *Journal of Architectural Education*, 71(1), 34–45. <https://doi.org/10.1080/10464883.2017.1260919>
- Paul J. Schramm, Christopher K. Uejio, Jeremy J. Hess, Gino D. Marinucci, & George Luber. (n.d.). *Climate Models and the Use of Climate Projections: A Brief Overview for Health Departments*. Department of Health & Human Services USA. Retrieved 29 April 2023, from https://www.cdc.gov/climateandhealth/pubs/climate_models_and_use_of_climate_projections.pdf
- Perkins, S. E., & Alexander, L. V. (2013). On the Measurement of Heat Waves. *Journal of Climate*, 26(13), 4500–4517. <https://doi.org/10.1175/JCLI-D-12-00383.1>
- Perkins, S. E., Alexander, L. V., & Nairn, J. R. (2012). Increasing frequency, intensity and duration of observed global heatwaves and warm spells. *Geophysical Research Letters*, 39(20), 2012GL053361. <https://doi.org/10.1029/2012GL053361>
- Portal München Betriebs GmbH & Co. KG. (n.d.). *Maxvorstadt: Alle Infos zum Münchner Stadtteil*. Retrieved 27 April 2023, from <https://www.muenchen.de/stadtteile/maxvorstadt-wissenswertes-tipps-und-infos>
- Powers, J. G., Klemp, J. B., Skamarock, W. C., Davis, C. A., Dudhia, J., Gill, D. O., Coen, J. L., Gochis, D. J., Ahmadov, R., Peckham, S. E., Grell, G. A., Michalakes, J., Trahan, S., Benjamin, S. G., Alexander, C. R., Dimego, G. J., Wang, W., Schwartz, C. S., Romine, G. S., ... Duda, M. G. (2017). The Weather Research and Forecasting Model: Overview, System Efforts, and Future Directions. *Bulletin of the American Meteorological Society*, 98(8), 1717–1737. <https://doi.org/10.1175/BAMS-D-15-00308.1>
- Prof. Dr.-Ing. Doris Haas-Arndt, Anja Bramkamp, Hans Weidinger, & Planungsbüro Schmitz. (n.d.). *Baualterstufe Gründerzeit/Jahrhundertwende*. Baunetz Wissen. Retrieved 27 April 2023, from <https://www.baunetzwissen.de/altbau/fachwissen/baualtersstufen/baualterstufe-gruenderzeit-jahrhundertwende-148198>

- Rajagopalan, P., & Leung Tony, C. Y. (2012). Progress on building energy labelling techniques. *Advances in Building Energy Research*, 6(1), 61–80. <https://doi.org/10.1080/17512549.2012.672002>
- Raji, B., Tenpierik, M. J., & van den Dobbelsteen, A. (2016). An assessment of energy-saving solutions for the envelope design of high-rise buildings in temperate climates: A case study in the Netherlands. *Energy and Buildings*, 124, 210–221. <https://doi.org/10.1016/j.enbuild.2015.10.049>
- Rajput, M., Augenbroe, G., Stone, B., Georgescu, M., Broadbent, A., Krayenhoff, S., & Mallen, E. (2022). Heat exposure during a power outage: A simulation study of residences across the metro Phoenix area. *Energy and Buildings*, 259, 111605. <https://doi.org/10.1016/j.enbuild.2021.111605>
- Resilient Design Institute. (n.d.). What is Resilience? Resilient Design Institute. Retrieved 22 January 2023, from <https://www.resilientdesign.org/defining-resilient-design/>
- Robinson, P. J. (2001). On the Definition of a Heat Wave. *Journal of Applied Meteorology*, 40(4), 762–775. [https://doi.org/10.1175/1520-0450\(2001\)040<0762:OTDOAH>2.0.CO;2](https://doi.org/10.1175/1520-0450(2001)040<0762:OTDOAH>2.0.CO;2)
- Rosen, R. (1991). *Life itself: A comprehensive inquiry into the nature, origin, and fabrication of life*. Columbia University Press.
- Saltelli, A., Ratto, M., Andres, T., Campolongo, F., Cariboni, J., Gatelli, D., Saisana, M., & Tarantola, S. (2008). *Global Sensitivity Analysis. The Primer*. John Wiley & Sons, Ltd. <https://doi.org/10.1002/9780470725184>
- Santamouris, M. (2016). Cooling the buildings – past, present and future. *Energy and Buildings*, 128, 617–638. <https://doi.org/10.1016/j.enbuild.2016.07.034>
- Santosh, P. (2022). *Eppy Documentation*. <https://buildmedia.readthedocs.org/media/pdf/eppy/latest/eppy.pdf>
- Schünemann, C., Son, S., & Ortlepp, R. (2022). Heat resilience of apartment buildings in Korea and Germany: Comparison of building design and climate. *International Journal of Energy and Environmental Engineering*, 13(3), 889–909. <https://doi.org/10.1007/s40095-022-00476-7>
- Seneviratne, S. I., X. Zhang, M. Adnan, W. Badi, C. Dereczynski, A. Di Luca, S. Ghosh, I. Iskandar, J. Kossin, S. Lewis, F. Otto, I. Pinto, M. Satosh, S.M. Vicente-Serrano, M. Werner, & B. Zhou. (2021). Chapter 11: *Weather and Climate Extreme Events in a Changing Climate* (Climate Change 2021: The Physical

- Science Basis. Contribution of Working Group I to the Sixth Assessment Report of the Intergovernmental Panel on Climate Change, pp. 1513–1766). Cambridge University Press.
- Simmie, J., & Martin, R. (2010). The economic resilience of regions: Towards an evolutionary approach. *Cambridge Journal of Regions, Economy and Society*, 3(1), 27–43. <https://doi.org/10.1093/cjres/rsp029>
- Simon Levin. (2013, April 3). *Ecological resilience*. Encyclopedia Britannica. <https://www.britannica.com/science/ecological-resilience>
- Siu, C. Y., O'Brien, W., Touchie, M., Armstrong, M., Laouadi, A., Gaur, A., Jandaghian, Z., & Macdonald, I. (2023). Evaluating thermal resilience of building designs using building performance simulation – A review of existing practices. *Building and Environment*, 234, 110124. <https://doi.org/10.1016/j.buildenv.2023.110124>
- SKYbrary Aviation Safety. (n.d.). *Temperate oceanic climate (Cfb)*. Retrieved 27 April 2023, from <https://www.skybrary.aero/articles/temperate-oceanic-climate-cfb-0>
- Sobol, I. M. (1993). *Sensitivity estimates for nonlinear mathematical models*. *Mathematical Modelling & Computational Experiment*. 1(4), 407–414.
- Solcast. (n.d.). *Historical and TMY Data*. Retrieved 28 April 2023, from <https://solcast.com/historical-and-tmy>
- Struck, C. (2012). *Uncertainty propagation and sensitivity analysis techniques in building performance simulation to support conceptual building and system design*. University of Technology, Department of the Built Environment.
- Sun, K., Specian, M., & Hong, T. (2020). Nexus of thermal resilience and energy efficiency in buildings: A case study of a nursing home. *Building and Environment*, 177, 106842. <https://doi.org/10.1016/j.buildenv.2020.106842>
- Sun, K., Zhang, W., Zeng, Z., Levinson, R., Wei, M., & Hong, T. (2021). Passive cooling designs to improve heat resilience of homes in underserved and vulnerable communities. *Energy and Buildings*, 252, 111383. <https://doi.org/10.1016/j.enbuild.2021.111383>
- Tartarini, F., & Schiavon, S. (2020). *pythermalcomfort: A Python package for thermal comfort research*. *SoftwareX*, 12, 100578. <https://doi.org/10.1016/j.softx.2020.100578>

- Ted Kesik & Liam O'Brien. (2019). *Thermal Resilience Design Guide*. John H. Daniels Faculty of Architecture, Landscape, and Design.
- The Intergovernmental Panel on Climate Change. (2020). *IPCC DDC Glossary*. https://www.ipcc-data.org/guidelines/pages/glossary/glossary_c.html
- Tian, W. (2013). A review of sensitivity analysis methods in building energy analysis. *Renewable and Sustainable Energy Reviews*, 20, 411–419. <https://doi.org/10.1016/j.rser.2012.12.014>
- Tian, W., & de Wilde, P. (2011). Uncertainty and sensitivity analysis of building performance using probabilistic climate projections: A UK case study. *Automation in Construction*, 20(8), 1096–1109. <https://doi.org/10.1016/j.autcon.2011.04.011>
- Trigo, R. M. (2005). How exceptional was the early August 2003 heatwave in France? *Geophysical Research Letters*, 32(10), L10701. <https://doi.org/10.1029/2005GL022410>
- UN Department of Economic and Social Affairs. (n.d.). *United Nations Sustainability Goals*. United Nations Sustainability Development. Retrieved 18 January 2018, from <https://sdgs.un.org/goals/goal11>
- UN. Secretary-General & UN. Open-ended Intergovernmental Expert Working Group on Indicators and Terminology relating to Disaster Risk Reduction. (2016). *Report of the open-ended intergovernmental expert working group on indicators and terminology relating to disaster risk reduction Reduction: Note / by the Secretary-General*.
- United Nations. (n.d.). *The Paris Agreement*. United Nations Nations Climate Action. Retrieved 22 January 2023, from <https://www.un.org/en/climatechange/paris-agreement>
- U.S. Environmental Protection Agency. (n.d.). *U.S. heat wave frequency and length are increasing*. GlobalChange. Retrieved 21 January 2023, from <https://www.globalchange.gov/browse/indicators/us-heat-waves>
- Visual Crossing Corporation. (n.d.). *Historical weather data for munich*. Retrieved 28 April 2023, from <https://www.visualcrossing.com/weather-history/munich>
- White, L. M., & Wright, G. S. (2020). *ASSESSING RESILIENCY AND PASSIVE SURVIVABILITY IN MULTIFAMILY BUILDINGS*. 144–144.

- Zhang, C., Kazanci, O. B., Levinson, R., Heiselberg, P., Olesen, B. W., Chiesa, G., Sodagar, B., Ai, Z., Selkowitz, S., Zinzi, M., Mahdavi, A., Teufel, H., Kolokotroni, M., Salvati, A., Bozonnet, E., Chtioui, F., Salagnac, P., Rahif, R., Attia, S., ... Zhang, G. (2021). Resilient cooling strategies – A critical review and qualitative assessment. *Energy and Buildings*, 251, 111312. <https://doi.org/10.1016/j.enbuild.2021.111312>
- Zhang, Y., Wang, J., Chen, H., Zhang, J., & Meng, Q. (2010). Thermal comfort in naturally ventilated buildings in hot-humid area of China. *Building and Environment*, 45(11), 2562–2570. <https://doi.org/10.1016/j.buildenv.2010.05.024>
- Zuo, J., Pullen, S., Palmer, J., Bennetts, H., Chileshe, N., & Ma, T. (2014). Impacts of heat waves and corresponding measures: A review. *Journal of Cleaner Production*, 92, 1–12. <https://doi.org/10.1016/j.jclepro.2014.12.078>

Appendix A

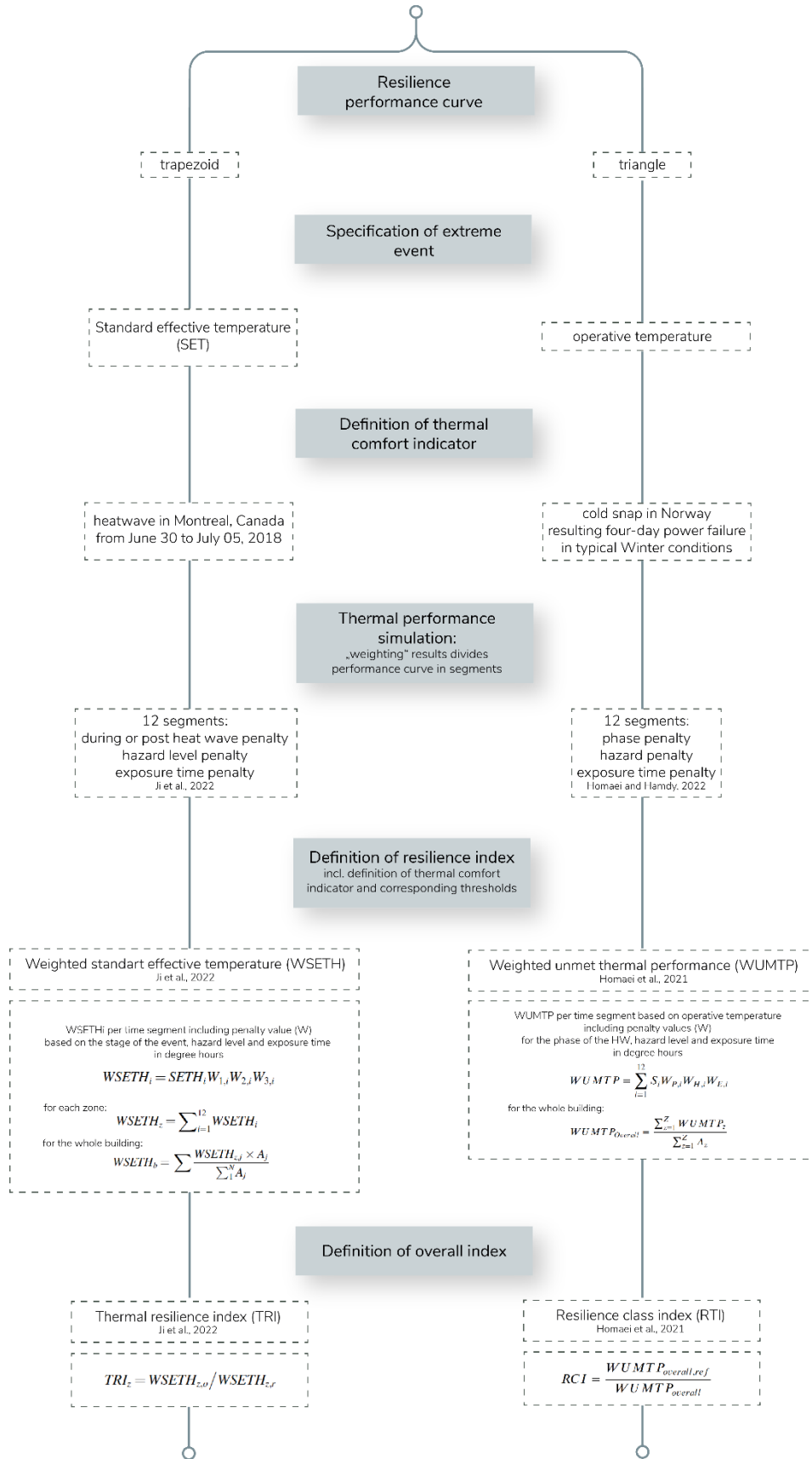


Figure 46: Comparison of thermal resilience assessment methodology
 From: Thesis author on basis of methodology of Homaei and Hamdy, 2021 and Ji et al., 2022

Appendix B

Link to online repository of relevant Python scripts developed for the purpose of this thesis:

<https://github.com/AVWagner/thermal-resilience-assessment.git>

